NASA TECHNICAL NOTE

NASA TN D-4580

NASA TN D-4580

C. 1

ATLAS-CENTAUR FLIGHT PERFORMANCE FOR SURVEYOR MISSION A

Lewis Research Center
Cleveland, Ohio

NATIONAL AERONAUTICS AND SPACE ADMINISTRATION • WASHINGTON, D. C. • MAY 1968

ATLAS-CENTAUR FLIGHT PERFORMANCE FOR SURVEYOR MISSION A

Lewis Research Center
Cleveland, Ohio

NATIONAL AERONAUTICS AND SPACE ADMINISTRATION

For sale by the Clearinghouse for Federal Scientific and Technical Information
Springfield, Virginia 22151 – CFSTI price $3.00

ABSTRACT

The first operational Atlas-Centaur launch vehicle AC-10, with Surveyor spacecraft SC-1, was launched May 30, 1966. Surveyor was the first Earth-launched spacecraft to soft land, under controlled conditions, on the lunar surface. Landing on the lunar surface occurred on June 2, 1966. This report includes a flight performance evaluation of the Atlas-Centaur launch vehicle systems from lift-off through spacecraft separation and Centaur retromaneuver.

STAR Category 31

CONTENTS

I. SUMMARY

The Atlas-Centaur launch vehicle AC-10 with Surveyor spacecraft SC-1, was successfully launched from Eastern Test Range Complex 36A on May 30, 1966, at 0941:00.99 hours eastern standard time. It was the first operational Atlas-Centaur vehicle and the first attempted launching of an operational Surveyor spacecraft into a lunar intercept trajectory. The mission was a complete success with the spacecraft being the first Earth launched vehicle to accomplish a successful controlled soft landing on the lunar surface. The Surveyor was injected into its lunar intercept trajectory in a single burn (direct ascent) mission. Landing on the lunar surface occurred on June 2, 1966.

Lift-off of the launch vehicle was achieved within 1 second after the launch window opened. It was launched on a flight azimuth of 102^{o}. The flight profile through boost phase, Centaur main engine firing, spacecraft separation, and Centaur retromaneuver was accomplished without incident. Spacecraft injection for lunar intercept was excellent and only a very slight midcourse velocity correction was required to place the Surveyor on target. Flight time from lift-off to lunar touchdown was about 64 hours.

This report includes an evaluation of the flight performance of the Atlas-Centaur launch vehicle systems from lift-off through spacecraft separation and Centaur retromaneuver.

II. INTRODUCTION

by John J. Nieberding

Atlas-Centaur launch vehicle AC-10, which boosted Surveyor SC-1 into a direct ascent lunar trajectory, was the first operational flight (Mission A) in a series of seven planned for 1966-1967.

Centaur was developed as a second stage for a modified Atlas D missile and was first flight tested, unsuccessfully, on May 8, 1962. A major redesign and institution of a program of extensive ground testing made a significant contribution to the subsequent success achieved by AC-2 on November 27, 1963. Seven months later, the flight of AC-3 on June 30, 1964, demonstrated the ability of the Atlas-Centaur to jettison the insulation panels and the nose fairing. This flight also firmly established Centaur's flight capability. This capability was further confirmed on December 11, 1964, by the success of AC-4. Despite the failure of AC-5 on March 2, 1965, caused by a premature shutdown of an Atlas engine, the Centaur single-burn development program was completed on August 11, 1965, with the flight of AC-6. This flight successfully demonstrated the ability of Atlas-Centaur to support the Surveyor mission using a direct ascent flight profile.

AC-10 was subsequently launched on May 30, 1966, with the objective of injecting the Surveyor spacecraft on a lunar trajectory with sufficient accuracy that the midcourse correction, required at 20 hours after injection, would not exceed 50 meters per second. The Centaur was also required to perform a retromaneuver after spacecraft separation to prevent impact of Centaur on the Moon and to avoid the possibility of the Surveyor star sensor mistaking Centaur for the star Canopus.

An evaluation of the results of the Atlas-Centaur flight AC-10 in support of the mission objectives is presented in this report. Both Atlas and Centaur systems and subsystems are described, and their performance is evaluated.

III. LAUNCH VEHICLE DESCRIPTION

by Eugene E. Coffey

The Atlas-Centaur AC-10 was a two-stage launch vehicle consisting of an Atlas first stage and a Centaur second stage. Illustrations of the general arrangement of the Atlas, Centaur, and Surveyor are shown in figures III-1, III-2, and III-3. Both stages were 10 feet in diameter and were connected by an interstage adapter. The composite vehicle was 113 feet in length and weighed 302 248 pounds at lift-off. The Atlas and the Centaur stages utilized thin-wall, pressurized, main propellant tank sections of monocoque construction to provide primary structural support for all vehicle systems.

The first-stage Atlas vehicle was 65 feet long. It was powered by a standard Rocketdyne MA-5 propulsion system consisting of two booster engines with 328 600 pounds thrust total, a single sustainer engine of 57 000 pounds thrust, and two small vernier engines of 670 pounds thrust each. These engines, which burned liquid oxygen and kerosene, were ignited simultaneously on the ground. The booster engines were gimbaled for roll and directional control during the booster phase of the flight. This phase was completed when the vehicle acceleration equaled 5.68 g's and the booster engines were cut off. The booster engines were jettisoned 3.1 seconds after booster engine cutoff. The sustainer engine and the vernier engines, which were ignited at lift-off, continued to burn after booster engine cutoff for the Atlas sustainer phase of the flight. During this phase, the sustainer engine gimbaled for directional control while the vernier engines gimbaled for roll control. The sustainer and vernier engines burned until propellant depletion, at which time the sustainer phase was completed. The Atlas was separated from the Centaur, after sustainer engine cutoff, by the firing of a shaped charge severance system. The firing of a retrorocket system, required to back the Atlas and the interstage adapter away from the Centaur, completed the separation of these stages. Other major systems of the Atlas first stage included flight control, structures and separation, propellant utilization, telemetry and instrumentation, flight termination (destruct) and electrical.

The second-stage Centaur vehicle, including the nose fairing, was 48 feet long. Centaur, a high-specific-impulse (433 sec) vehicle was powered by two Pratt & Whitney RL-10A3CM-1 engines which generated 30 045 pounds thrust total. These engines burned liquid hydrogen and liquid oxygen. The Centaur main engines gimbaled to provide directional and roll control during Centaur powered flight. Hydrogen peroxide engines (3.5, 6, and 50 lb thrust) mounted on the aft periphery of the tank, provided attitude control

and additional thrust for vehicle reorientation after Centaur main engine cutoff. The Centaur was equipped with four insulation panels (1-in.-thick glass fabric sandwich construction with a polyurethane foam core) for insulating the hydrogen tank. The insulation panels and nose fairing were jettisoned during the Atlas sustainer phase. A fiberglass nose fairing was used to provide an aerodynamic shield for the Surveyor spacecraft, guidance equipment, and electronic packages during launch. The Centaur used an inertial guidance system. Additional major systems of the Centaur included flight control, structures and separation, propellant utilization, telemetry and instrumentation, flight termination (destruct), C-band radar tracking beacon, guidance, and electrical.

The Atlas-Centaur launch vehicle AC-10, which injected Surveyor SC-1 into a lunar intercept trajectory, was substantially similar to AC-6, the final launch vehicle flown in the single-burn, direct-ascent development program (see ref. 1). The only exception was the removal of instrumentation not necessary for an operational vehicle.

The major systems, as they were configured for the Atlas-Centaur launch vehicle AC-10, are delineated in the subsequent sections of this report.

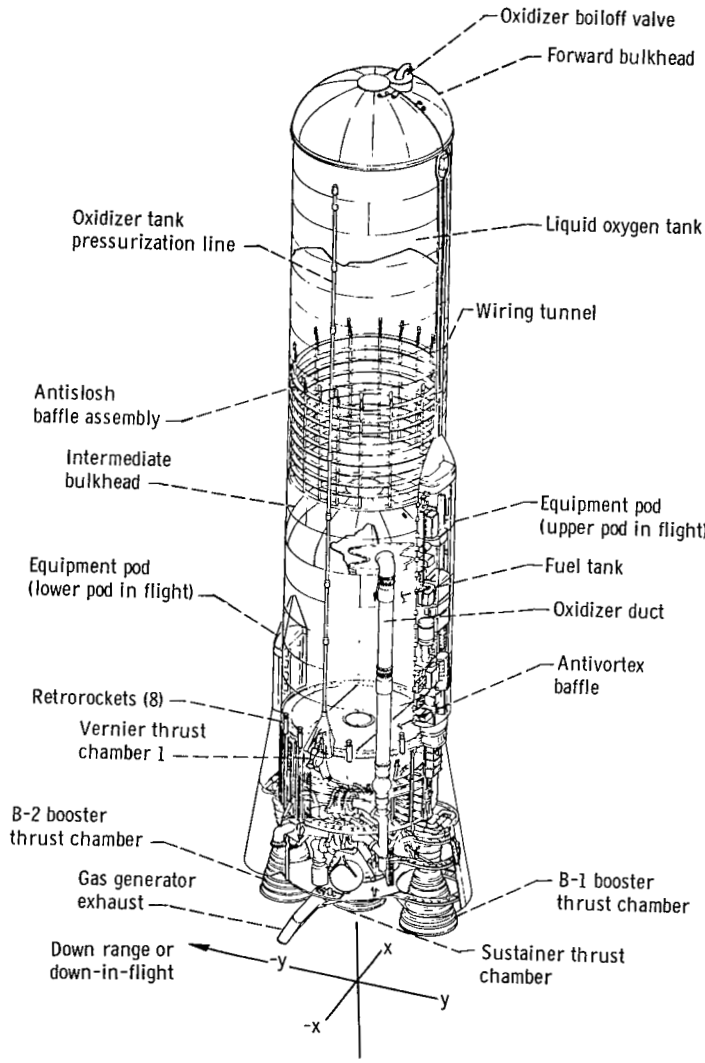

Figure III-1. - General arrangement of Atlas launch vehicle.

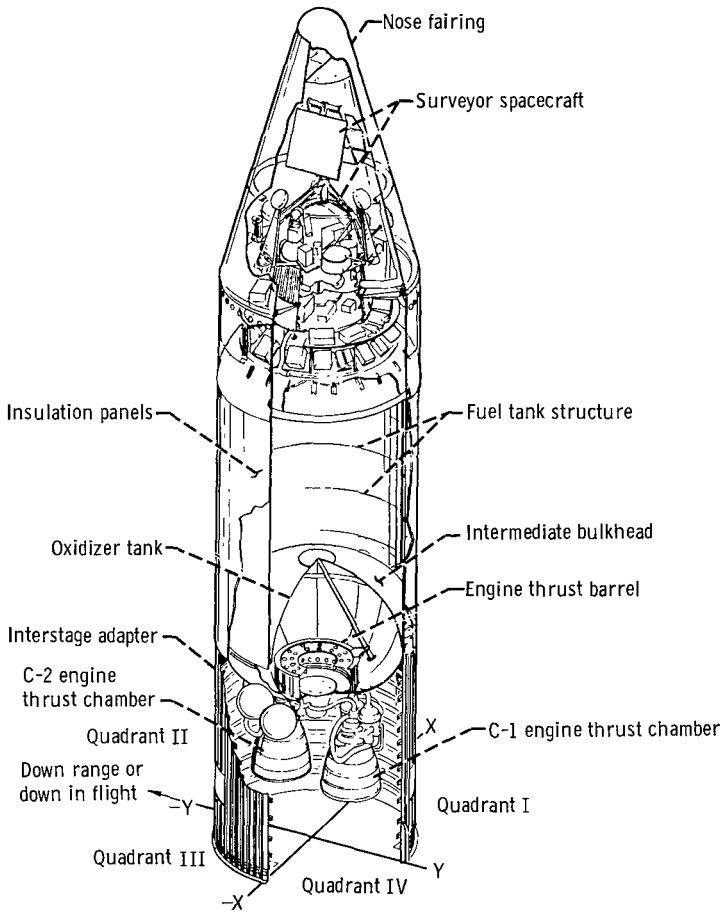

Figure III-2. - General arrangement of Centaur vehicle.

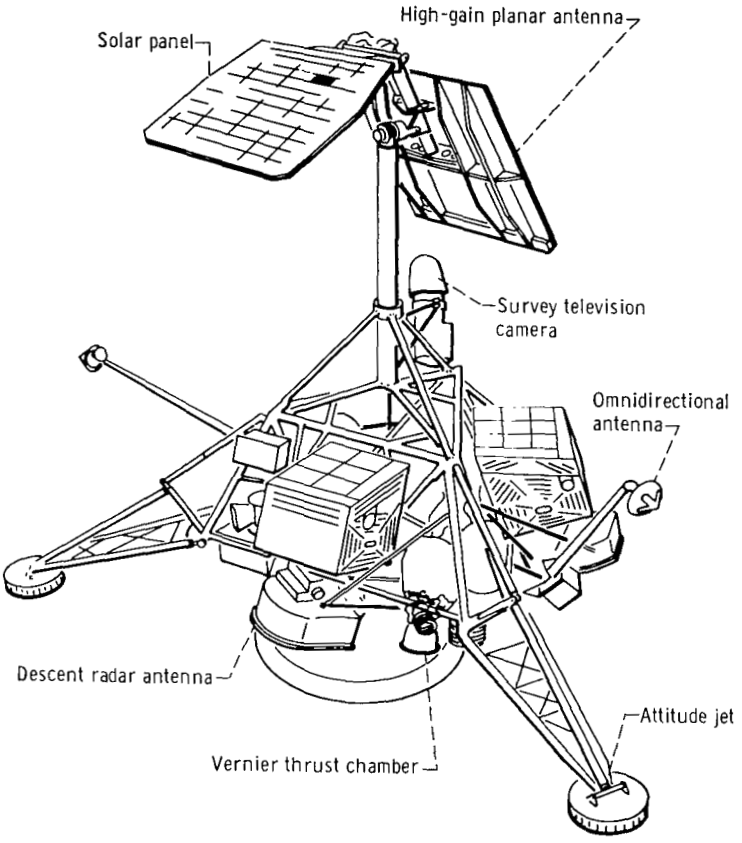

Figure III-3. - Surveyor spacecraft in landing configuration.

IV. MISSION PERFORMANCE

by William A. Groesbeck

ATLAS FLIGHT PHASE

The first operational Atlas Centaur launch vehicle AC-10, with Surveyor I, was launched from Eastern Test Range Complex 36A on May 30, 1966, at 0941:00.99 hours eastern standard time. AC-10 was programmed to fly a single-burn direct-ascent lunar intercept trajectory from which the first operational Surveyor spacecraft would attempt a controlled soft landing on the lunar surface. Countdown for the launch proceeded without a single interruption, and lift-off was achieved within 1 second after the launch window opened. Weight of the combined vehicle at lift-off was 302 248 pounds, which gave a thrust to weight ratio of 1.28. A compendium of the AC-10 mission profile and the Surveyor-Earth-Moon trajectory is shown in figures IV-1 and IV-2. For reference also, the postflight vehicle weights summary, atmospheric sounding data, Surveyor launch windows, flight events record, and trajectory data are given in appendix A.

Vehicle lift-off was normal and, from lift-off (T + 0 sec) through Atlas booster staging, the vehicle was flown without guidance generated steering commands on a preprogrammed trajectory. The guidance system inertial reference, however, was locked in at T - 7.5 seconds. The Atlas flight control system initiated the preset roll program at T + 2 seconds in order to realine the vehicle from the launch pad azimuth of 105° to a flight azimuth of 102.285°. With the roll attitude stabilized on the flight azimuth, the flight programmer initiated the booster pitchover program at T + 15 seconds. Winds aloft and maneuvering requirements were not severe and the maximum booster engine gimbal deflections during the ascent did not exceed 3.6°.

The programmed Centaur hydrogen tank nonventing period following lift-off was interrupted at T + 53.8 seconds as tank pressure reached the relief pressure of the high range secondary vent valve. The valve cycled once emitting a momentary puff of hydrogen. A few seconds later, at T + 69.3 seconds and an altitude of 25 500 feet, the primary vent valve was programmed to the relief mode allowing tank pressure to blow down. The ullage pressure was then controlled at a lower pressure within the regulating range of the primary vent valve.

Thrust buildup and vehicle acceleration during boost phase proceeded according to the mission plan, and at an acceleration of 5.68 g's, which occurred at T + 142.04 seconds, the Centaur guidance issued the booster engine cutoff signal. Three seconds

later, at T + 145.04 seconds, the staging command was given by the Atlas programmer and the booster engine separated from the vehicle. Staging transients were mild, and momentary vehicle rate excitation in pitch, yaw, or roll did not exceed 1.0 degree per second. Low amplitude slosh was excited in the Atlas liquid oxygen tank but it was almost completely damped out within a few seconds. When guidance steering commands were first admitted to the Atlas flight control system 8 seconds after booster engine cutoff, the vehicle was 18^{o} nose low and 1.0^{o} nose right of the required steering vector. These differences, however, were not serious and were corrected in approximately 11 seconds; the guidance system continued to command a pitchover during the Atlas sustainer phase.

Insulation panels were jettisoned during the sustainer phase at T + 175.84 seconds. All panels were completely severed by the shaped charge and cleared the vehicle within 0.2 second. Similarly, the nose fairing unlatch command was given at T + 202.26 seconds, and the thrustor bottles, firing 0.5 second later, rotated the fairing halves clear of the vehicle within 0.28 second. Vehicle angular rates due to the jettisoning of the insulation panels and nose fairing were low and did not exceed 0.25 degree per second in pitch or yaw, or 1.5 degrees per second in roll. Sustainer and vernier engine systems performed satisfactorily, building up from a rated sea level thrust of 58 340 pounds to a total vacuum thrust of 81 000 pounds at engine cutoff. This thrust boosted the vehicle to an Earth referenced velocity of 11 428 feet per second and an acceleration of 1.8 g's at engine shutdown. The propellant utilization system operated satisfactorily throughout the Atlas flight phase, and the sustainer shutdown sequence was initiated in a normal manner with a gradual thrust decay due to depletion of usable liquid oxygen. Sustainer and vernier engine cutoff occurred at T + 239.4 seconds.

Coincident with sustainer engine cutoff, the guidance steering was disabled allowing the vehicle to coast on a noncontrolled flight mode. The guidance disable prevented gimbaling the Centaur engines under nonthrusting conditions and helped maintain required clearances between the engines and the interstage adapter during staging.

The Atlas staging command from the flight programmer was given at T + 241.3 seconds and the shaped charge fired severing the two vehicles. Eight retrorockets on the Atlas then fired and pushed the Atlas stage clear of the Centaur. The Centaur stage, however, did experience some slight disturbances during the Atlas sustainer engine shutdown and vehicle staging sequence, which caused the vehicle to drift off the steering vector. The angular rates did not exceed 0.2 degree per second, and the drift error was quickly corrected after the start of Centaur main engines when guidance steering was readmitted.

CENTAUR FLIGHT PHASE

Centaur stage boost pumps were started prior to sustainer engine cutoff and were

deadheaded through staging until main engine start. Required net positive suction pressure during the near-zero-gravity period from sustainer engine cutoff until main engine start at T + 250.9 seconds was provided by pressure pulsing the propellant tanks with helium. Ullage pressures were increased from 29.8 to 39.8 psia in the oxygen tank and from 19.7 to 21.2 psia in the hydrogen tank. Eight seconds prior to main engine start, the Centaur programmer issued preparatory commands for main engine firing. Main engines were gimbaled to the zero position. Cooldown valves were opened to flow liquid propellants through the lines and to chill down the engine turbopumps. Chilldown of the lines ensured liquid at the pump inlets and enhanced a uniform and rapid thrust buildup at engine ignition. At T + 250.9 seconds, the ignition command was given by the flight control programmer, and the engine thrust increased to full flight levels. The difference between engines in start total impulse during the first 2 seconds following engine ignition was only 1289 pound-seconds.

Guidance steering for the Centaur stage was enabled at T + 254.9 seconds, when the engine thrust was fully established. During the main engine start sequence, guidance steering was disabled temporarily to allow the engines to be centered and to prevent excessive vehicle angular rates induced by correction of vehicle position errors. However, without steering control during this interval, residual angular rates and disturbing torques caused the vehicle to drift off the steering vector 1^{o} nose high and 4^{o} nose right. These errors were corrected within 4 seconds, and the steering commands again provided the required pitchdown rate to home in on the injection velocity vector.

The propellant utilization system controlled the mixture ratio during main engine firing to an average value of 5.06. Propellant consumption was controlled so that the burnable residuals at engine cutoff were within 12 pounds of hydrogen at a mixture ratio of 5.

About 60 seconds prior to the end of Centaur powered flight the pitchover rate decreased as the vehicle homed in on the desired orbital injection conditions for the Surveyor lunar transfer intercept. At T + 689.2 seconds, the guidance computed velocity-to-be-gained was zero, and the main engines were cut off. The injection velocity was 34 496 feet per second at an altitude of about 90 nautical miles. At injection, approximately 1700 nautical miles southeast of Cape Kennedy, the vehicle had pitched over a total of 135^{o} from its inertial attitude at lift-off. Engine cutoff occurred with 189 pounds of burnable propellants remaining, or enough for 2 more seconds of engine firing.

SPACECRAFT SEPARATION

Coincident with main engine cutoff, the guidance steering commands were disabled and the coast phase hydrogen peroxide attitude control system was activated. Rates im-

parted to the vehicle at main engine cutoff were mild (not in excess of 0.76 deg/sec), and were quickly damped by the attitude control system to rates less than 0.2 degree per second. The residual motion below this threshold allowed only a negligible drift in vehicle attitude. This drift did not interfere with the subsequent spacecraft separation.

The Centaur with the Surveyor spacecraft then coasted in a near-zero-gravity field for about 68 seconds. This coast period allowed for canceling the residual vehicle rates and preparing the spacecraft for separation. Signals from the Centaur programmer were given to the spacecraft to extend landing gear and omniantennas, to turn on spacecraft transmitter high power, and to arm the spacecraft for separation. All commands were received and executed by the spacecraft.

Separation of the spacecraft was commanded at T + 756.9 seconds. Pyrotechnically operated latches were fired, and the spring loaded mechanism pushed the Surveyor to impart an approximate 0.75-foot-per-second separation velocity. Full extension of all three springs occurred within 2 milliseconds of each other. Maximum turning rates imparted to the spacecraft were only 0.34 degree per second, which was well below the maximum allowable of 3.0 degrees per second. The attitude control system had been disabled at spacecraft separation in order to minimize vehicle turning rates which could have caused interference between the two vehicles.

CENTAUR RETROMANEUVER

The Centaur vehicle was required to execute a turnaround and retrothrust maneuver after spacecraft separation in order to eliminate the possibility of the Surveyor acquiring the reflected light of Centaur rather than the star Canopus. A second objective was to avoid impact of Centaur on the Moon. A guidance vector for the turnaround was selected which was the reciprocal of the velocity vector at main engine cutoff. Execution of the turnaround was commanded at T + 761.9 seconds, 5 seconds after spacecraft separation. Guidance system logic accounted for any vehicle drift since main engine cutoff and steering commands were given which rotated the Centaur in the shortest arc from its actual position to the new retrovector. Turning rate during the reorientation was limited, for structural considerations, to a maximum of 1.6 degrees per second.

About half way through the turnaround at T + 801.9 seconds, two 50-pound-thrust hydrogen peroxide engines were fired for 20 seconds to provide lateral as well as additional longitudinal separation from the spacecraft. The lateral separation was necessary to minimize particle impingement of residual propellants on the spacecraft during the subsequent Centaur propellant tank blowdown. During this lateral thrust maneuver, the impingement forces on the vehicle from the engine exhaust plumes were unexpectedly high and produced a clockwise roll disturbing torque. These impingement forces required the 3.5- and 6.0-pound-thrust attitude control engines to operate 50 percent of the time in

order to maintain vehicle orientation.

The turnaround maneuver was completed at T + 860 seconds after rotating the vehicle through 161°. Once the retrovector was acquired, the attitude control maintained the vehicle position on the vector within 1.5°.

The retrothrust maneuver was initiated by programmer command at T + 996.9 seconds. The main engines were gimbaled to aline the thrust vector with the vehicle center of gravity, and the engine prestart valves were opened in order to allow the residual propellants to blow down through the engines. Expelling the residual propellants provided sufficient thrust to alter the Centaur orbit, and the relative separation distance from the spacecraft at the end of 5 hours was 1054 kilometers. This distance was more than three times the required minimum. At completion of the retromaneuver at T + 1246.9 seconds, all vent valves were enabled to the relief or normal regulating mode. Flight control and all other systems were deenergized allowing the spent vehicle to continue its orbit in a nonstabilized flight mode.

SURVEYOR TRANSIT PHASE

The Surveyor spacecraft was injected into its lunar intercept trajectory with such accuracy that lunar impact would have occurred without any midcourse correction. To impact on its preselected target, a slight midcourse velocity correction of only 3.8 meters per second for miss only, or 6.4 meters per second for miss plus time of arrival would have been required. However, the Surveyor Mission Manager elected to change the landing site during the flight to optimize the landing configuration. A new target, as shown in figure IV-3, was established at 2.33° South latitude, and 43.83° West longitude, and the actual midcourse maneuver was executed at T + 16 hours 4 minutes from lift-off. A total correction of 20.35 meters per second was made. This correction was the vector sum of 3.74 meters per second for miss only, 5.7 meters per second for time of flight, and 15.66 meters per second for optimizing fuel margin and burnout velocity.

On June 2, 1966 at 0117:37 hours eastern standard time, after an elapsed flight time of 63 hours, 36 minutes, and 36 seconds, the Surveyor spacecraft successfully touched down on the lunar surface. The touchdown point, only 9 miles off the revised aiming point, was at a position of 2.58° South latitude and 43.35° West longitude. This location was approximately 60 miles North of the crater Flamsteed. The Surveyor touchdown, and the subsequent pictorial data transmission, was completely successful and was the first controlled soft landing of an Earth launched interplanetary space vehicle on the Moon. An evaluation of the Surveyor spacecraft performance is given in reference 2.

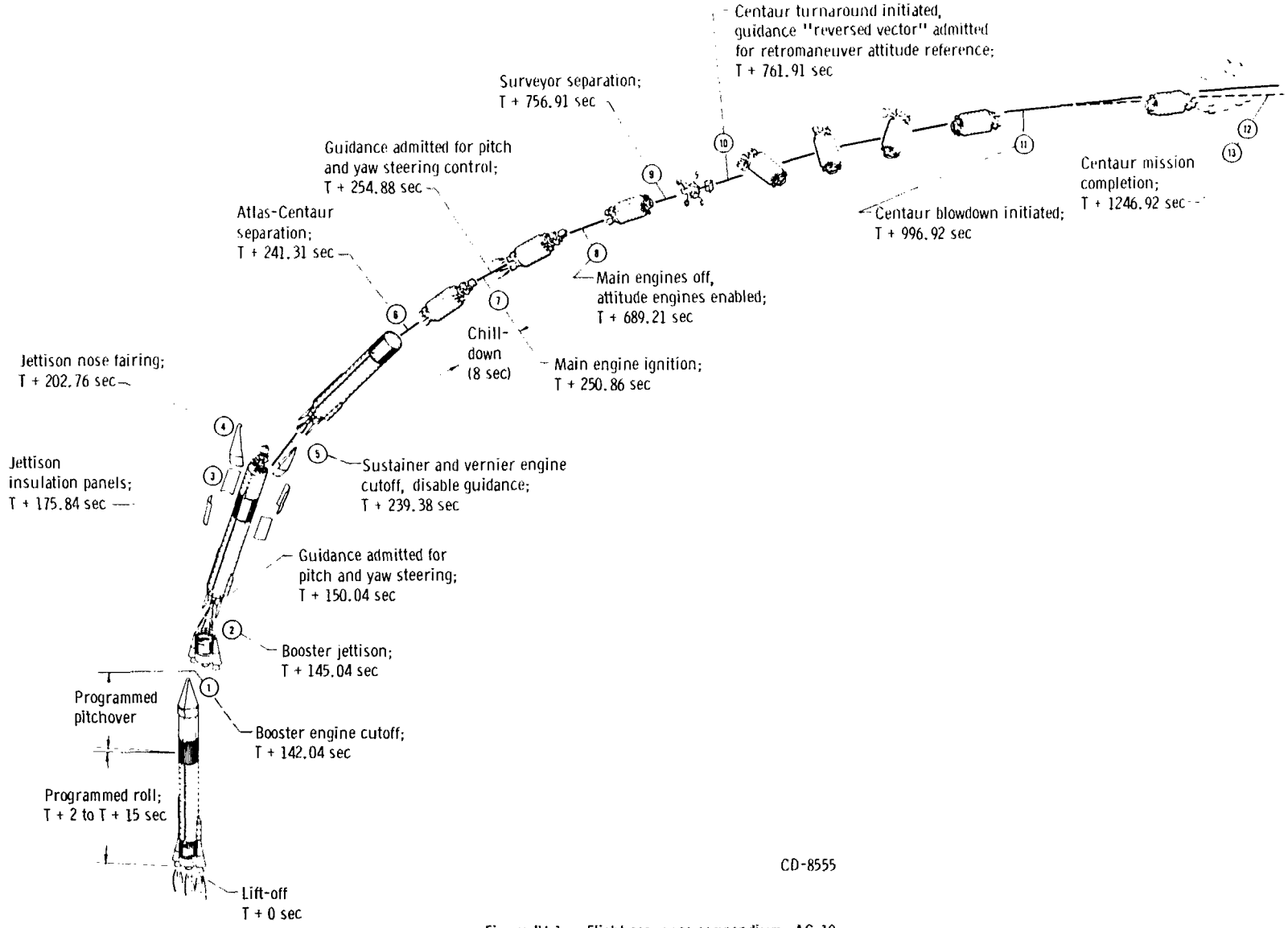

Figure IV-1. - Flight sequence compendium, AC-10.

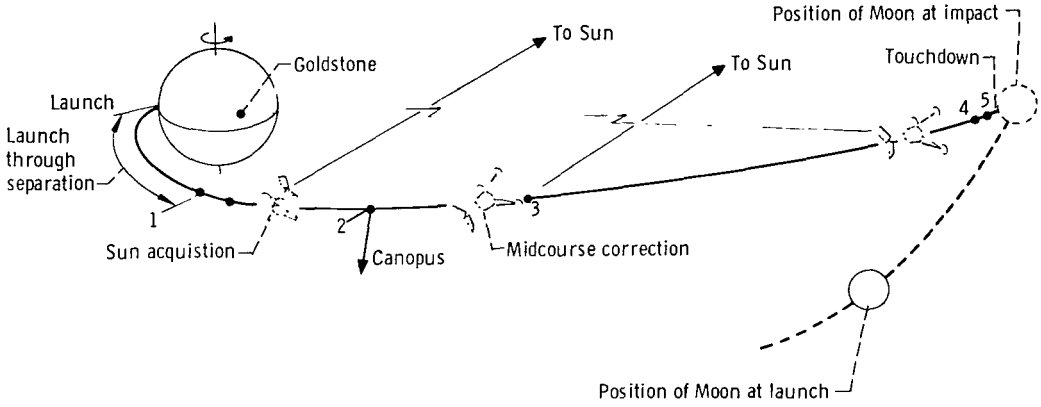

Figure IV-2. - Surveyor-Earth-moon trajectory: 1, injection and separation; 2, star acquistion and verification; 3, reacquisition of Sun and star after midcourse correction; 4, retrophase initiated about 60 miles from Moon; 5, vernier descent initiated 35 000 feet above surface of Moon.

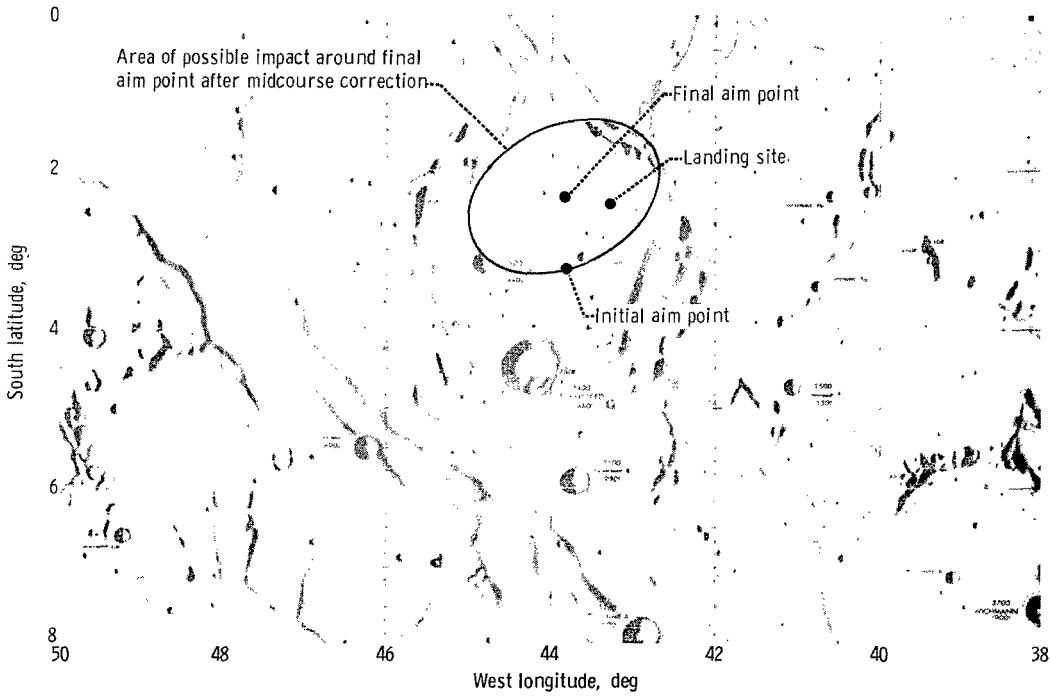

Figure IV-3. - Surveyor I landing location.

V. LAUNCH VEHICLE SYSTEM ANALYSIS

PROPULSION SYSTEM

by Ronald W. Ruedele, Steven V. Szabo, Jr., Kenneth W. Baud, and Donald B. Zelten

Atlas

System description. - The Rocketdyne MA-5 engine system used on the Atlas vehicle consisted of two booster engines, a sustainer engine, two vernier engines, an engine start system, a logic control package, and associated electrical equipment. The system schematic is shown in figure V-1. All engines were single start and used liquid oxygen and kerosene (RP-1) as propellants. The engines were hypergolically ignited through the use of pyrophoric fuel cartridges. The pyrophoric fuel preceeded the RP-1 into the thrust chamber and initiated ignition with the liquid oxygen. Combustion was then sustained by the RP-1 and liquid oxygen.

All thrust chambers were regeneratively cooled by using the fuel as the coolant. The engine acceptance test thrust values are given in the following table:

Engine	Thrust, lb
Booster (2)	328 600
Sustainer	57 000
Vernier (2)	1 340
Total thrust (sea level)	386 940

The booster engine system consisted of two gimbaled thrust chamber assemblies and a common power package consisting of a gas generator, two turbopumps, and a supporting control system. The sustainer engine was a single gimbaled engine assembly consisting of a thrust chamber, gas generator, turbopump and a supporting control system. The vernier engines consisted of thrust chamber assemblies, propellant valves, gimbal bodies, and mounts. The self-contained engine start system consisted of an oxidizer start tank, a fuel start tank, and the associated control system.

TABLE V-I. - ATLAS ENGINE SYSTEM PERFORMANCE DATA, AC-10

Parameter	Flight time, sec		
	T + 10	Booster engine cutoff, T + 142.04	Sustainer engine cutoff, T + 239.38
Booster engine 1:			
Chamber pressure, psia	577	577	------
Pump speed, rpm	6 368	6 339	------
Oxidizer pump inlet pressure, psia	57	79	------
Fuel pump inlet pressure, psia	67	51	------
Booster engine 2:			
Chamber pressure, psia	575	579	------
Pump speed, rpm	6 300	6 300	------
Oxidizer pump inlet pressure, psia	58	82	------
Fuel pump inlet pressure, psia	67	53	------
Booster gas generator combustion chamber pressure, psia	534	528	------
Booster liquid oxygen regulator reference pressure, psia	629	619	------
Sustainer engine chamber pressure, psia	707	692	682
Sustainer pump speed, rpm	10 080	9 958	10 080
Sustainer oxidizer injector manifold pressure, psia	812	812	802
Sustainer fuel pump discharge pressure, psia	917	932	924
Sustainer oxidizer regulator reference pressure, psia	831	821	821
Sustainer gas generator discharge pressure, psia	643	643	643
Sustainer fuel pump inlet pressure, psia	70	63	40
Sustainer oxidizer pump inlet pressure, psia	63	87	32
Sustainer oxidizer pump inlet temperature, ^{o}F	-284	-281	-281
Vernier engine 1 chamber pressure, psia	267	265	265
Vernier engine 2 chamber pressure, psia	264	260	264

Engine performance. - All engine system operations were satisfactory during flight. The total calculated lift-off thrust was 387 500 pounds (acceptance test value was 386 940 lb), well within the limits of allowable engine performance. All system parameters displayed values indicative of proper engine operation. Engine performance data for T + 10 seconds, booster engine cutoff, and just prior to thrust decay at sustainer engine cutoff are summarized in table V-I.

Centaur Main Engines

System description. - Two Pratt & Whitney RL 10A3CM-1 engines were used to provide thrust for the Centaur stage on AC-10. These were high energy hydrogen-oxygen engines with a nozzle expansion ratio of 40. Rated vacuum thrust of each engine was 15 000 pounds (acceptance test values were 14 994 and 15 051 lb of thrust for the C-1 and C-2 engines, respectively) at a design thrust chamber pressure of 300 psia and an oxidizer to fuel mixture ratio of 5.0. The specific impulse was 433 seconds.

The engine system, shown schematically in figure V-2, utilized a regeneratively cooled thrust chamber and a turbopump-fed propellant flow system. Pumped fuel, after cooling the thrust chamber, was expanded through a turbine, which drove the propellant pumps. By regulating the amount of fuel bypassed around the turbine as a function of combustion chamber pressure, it was possible to vary turbopump speed and thereby control engine thrust. The oxidizer was pumped directly to the propellant injector through the propellant utilization (mixture ratio control) valve. Ignition was accomplished by a spark igniter recessed in the propellant injector face. Engine start and stop sequences were controlled by pneumatically operated valves actuated by electrical signals from the vehicle. The engines were gimbal mounted to permit thrust vector control for steering the vehicle.

System performance. - Main engine performance appeared normal throughout the Centaur flight. Eight seconds prior to main engine start, the engine inlet valves were opened to flow liquid propellants through the lines and to chill down the engine pumps. Command for engine ignition was given by the flight control programmer at T + 250.9 seconds, and thrust increased normally to full flight levels. The thrust chamber pressure rise for the engine start is shown in figure V-3. Ignition of the C-1 engine required approximately 0.28 second, which was somewhat longer than normal. The time, however, was within the limits of previous experience, and it did not produce any adverse effect on the engine start transient. No thrust overshoot, as experienced on AC-6, was observed from either the chamber pressure or oxidizer pump speed rise data, which are presented in figure V-4. The start total impulse to 95 percent of rated thrust was calculated to be 1970 and 2373 pound-seconds for the C-1 and C-2 engines, respectively. Cor-

responding engine acceleration times were 1.11 and 1.21 seconds. The start total impulse from engine start to 2 seconds was calculated to be 15 073 and 13 784 pound-seconds for the two engines, respectively. The difference in these total impulse values was acceptable.

Liquid hydrogen and liquid oxygen pump inlet temperature and pressure data are presented in figures V-5 and V-6. The pump inlet pressures remained well above saturation for any fluid inlet temperature. The margin between the steady-state operating limit and the actual inlet conditions ensured satisfactory values of net positive suction pressure.

Steady-state engine operating conditions are summarized and compared with corresponding predicted values in table V-II. All actual flight values were within the allowable tolerances.

TABLE V-II. - CENTAUR PROPULSION SYSTEM DATA

Parameter	Expected range	Time from main engine start, sec					
		90		200		435	
		Engine					
		C-1	C-2	C-1	C-2	C-1	C-2
Hydrogen total pressure at pump inlet, psia	21.9 to 48.1	35.7	36.2	35.6	35.2	33.3	33.4
Hydrogen temperature at pump inlet, ^{o}R	34 to 39.8	38.5	38.6	38.2	38.1	37.3	37.1
Oxidizer total pressure at pump inlet, psia	45 to 77	63.0	65.3	64.3	66.1	61.1	63.8
Oxidizer temperature at pump inlet, ^{o}R	171 to 182.5	176.6	176.4	176.0	175.9	172.5	172.3
Oxidizer pump speed, rpm	11 140 to 11 676	11 569	11 420	11 569	11 340	11 460	11 510
Hydrogen pressure upstream of venturi, psia	647 to 695	657.8	666.7	653.7	665.7	652.7	665.7
Hydrogen temperature at turbine inlet, ^{o}R	302 to 348	318.2	329.5	311.5	327.3	312.8	324.3
Oxidizer injector differential pressure, psid	43 to 59	58.4	55.3	58.9	54.4	57.7	55.3
Engine chamber pressure, psia	292 to 300	297.3	295.2	296.0	295.8	295.5	294.5

Engine performance values of thrust, specific impulse, and mixture ratio during main engine firing were within specification. Engine performance values at T + 90 seconds are shown in table V-III. Performance values in table V-III are based on the Pratt & Whitney C* method. From the guidance acceleration data, the calculated vehicle specific impulse was a little lower at 431.6 seconds. This agreement is very good considering the accuracy of the telemetry data used in the C* calculation. A more complete summary and discussion of these performance calculation methods is given in appendix B.

TABLE V-III. - CENTAUR ENGINE PERFORMANCE

SUMMARY AT T + 90 SECONDS, AC-10

Parameter	Expected value[a]	C-1 engine	C-2 engine
Engine thrust, lb	14 700 to 15 226	14 997	15 069
Specific impulse, sec	429.7 to 438.3	433.7	434.8
Mixture ratio	4.921 to 5.079	5.102	5.124

[a]Tolerances apply only for zero angle of propellant utilization valve.

The overall variation in performance with time was slight. Normally, the main reason for any performance change can be related to control movement of the propellant utilization valve. However, on AC-10, the movement of the propellant utilization valve was less than usual, and the engine performance remained relatively constant.

Engine shutdown appeared normal. Chamber pressure began to decay 0.05 and 0.07 second following the main engine cutoff signal for the C-1 and C-2 engines, respectively. These values compared favorably with those obtained on previous vehicles. Vehicle shutdown impulse was calculated to be 3304 pound-seconds which was higher than the predicted level of 3050 pound-seconds. This difference was a big contributor to the required midcourse correction of 3.8 meters per second. However, 3.8 meters per second was much smaller than the allowable specification, as discussed in the GUIDANCE AND FLIGHT CONTROL SYSTEMS section of this report.

Engine burn time was 3.1 seconds longer than predicted, but this difference was within the allowable engine operating limits. If the Atlas performance was assumed to be normal, three possible causes for the longer Centaur burn time were (1) low engine thrust, (2) high specific impulse, and (3) high propellant loading. Any of these factors would have the effect of increasing vehicle weight at any given time during the ascent. A longer burn time would thus be necessary to drive the heavier vehicle to its required energy level at engine cutoff.

A computer investigation was conducted to determine the effect of slight changes in engine thrust, specific impulse, and propellant loading on engine burn time. These values of thrust, specific impulse, and propellant loading were varied separately while holding the other two constant. With thrust 400 pounds low, specific impulse 3 seconds high, and propellant weight 300 pounds high, engine burn time was increased by 5.94, 1.90, and 3.63 seconds, respectively. The assumed low thrust level of 400 pounds caused the residuals following main engine cutoff to be only 6 pounds low, while the high specific impulse and high propellant loading increased the residual level by 74 and 50 pounds, respectively. The variation of these parameters was within specification

limits, and yet the combination, when root sum squared, could increase engine burn time by approximately 7.2 seconds. When all factors are considered, the preflight uncertainty for engine burn time was +8.4, -10.4 seconds.

Centaur Boost Pumps

System description. - Boost pumps were used in the liquid oxygen and liquid hydrogen tanks on Centaur to supply propellants to the main engine pumps at required inlet pressures. Both pumps were a mixed flow type and were powered by gas driven turbines as shown in figures V-7 to V-10. Superheated steam and oxygen from the catalytically decomposed products of hydrogen peroxide were supplied to drive the turbines. A constant turbine power on each unit was maintained by metering the hydrogen peroxide through fixed area orifices upstream of the catalyst bed.

Boost pump performance. - Performance of the boost pumps was satisfactory during the entire flight. Boost pump start command was initiated at lift-off + 203.7 seconds and was terminated simultaneously with main engine cutoff at lift-off + 689.2 seconds. First indications of turbine inlet pressures were evident 1.0 and 3.2 seconds after boost pump start for fuel and oxidizer boost pumps, respectively. The slow pressure response on the liquid oxygen turbine relative to the liquid hydrogen turbine was unusual. Normally, the first indication of pressure occurs on the oxidizer pump because it has a shorter hydrogen peroxide supply line. The most common causes for delay in pressure rise are (1) gas trapped in the hydrogen peroxide bottle and supply lines to the boost pump turbines, and (2) slow catalyst bed reaction due to a cold or slightly contaminated catalyst bed. However, ground test experience has shown that less than 1 second of differential response time can be expected due to gas trapped in the bottle and supply lines. The principal cause of delay has been one catalyst bed being slightly contaminated or colder than the other (up to 2.5 sec of differential response time has been observed in ground tests). Prior to lift-off, the AC-10 landline turbine bearing temperature data did indicate that the oxidizer turbine was 10^{o} colder than the fuel turbine (64^{o} and 74^{o} F, respectively). The longer oxidizer delay therefore was probably caused by a cold or slightly contaminated catalyst bed. The 3.2-second delay was well within the time allowed in the start sequence, which was 16 seconds.

Steady-state turbine inlet pressures are shown in table V-IV. Average values were within 2 psi of the expected values with up to 32-psi peak-to-peak pressure oscillations superimposed. Oscillations of 100 psi peak to peak have been experienced on previous flights and in ground tests with no apparent effect on turbine performance.

Steady-state oxidizer boost pump headrise, oxidizer turbine speed, and fuel turbine speed data, as shown in figures V-11 to V-13, were all higher than the expected values

TABLE V-IV. - CENTAUR BOOST PUMP TURBINE INLET PRESSURE, AC-10

Parameter	Expected range	Time from boost pump start, sec					
		40	100	200	300	400	485
Oxidizer[a] turbine inlet pressure, psia	96 to 108	100	100	101	102	103	104
Fuel[b] turbine inlet pressure, psia	128 to 140	132	135	135	135	135	136

[a]Values are averages of oscillations which started 30 sec after boost pump start and continued throughout boost pump operation with maximum amplitude of 32 psi peak to peak.

[b]Values are averages of oscillations which started immediately after boost pump start and continued throughout boost pump operation with maximum amplitude of 20 psi peak to peak.

calculated from ground acceptance test data. The differences were attributed to the inability of the ground tests to simulate correctly the actual flight conditions.

Oxidizer boost pump headrise, oxidizer turbine speed, and fuel turbine speed data indicated that the propellants moved away from the boost pump inlets immediately following main engine cutoff. This liquid displacement was expected for a single-burn mission as no means were provided or were necessary to retain the propellants in a settled condition. The fuel turbine speed began a linear decay 2 seconds after main engine cutoff, and the oxidizer pump headrise decayed to zero by main engine cutoff + 5 seconds with a corresponding linear decay in oxidizer turbine speed. Linear turbine speed decay and zero headrise are typical coastdown characteristics without liquid in the pump.

Oxidizer temperatures at the boost pump inlet, as shown in figure V-14, were normal throughout the flight. Temperature data indicated the presence of liquid at the pump inlet from lift-off through main engine cutoff. At booster engine cutoff, the reduction in vehicle acceleration reduced the static head pressure causing some local boiling and a slight drop in temperature as the liquid oxygen equilibrated at the lower saturation pressure.

Fuel boost pump turbine bearing temperature data are shown in figure V-15. The temperature dropped 6^{o} F from lift-off through boost pump start and then increased to 338^{o} F by main engine cutoff at an average rate of 0.56 degree per second, which was normal.

Centaur Hydrogen Peroxide Attitude Control Engines

System description. - Attitude control of the Centaur vehicle during the coast phase after main engine cutoff and during the Centaur reorientation and retromaneuver was provided by a combination of fixed-axis constant-thrust hydrogen peroxide engines. The system is shown in figure V-16. Propellants were fed to the engines from a positive expulsion, bladder type storage bottle which was pressurized to about 300 psia by the pneumatics system. Firing commands to the engines were given by the Centaur autopilot in response to guidance steering information.

On AC-10 the attitude control system was composed of four engines with 50 pounds thrust each, and two clusters of three engines each. Each cluster contained one 6-pound-thrust and two 3.5-pound-thrust engines. These engines were used for attitude control and vehicle reorientation after main engine cutoff and spacecraft separation. The 50-pound engines provided thrust midway through the Centaur reorientation to provide lateral as well as increased axial separation distance from the spacecraft. These engines were also called upon by control logic if attitude errors exceeded the control capability of the cluster engines.

Engine performance. - All engine systems operated satisfactorily throughout the flight. Engine chamber temperature data were all normal, and there was no indication of propellant leakage. The hydrogen peroxide consumption for the attitude control system was computed to be 17.5 pounds from ground-test flow rates and actual engine firing times. With 49.4 pounds of hydrogen peroxide used by the boost pump turbines, 66.9 pounds of propellants were consumed during the flight. At lift-off, 132 pounds of propellants were tanked.

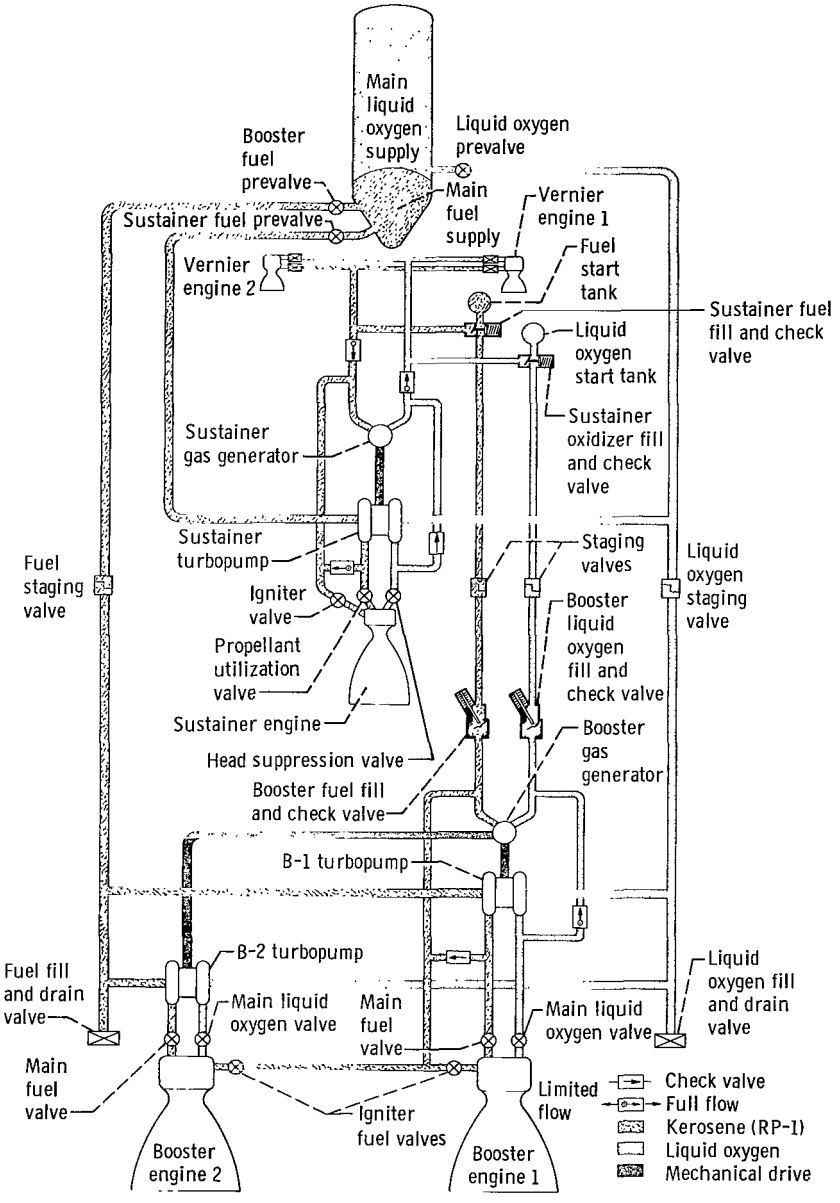

CD-8104

Figure V-1. - Atlas propulsion system schematic drawing, AC-10.

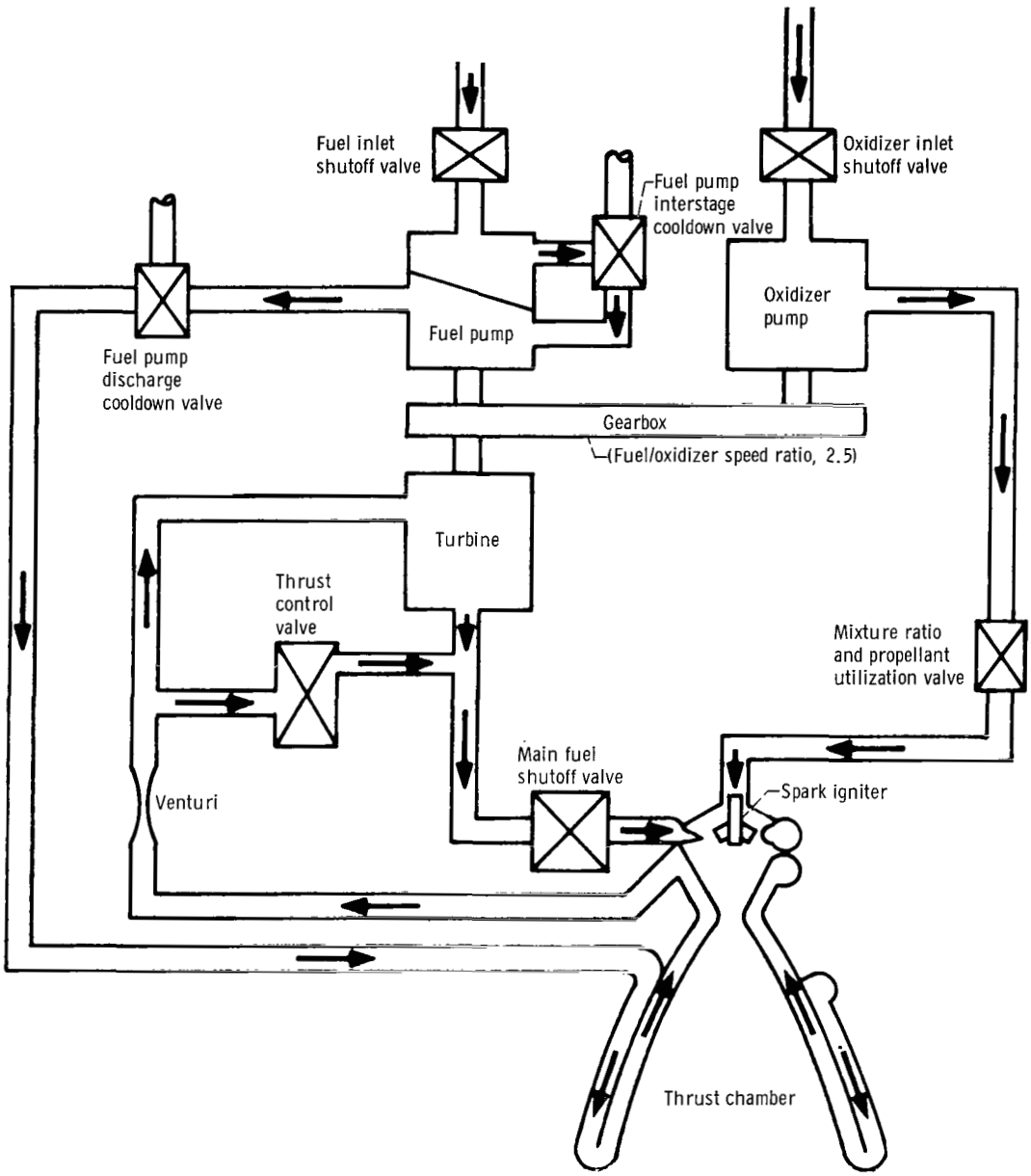

Figure V-2. - Centaur engine system schematic drawing, AC-10.

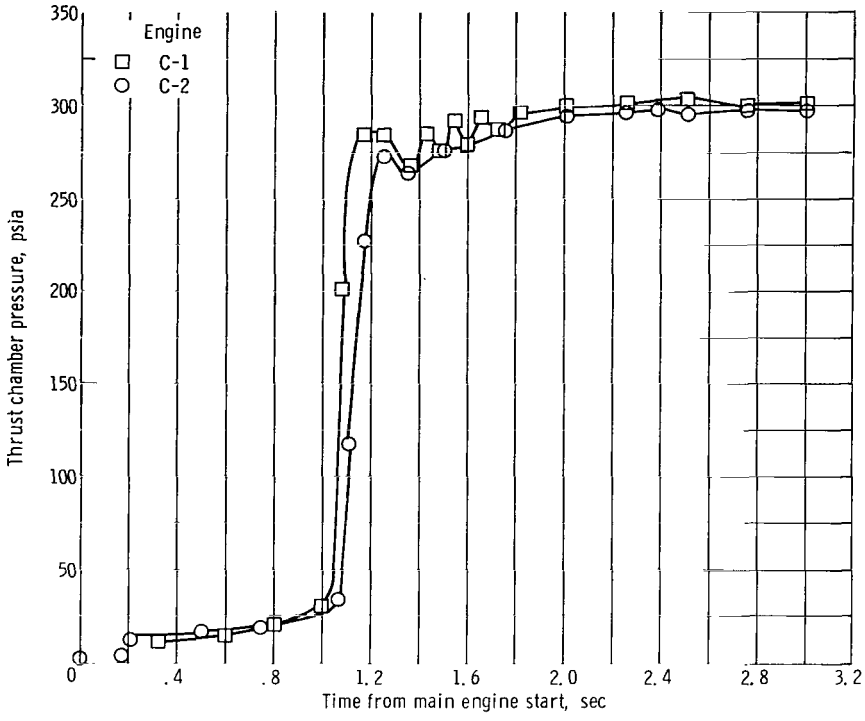

Figure V-3. - Centaur engine chamber pressure start transient, AC-10.

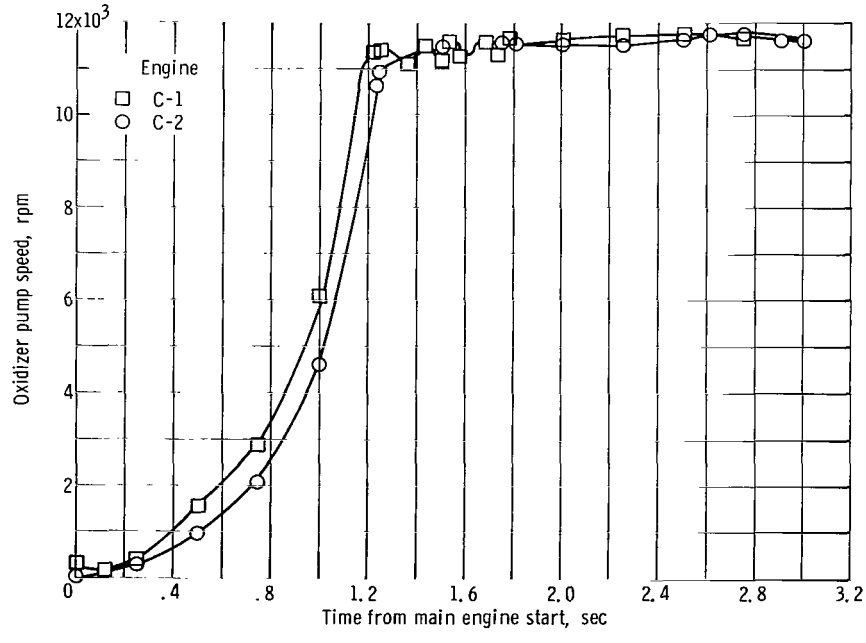

Figure V-4. - Centaur engine oxidizer pump speed start transient, AC-10.

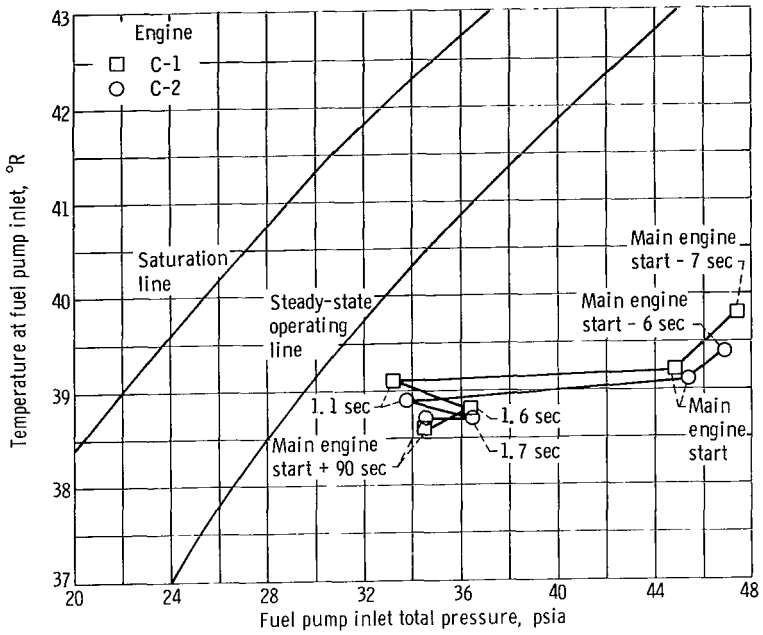

Figure V-5. - Centaur fuel pump inlet conditions, AC-10.

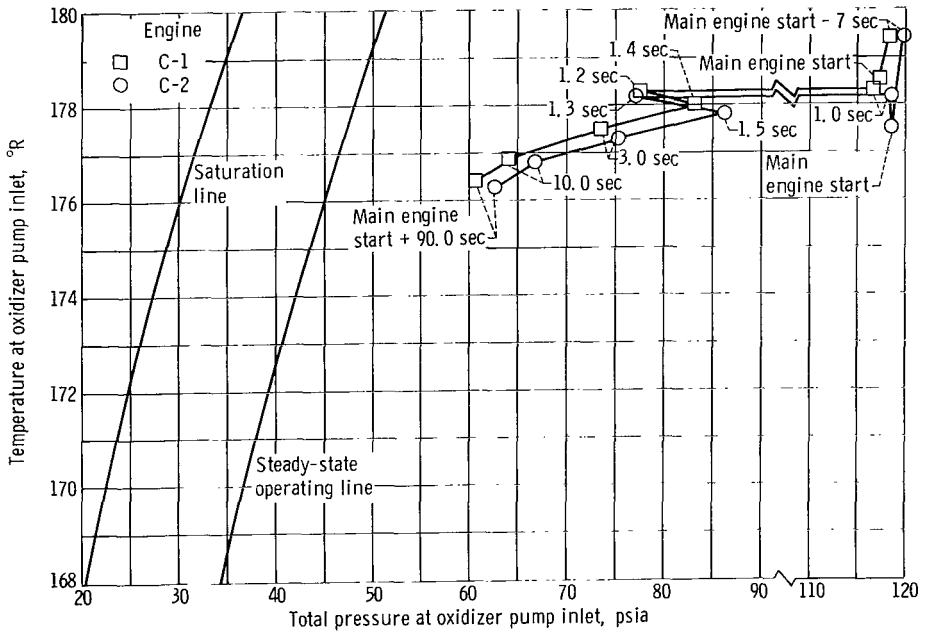

Figure V-6. - Centaur oxidizer pump inlet conditions, AC-10.

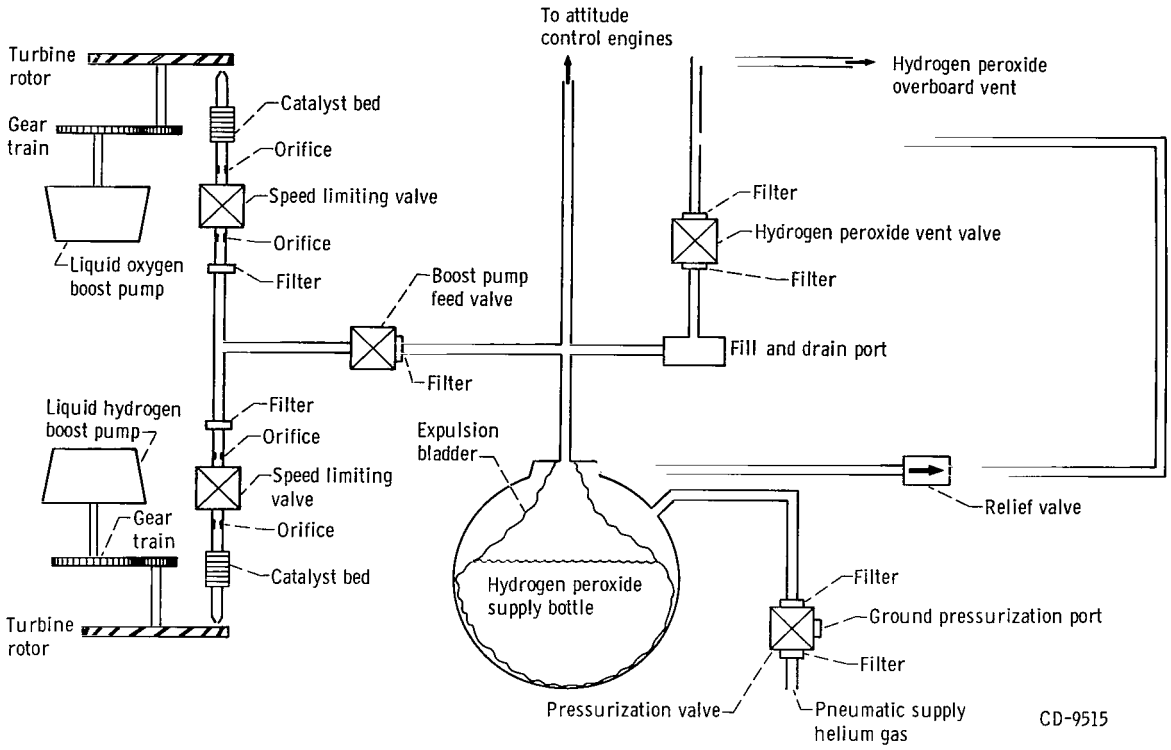

Figure V-7. - Schematic drawing of Centaur boost pump hydrogen peroxide supply, AC-10.

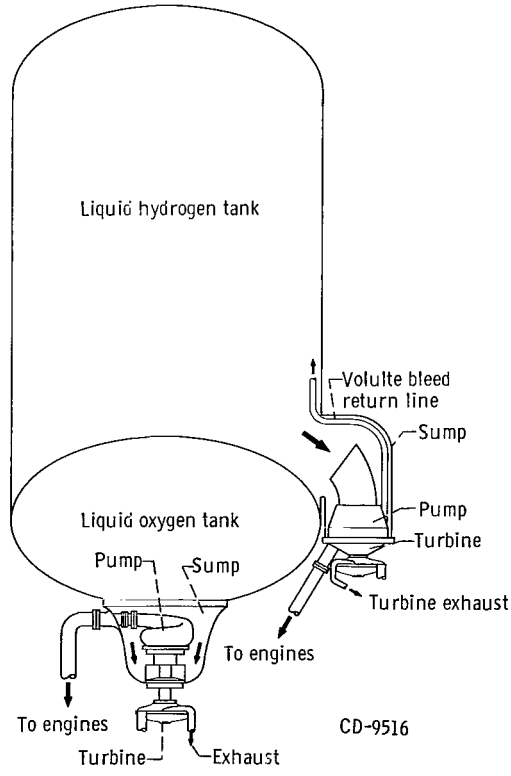

Figure V-8. - Centaur tank-mounted boost pumps, AC-10.

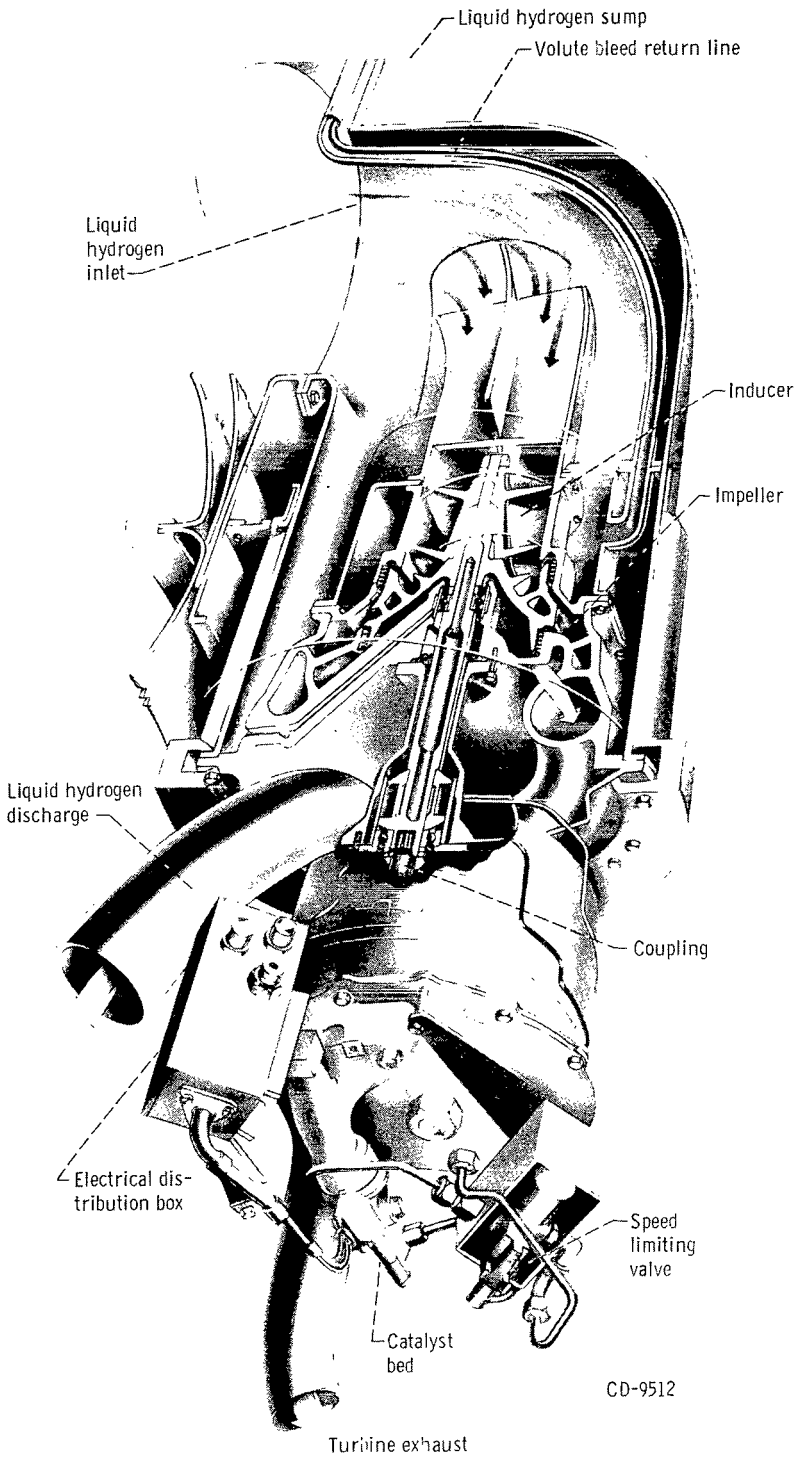

Figure V-9. - Centaur liquid hydrogen boost pump and turbine cutaway, AC-10.

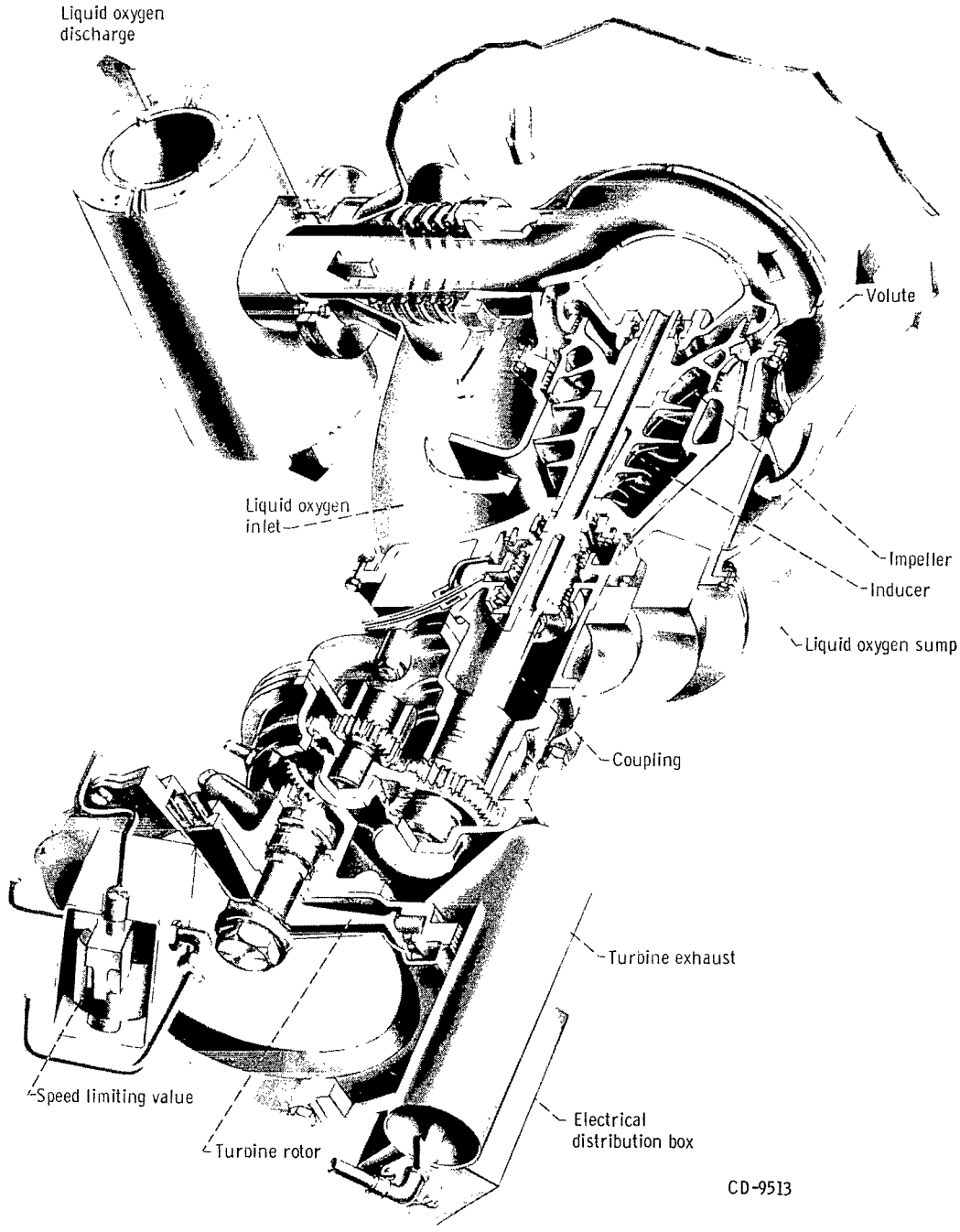

Figure V-10. - Centaur liquid oxygen boost pump and turbine cutaway, AC-10.

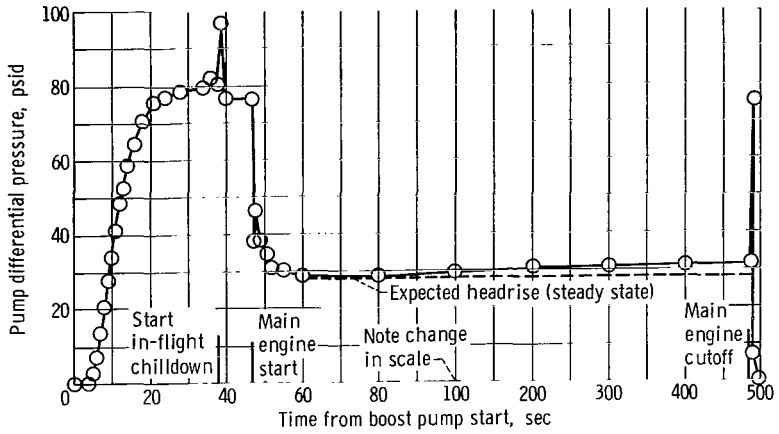

Figure V-11. - Centaur oxidizer boost pump headrise, AC-10.

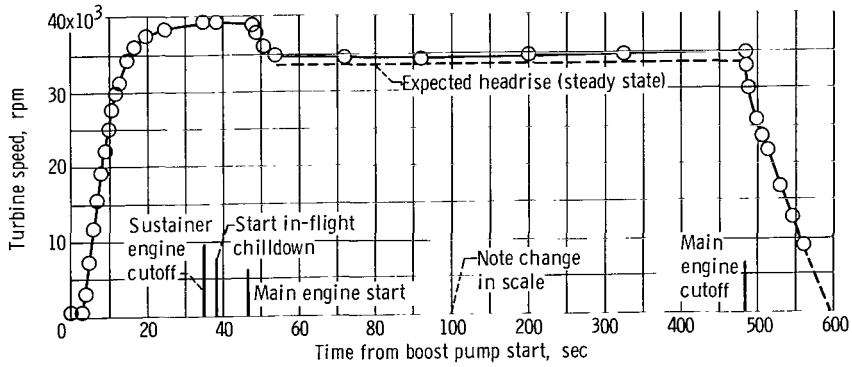

Figure V-12. - Centaur oxidizer boost pump turbine speed, AC-10.

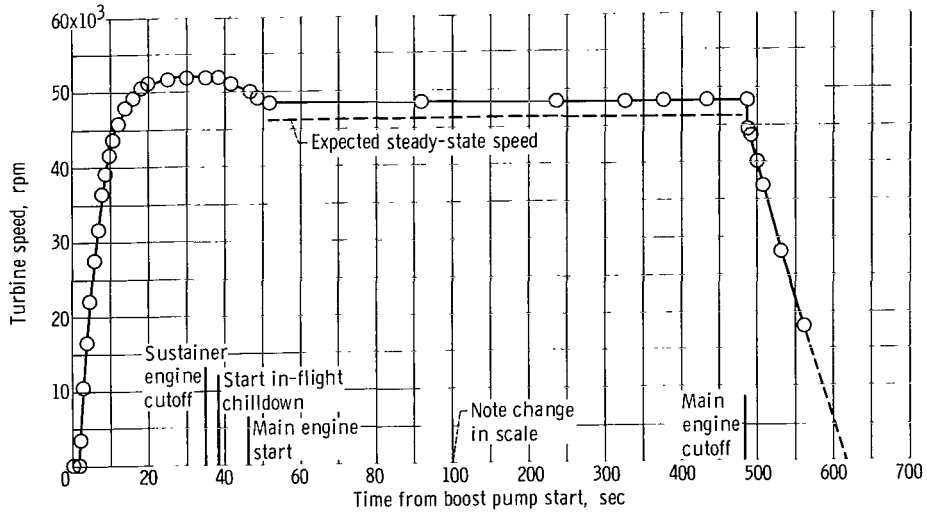

Figure V-13. - Centaur fuel boost pump turbine speed, AC-10.

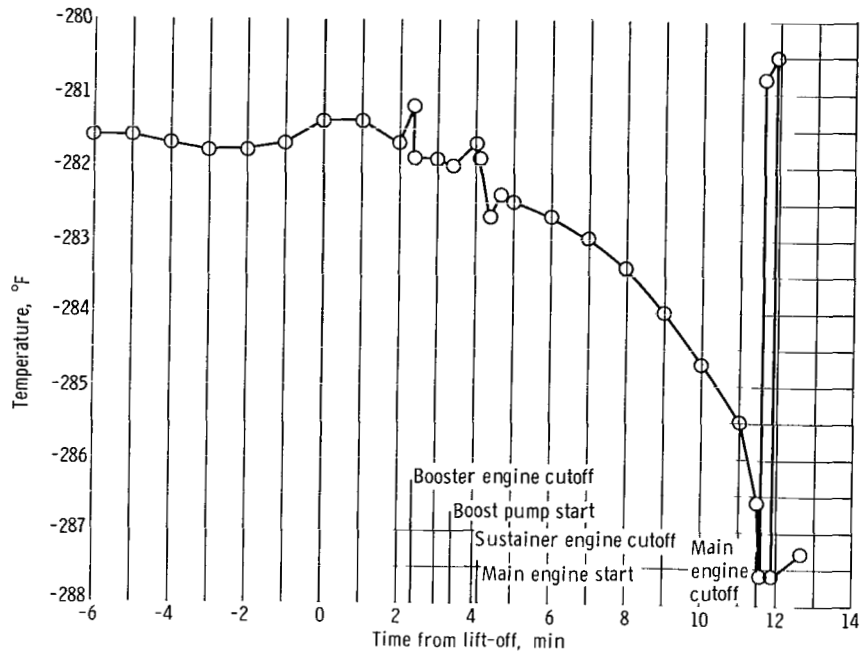

Figure V-14. - Oxidizer temperature at Centaur boost pump inlet, AC-10.

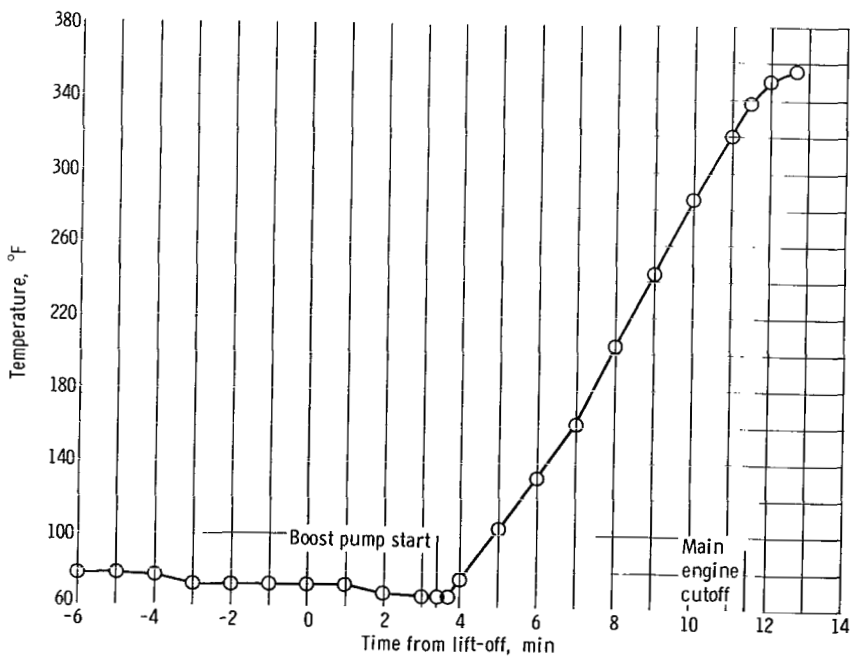

Figure V-15. - Centaur fuel boost pump turbine bearing temperature, AC-10.

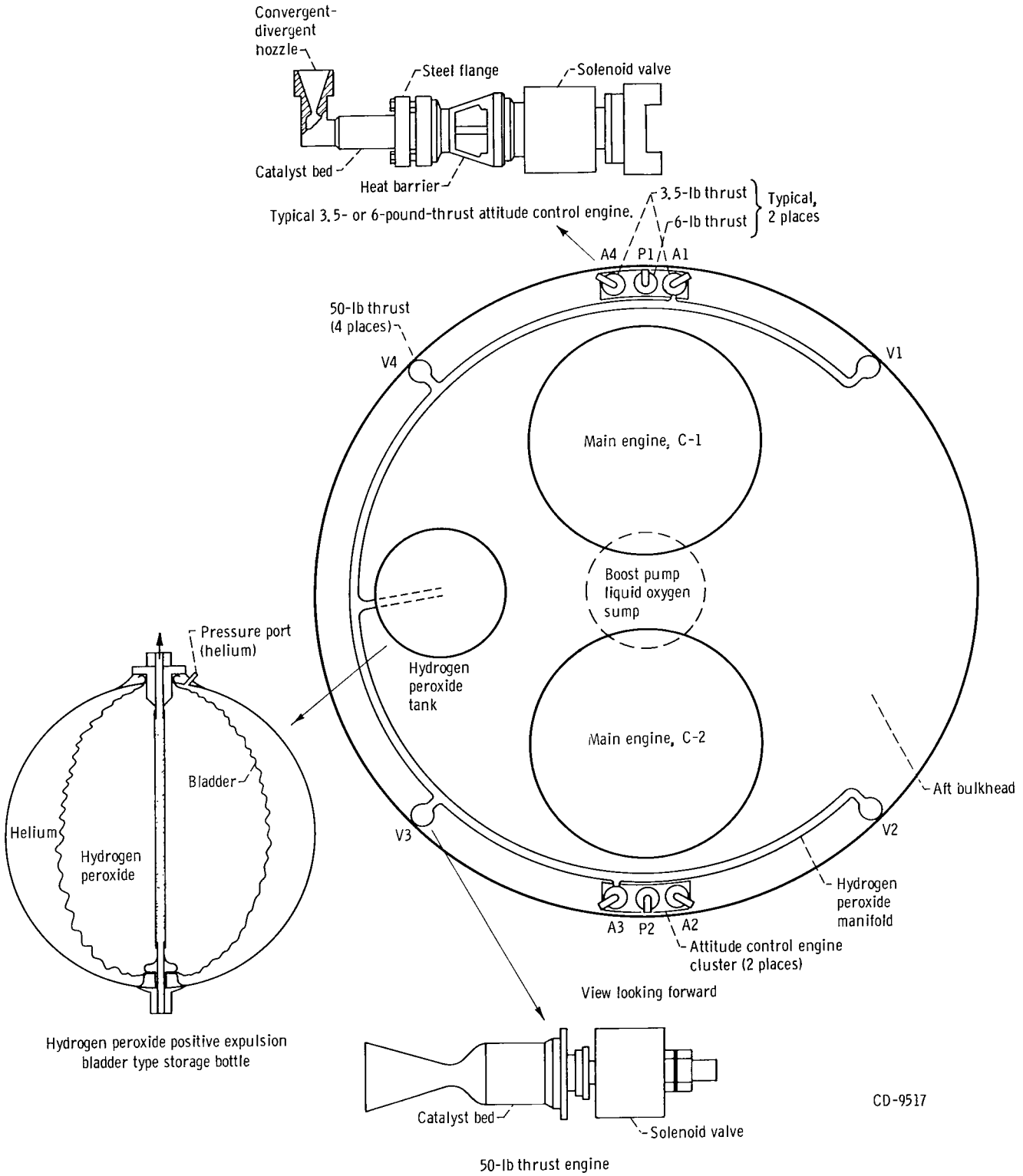

Figure V-16. - Centaur hydrogen peroxide engine system, AC-10.

PROPELLANT LOADING AND PROPELLANT UTILIZATION

by Steven V. Szabo, Jr.

Level Indicating System for Propellant Loading

System description. - Atlas propellant levels in the tanks before flight were determined by using liquid level sensors located at discrete points in the fuel (RP-1) and liquid oxygen tanks, as shown in figure V-17. The sensors located in the fuel tank were vibrating piezoelectric crystals. The sensors in the liquid oxygen tank were the platinum hot-wire type.

The associated control circuitry for the fuel level sensors was an oscillator circuit using the resonant characteristics of the piezoelectric crystal to maintain oscillations. When the sensor was immersed in liquid, the vibratory oscillations of the crystal were damped causing the control circuit to stop oscillating. This cessation of oscillations caused a control relay to deenergize and provide a signal to the propellant loading operator.

The control unit for the platinum hot-wire liquid oxygen sensors was an amplifier that detected a change in voltage level (similar to a Schmidt trigger circuit). The liquid oxygen sensors were supplied with a near constant current source (approximately 200 mA). The voltage drop across a sensor reflected the resistance value of the sensor. The sensing element was a 1-mil platinum wire which had a linear resistance temperature coefficient. When dry or warm, the wire had a high resistance and therefore a high voltage drop; when it was cold, as immersed in a cryogenic, the wire had a low resistance and a low voltage drop. When the sensor was wetted, a control relay was deenergized, and a signal was transmitted to the propellant loading operator.

The Centaur propellant level indicating system is shown in figure V-18. It utilized hot-wire level sensors in both the liquid oxygen and liquid hydrogen tanks. The sensors were similar in operation to the ones used in the Atlas liquid oxygen tank.

Propellant weights. - Atlas fuel (RP-1) was 76 951 pounds at lift-off at a density of 49.75 pounds per cubic foot. Atlas liquid oxygen at lift-off was 173 426 pounds at a density of 69.27 pounds per cubic foot.

Centaur propellant loading was satisfactorily accomplished with 5277 pounds of liquid hydrogen and 25 520 pounds of liquid oxygen on board at lift-off. Data used to determine propellant weights at lift-off are given in table V-V.

TABLE V-V. - CENTAUR PROPELLANT LOADING DATA, AC-10

Quantity or event	Propellant	
	Hydrogen	Oxygen
Sensor required to be wet at T - 90 sec, percent	99.8	100.2
Sensor station, in.	174.99	373.16
Volume at sensor[a], cu ft	1256.69	370.94
Ullage volume at sensor, cu ft	11.22	6.58
Liquid hydrogen 99.8 percent sensor dry, sec	T - 71	------
Liquid oxygen 100.2 percent sensor dry, sec	-------	Wet at T - 0
Ullage pressure, psia	20.5	30.3
Propellant density[b], lb/cu ft	4.215	68.8
Weight in tank at time sensor goes dry, lb	5297	Sensor wet at lift-off
Liquid hydrogen boiloff to vent valve lock, lb	20	------
Ullage volume at lift-off, lb/cu ft	15.8	6.58
Weight at lift-off, lb	5277	25 520

[a]Volumes include 1.85 cu ft liquid oxygen and 2.53 cu ft liquid hydrogen for lines from boost pumps to turbopump inlet valves.

[b]Densities are taken from vapor pressure against density curves for effective density of boiling hydrogen and oxygen.

Atlas Propellant Utilization System

System description. - The Atlas propellant utilization system (fig. V-19) was used to ensure near simultaneous propellant depletion and minimum residuals at sustainer engine cutoff. This was accomplished by controlling propellant mixture ratio (ratio of oxidizer flow rate to fuel flow rate) to the sustainer engine. The system consisted of two mercury manometer assemblies which sensed fuel and oxidizer head pressures, a computer-comparator package, a hydraulically actuated propellant utilization (fuel) valve, sensing lines, and associated electrical harnessing. During flight, the manometers sensed propellant head pressures which were indicative of propellant mass. The mass ratio was then compared with a reference ratio in the computer-comparator, and if needed, a correction signal was sent to the valve controlling the main fuel flow to the sustainer engine. The oxidizer flow was regulated by the head suppression valve. This valve sensed propellant utilization valve movement and moved in a direction opposite to that of the propellant utilization valve. The head suppression valve thus varied propellant mixture ratio, but maintained a constant total propellant mass flow to the sustainer engine.

System performance. - The Atlas propellant utilization system performance during the AC-10 flight was satisfactory. The propellant flow rates were controlled to a nearly simultaneous depletion of usable propellants. The fuel valve responded properly to the

system error signal given by the error demodulator output, as shown in figure V-20. During sustainer flight, the system was controlled to a full oxygen-rich position to reduce residuals. This caused a characteristic liquid oxygen depletion mode, as shown in figure V-21. Sustainer liquid oxygen pump inlet pressure began to decay approximately 6 seconds prior to sustainer engine cutoff. The engine cutoff signal was given by the pressure switches on the sustainer fuel injector manifold. Approximately 0.2 second after the engine cutoff signal, the fuel depletion sensors indicated dry, corroborating the nearly simultaneous propellant depletion.

Propellant residuals. - The nearly simultaneous depletion of usable propellants resulted in residuals of 369 pounds of liquid oxygen and 137 pounds of fuel. These values are based on densities of 68.6 pounds per cubic foot for liquid oxygen and 50 pounds per cubic foot of fuel at this time in flight. The liquid oxygen residual was calculated by using the propellant utilization head sensing port uncovery (see fig. V-19) as a reference. The fuel residual represents the amount between the fuel depletion sensors and the sustainer engine pump inlet.

Centaur Propellant Utilization System

System description. - The Centaur propellant utilization system was used during flight to optimize propellant consumption for minimum residuals. The system is shown schematically in figure V-22. It was also used during tanking to indicate propellant levels. In flight, the mass of propellant remaining in each tank was sensed by a capacitance probe and compared in a bridge circuit. If the mass ratio of propellants remaining in the tanks varied from a predetermined value (oxidizer to fuel ratio, 5.0), an error signal was sent to the proportional servopositioner which controlled the liquid oxygen flow control valve. If the mass ratio in the tank was greater than 5.0, the liquid oxygen flow was increased to return the ratio to 5.0. If the ratio in the tank was less than 5.0, the liquid oxygen flow was decreased. Since the sensing probes did not extend to the top of the tank, system control was not effected until approximately 90 seconds after main engine start. For this 90 seconds of engine burn, the liquid oxygen flow control valves were nulled (locked at a propellant mixture ratio of 5.0).

System performance. - Prelaunch checks and calibrations of the system were within specifications. The in-flight operation of the propellant utilization system was satisfactory. The system liquid oxygen valve positions during flight are shown in figure V-23. The valves were unnulled by the programmer at approximately main engine start + 90 seconds. Probe uncovery (liquid levels passing the top of the probe) occurred as expected also at approximately main engine start + 90 seconds. The valves were placed in a null position by the programmer at approximately 30 seconds prior to engine

cutoff. This nulling was done because the probes do not extend to the bottom of the tank.

System accuracy. - The Centaur propellant utilization system controlled propellant consumption so that the burnable residual propellants were within 12 pounds of hydrogen of a mixture ratio of 5.0 at engine cutoff. This error accounts for the system bias which was used to ensure that liquid oxygen would deplete first.

Propellant residuals. - The propellant residuals remaining at engine cutoff were calculated with end sensing times as reference points. The residuals were as follows:

Oxygen:

Total residual weight, lb	199±20
Burnable, lb	131±13
Available burn time, sec	2.3

Hydrogen:

Total residual weight, lb	130±13
Burnable, lb	58±6
Available burn time, sec	5.2

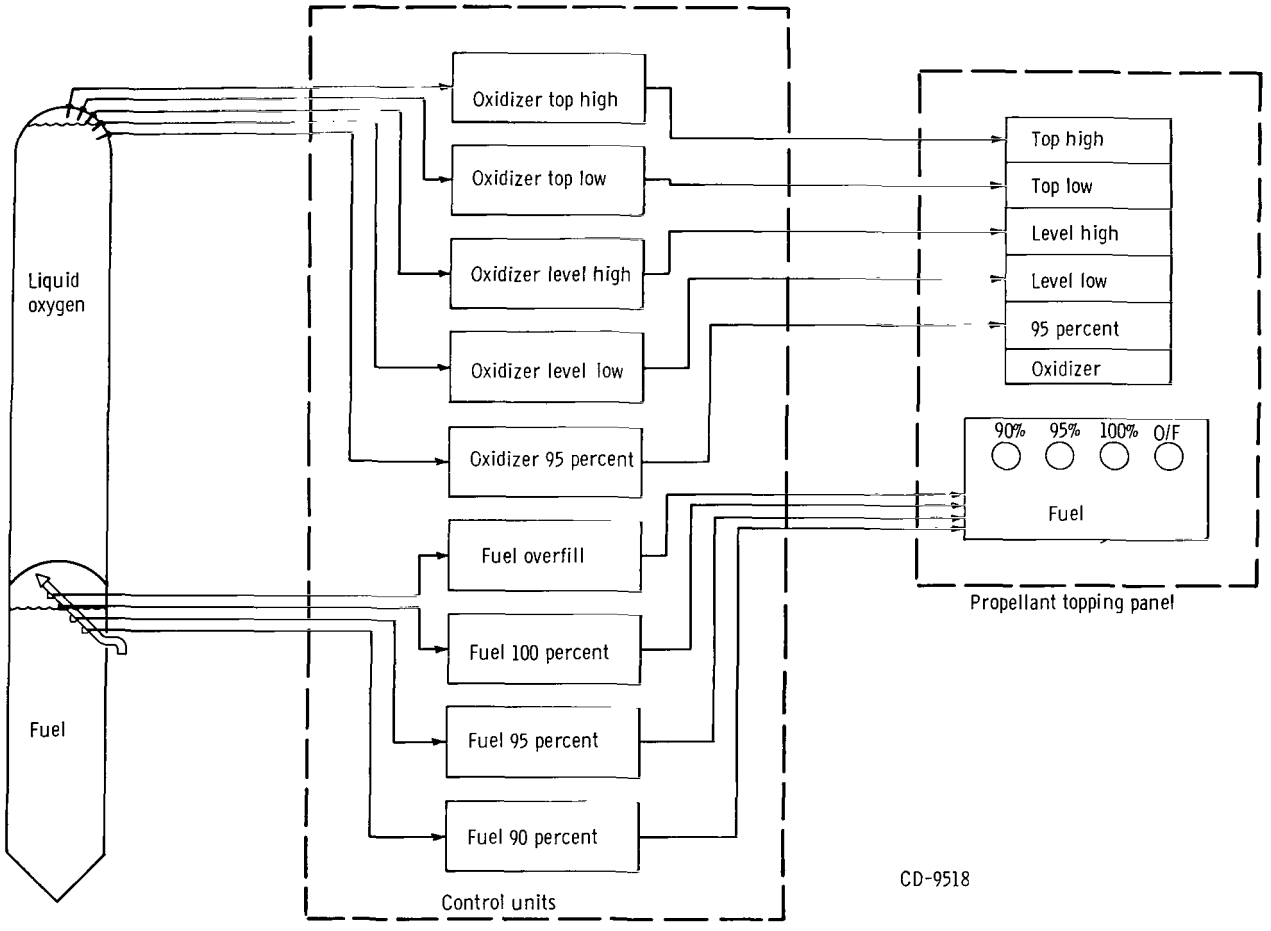

Figure V-17. - Level indicating system for Atlas propellant loading, AC-10. (Percent levels are indications of required flight levels and not percent of total tank volume.)

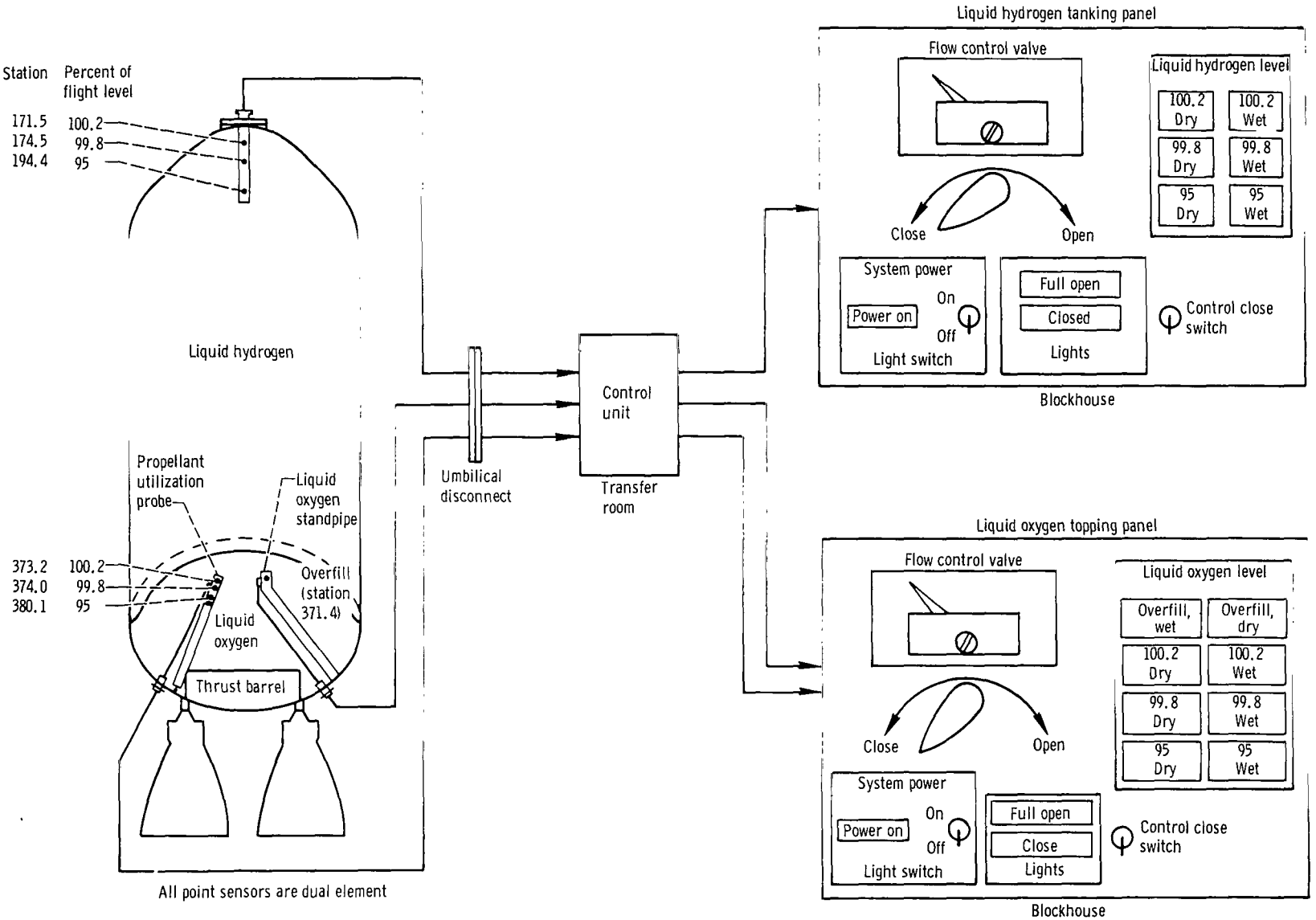

Figure V-18. - Level indicating system for Centaur propellant loading, AC-10. (All point sensors are dual element. Percent levels are indications of required flight levels and not percent of total tank volume.)

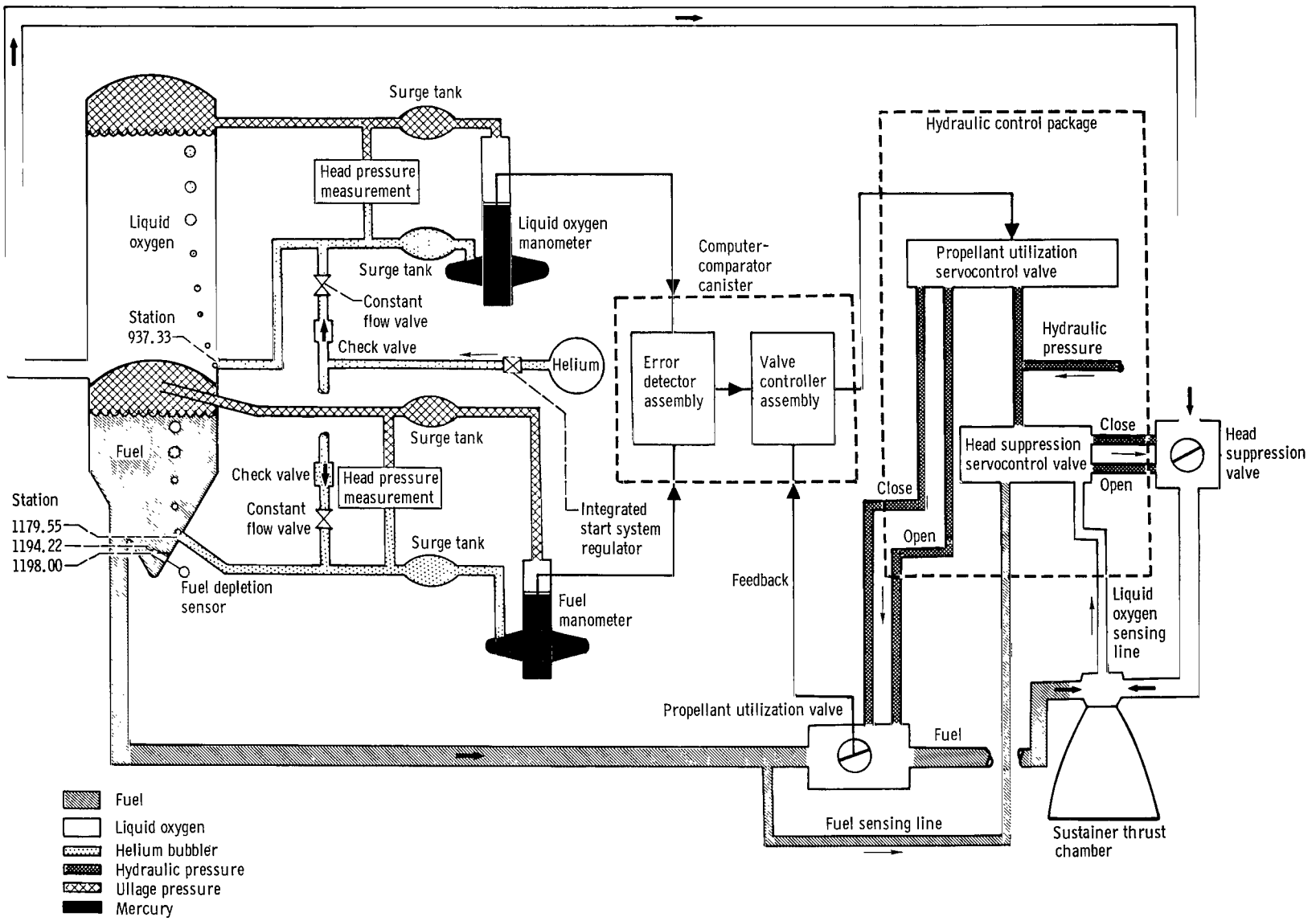

Figure V-19. - Atlas propellant utilization system, AC-10.

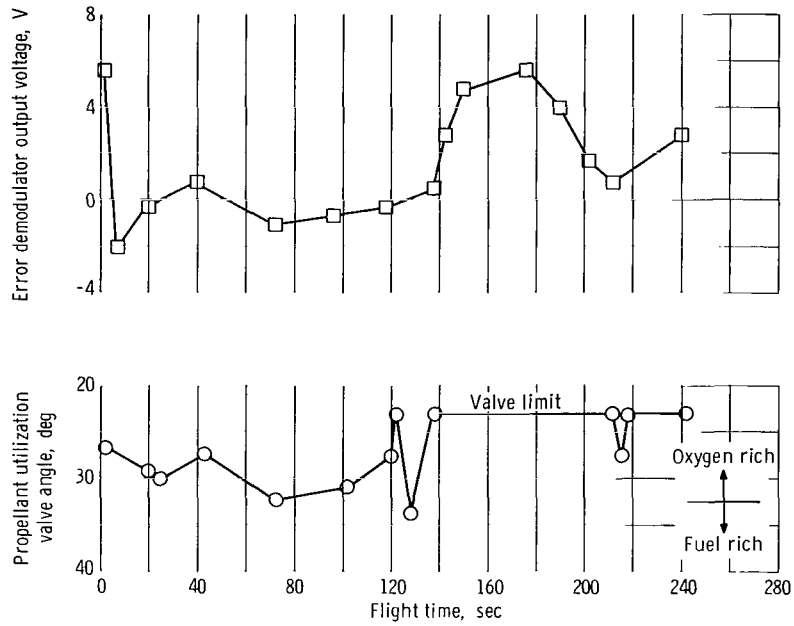

Figure V-20. - Atlas propellant utilization valve angle and error demodulator output, AC-10.

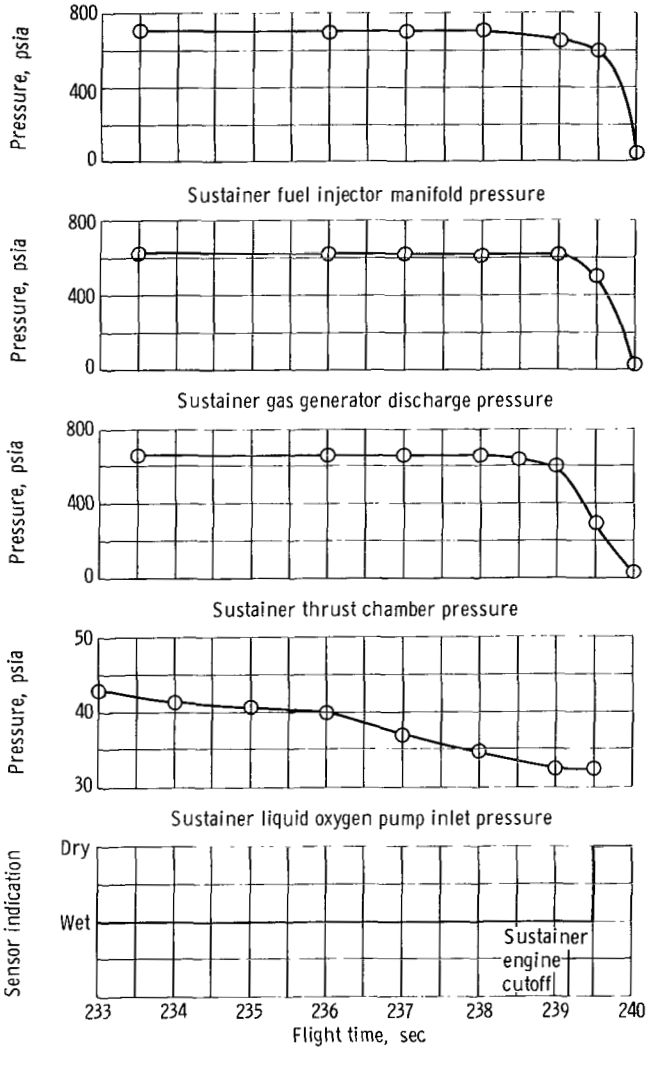

Figure V-21. - Sustainer engine system data at engine cutoff, AC-10.

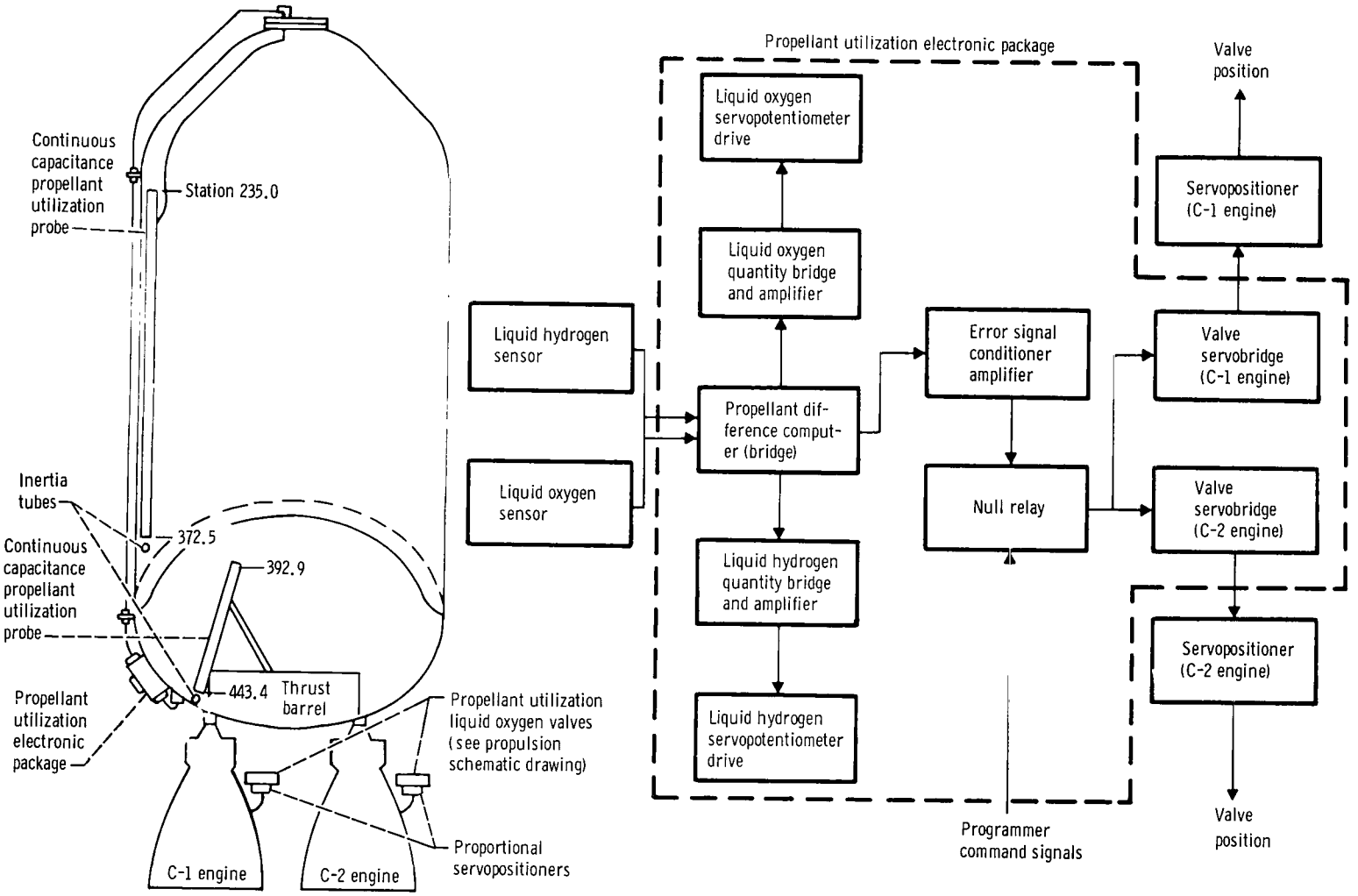

Figure V-22. - Centaur propellant utilization system, AC-10.

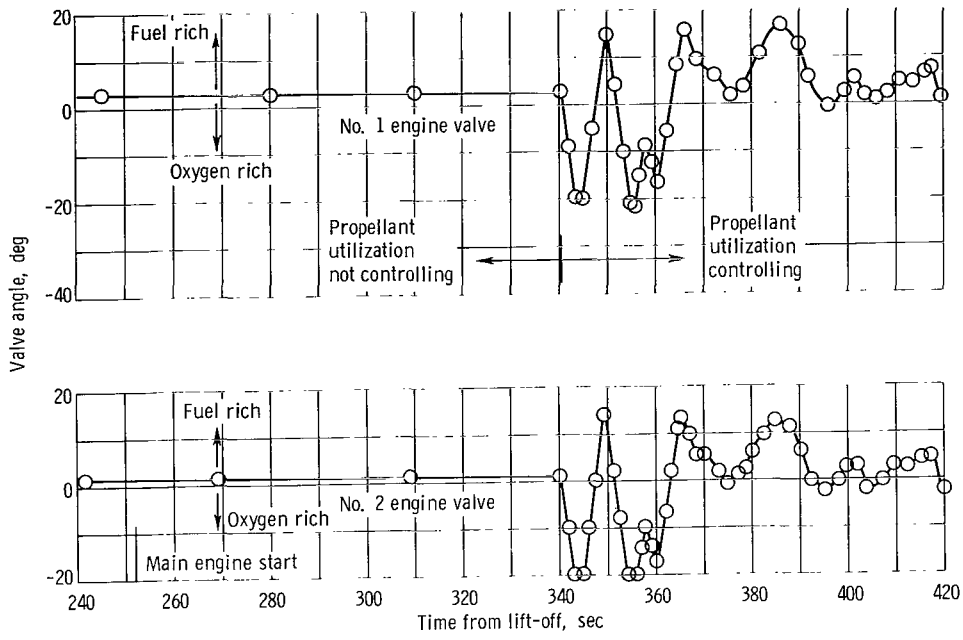

(a) Time, 240 to 420 seconds.

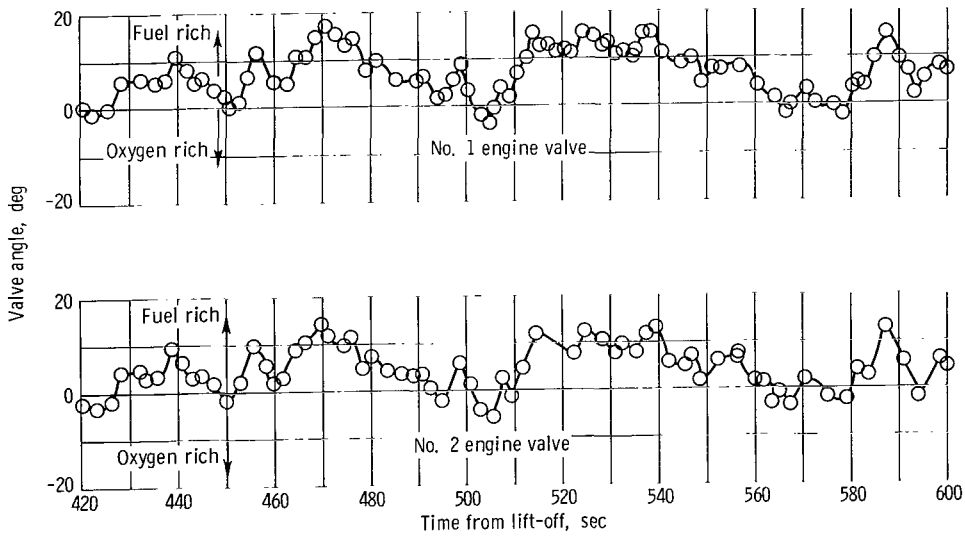

(b) Time, 420 to 600 seconds.

Figure V-23. - Propellant utilization valve angles, AC-10.

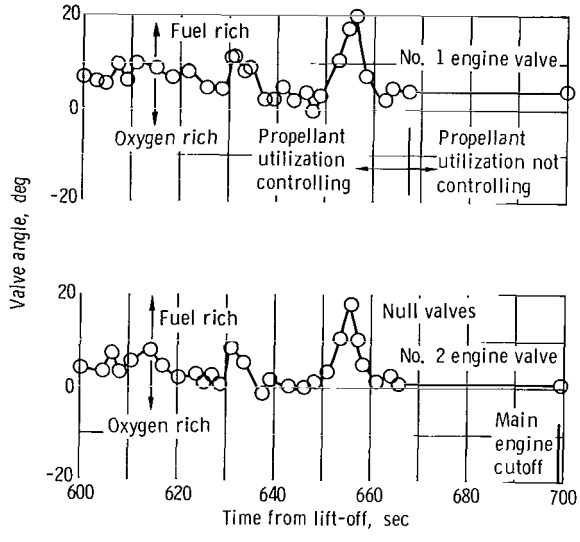

(c) Time, 600 to 700 seconds.

Figure V-23. - Concluded.

PNEUMATIC SYSTEMS

by William A. Groesbeck and Merle L. Jones

Atlas

System description. - The Atlas pneumatic system, shown in figure V-24, supplied helium at regulated pressures for several pressurization and control functions. The propellant tanks were pressurized to provide sufficient pressure to prevent propellant pump cavitation and to maintain stability of the pressure supported tank structure. Pressurized helium was bled off the fuel tank pressurization duct to pressurize the hydraulic reservoirs and turbopump lubrication tanks. Helium was supplied to these systems from six bottles mounted in the jettisonable booster section. Prior to launch, the bottles were chilled with liquid nitrogen to increase the stored mass of helium. The cold gas was heated and expanded by a heat exchanger in the booster engine turbine exhaust duct before being supplied to the tank pressure regulators.

A separate system provided pressurized helium to pneumatic regulators in the booster and sustainer engine control systems. Helium for this purpose was supplied from a bottle mounted in the sustainer section. Helium for actuation of the ten staging latches was supplied from a storage bottle mounted in the jettisonable booster section.

Propellant tank pressurization. - Control of propellant tank pressures was switched from ground to airborne systems at T - 60 seconds. At this time the liquid oxygen boiloff valve was locked closed, and the airborne pressure regulator began controlling tank pressure. Pressures were held within requirements. At lift-off the oxygen tank pressure was 24.2 psig, and the fuel tank pressure was 60.0 psig.

Ullage pressure history, shown in figure V-25, indicated that tank pressures were maintained satisfactorily during flight. The fuel tank pressure was stable at about 60.0 psig until termination of pneumatic control at booster staging. From about T - 2 minutes to T + 20 seconds, the liquid oxygen pneumatic regulator was biased by a slight helium bleed flow into the ullage pressure sensing line. This bias caused the regulator to control oxygen tank pressure at a lower level than the regulator setting. Reducing the oxidizer tank pressure caused an increase in the differential pressure across the intermediate bulkhead. The increased differential pressure ensured against bulkhead reversal due to launch transient loads and an initially large liquid oxygen head pressure. At T + 20 seconds, when the launch transient loads had passed and the liquid oxygen head pressure was less, the bias was removed and the regulator increased tank pressure to within the normal control range of 28.5 to 31.0 psig. This pressure provided sufficient vehicle structural stiffness to withstand bending loads during ascent.

Liquid oxygen tank pressure increased above the regulator control band at T + 70 seconds due to normal gas boiloff. At T + 109 seconds and a pressure of 33.1 psig, the

system relief valve opened and slowly bled tank pressure down to 31.3 psig at booster engine cutoff. Immediately after booster engine cutoff, the ullage pressure rose abruptly because of a reduction in liquid oxygen consumption rate, and also an increased boiloff rate resulting from a decrease in hydrostatic head caused by a reduction in vehicle acceleration.

The total helium usage for tank pressurization during the boost phase was 74.4 pounds. At lift-off, 159.8 pounds of cold helium were tanked. A summary of tank pressurization data is given in table V-VI.

Engine control regulators. - The booster and sustainer pneumatic regulators provided the required helium pressures for engine control throughout the flight. Performance values are shown in table V-VI.

TABLE V-VI. - ATLAS PNEUMATIC SYSTEM DATA, AC-10

Parameter	Time, sec				
	T - 10	Specification T - 0	Actual T - 0	Booster engine cutoff T - 142.04	Sustainer engine cutoff T - 239.38
Oxygen tank ullage pressure, psig	26.1	23.3 to 28.5	24.3	31.1	32.1
Fuel tank ullage pressure, psig	59.5	57.8 to 61.5	58.3	58.2	48.0
Intermediate bulkhead differential pressure, psid	17.2	----------	12.5	16.1	14.9
Booster controls pneumatic regulator outlet, psig	746	715 to 785	746	740	---
Sustainer controls pneumatic regulator outlet, psig	590	565 to 635	600	593	593
Controls bottle pressure, psig	3330	2900 to 3400	3220	2875	2775
Booster bottles pressure, psig	3345	3100 to 3400	3210	985	----
Booster bottles temperature, ^{o}F	-316	-309 (max)	-317	-365	----
Staging bottle pressure, psig	3354	2900 to 3400	3354	----	----

Centaur

System description. - The Centaur pneumatic system, as shown in figure V-26, was used to supply helium gas at regulated pressures for propellant tank pressurization, actuation of engine control valves, pressurization of hydrogen peroxide storage bottle, and purge systems.

Propellant tank pressure control was necessary to prevent rupture of the tank, to

maintain sufficient pressure at the boost pump inlets, and to provide stability of the pressure supported tank structure. Tank pressures were regulated by a dual vent valve configuration on the hydrogen tank and by a single vent valve on the oxygen tank. Two of these valves, one on each tank, were solenoid controlled and on programmer command could be positioned in either a locked closed or normal regulating mode. The second vent valve on the hydrogen tank, however, was able to regulate at all times but at a higher control range about 4 psi above the regulating range of the primary vent valve. The control range for this secondary valve was selected to guard against overpressure in the tank when the primary vent valve was locked closed. The primary vent valve was programmed locked closed to (1) allow tank pressure buildup for increased structural strength during the atmospheric ascent; (2) restrict hydrogen venting to nonhazardous times; (3) allow pressure pulsing of the propellant tanks, required during the near-zero-gravity conditions of stage separation, to prevent liquid boiling and boost pump cavitation; (4) sustain tank pressure during main engine firing; and (5) avoid vehicle disturbance as a result of venting during the interval from main engine cutoff through execution of spacecraft separation, Centaur turnaround, and propellant tank blowdown. The pressure pulsing of the propellant tanks was effected by a controlled injection of helium gas into the ullage.

Pneumatic pressure supplied by the engine controls regulator was used to actuate the propellant inlet valves and the engine cooldown valves during operation of the main engines. The engine controls regulator also supplied helium to a second regulator for pressurization of the bladder-type hydrogen peroxide storage bottle.

The purge system, as shown in figure V-27, was separate from the pressurization system. This system supplied helium gas until T - 9.7 seconds from a ground source for purging the cavity between the hydrogen tank and the insulation panels, the seal and cavity between the nose fairing and forward bulkhead insulation, the propellant feed lines and boost pumps, engine chilldown vent ducts and thrust chambers, and hydraulic power packages. Purging of the cavities under the nose fairing seal and under the insulation panels was vital to prevent cryopumping nitrogen or air which could freeze the jettisonable fairings to the tank. At T - 9.7 seconds, just prior to lift-off, the purge was transferred to an airborne bottle which blew down and extended the purge through the atmospheric ascent.

Propellant tank pressurization. - The flight pressure profiles for the hydrogen and oxygen tanks in support of the AC-10 flight are shown in figure V-28. There were no unusual incidents or anomalies noted throughout the flight. Pressure regulation was within specification and there was no evidence of leaking or malfunctioning vent valves. Overboard discharge of the propellant boiloff gases during boost flight phase was also accomplished without incident.

Tank pressures just prior to lift-off were stable at 30.3 psia in the oxygen tank and

20.5 psia in the hydrogen tank. At T + 7.1 seconds, the primary hydrogen vent valve was programmed to a closed, or nonventing mode and the tank pressure began increasing at an average rate of 5.62 psi per minute. Closing the primary vent valve just prior to lift-off was necessary to provide increased tank pressure buildup for minimum required structural strength during the atmospheric ascent, and to avoid possible fire hazards of hydrogen venting. A hydrogen plume from the vent early in flight, while the vehicle velocity was low, could wash back over the vehicle and possibly be exposed to some ignition source. Wind tunnel tests on Centaur hydrogen venting are reported in reference 3.

The first scheduled blowdown of the hydrogen tank occurred at T + 69.3 seconds as the primary vent valve was programmed back to the open or normal regulating mode. Prior to the blowdown, however, at T + 53.8 seconds, the tank pressure had reached the control range and was being regulated by the secondary vent valve. The secondary valve regulated the pressure between 26.2 and 25.5 psia. This range was well within the required specification of 24.8 to 26.8 psia. Following the blowdown, tank pressure was regulated by the primary vent valve at 21.3 psia. This valve was within the required control range of 19 to 21.5 psia.

The primary hydrogen vent valve was again locked closed at T + 142.04 seconds to prevent vented hydrogen gas from mixing with the residual gaseous oxygen which envelopes a large portion of the vehicle during booster engine staging. During this nonventing period, which lasted until T + 149.04 seconds, the hydrogen tank ullage pressure increased from 20.2 to 21.6 psia.

Oxygen tank pressures were controlled normally throughout the boost flight phase with the vent valve in the unlocked or normal regulating mode. The liquid oxygen was in a near-thermal-equilibrium state and venting was regular. During booster engine shutdown, a sudden perturbation in the ullage pressure was generated causing the pressure to rise from 30.3 to 32.2 psia. This pressure change resulted from the decrease in hydrostatic head, due to a sudden reduction in vehicle acceleration, causing an increase in the liquid oxygen boiloff.

The ascent heating of the Centaur propellants could also have resulted in boiling of the saturated liquids at Atlas sustainer thrust termination for stage separation. However, to prevent this boiling and avoid boost pump cavitation (boost pumps were started prior to sustainer engine cutoff), helium gas was injected into the propellant tanks to step up the pressure. This pressure pulsing of the tanks, also called "burping", was controlled by metering helium flow through a 0.089-inch-diameter orifice in the line to the hydrogen tank, and a 0.043-inch-diameter orifice in the line to the oxygen tank.

The primary hydrogen vent valve was closed at sustainer engine cutoff, T + 239.4 seconds, and the tank pressure was pulsed for 1 second. This pressure pulse increased the ullage pressure from 19.9 to 20.6 psia.

Oxygen tank pressure pulsing, however, was more complex because of a small ullage volume, 11 cubic feet, and a much higher pressure pulse requirement. Reduction in hydrostatic pressure in the oxygen tank at sustainer thrust cutoff was more pronounced because of the greater density of the liquid oxygen. Consequently, a higher ullage pressure was necessary to hold pressure well above saturation during staging. To guard against overpressure in pulsing the small ullage, the pressure pulse was limited by a regulator which controlled between 38 and 40 psia. The oxygen tank vent valve was closed and pressure pulsing of the tank was enabled coincident with boost pump start at T + 203.7 seconds. Ullage pressure increased abruptly from 29.8 to 39.8 psia and was controlled well within the specified range of the regulator.

Ullage pressures in both propellant tanks decayed normally during main engine firing due to fuel consumption. At main engine cutoff, the ullage pressure in the hydrogen tank was down to 14.7 psia and to 23.8 psia in the oxygen tank. Shutdown transients at main engine cutoff were sufficient to geyser the liquid residuals upward throughout the tanks. This action was verified by the ullage temperature probe at the top of the hydrogen tank which sensed a liquid hydrogen temperature, as shown in figure V-29, a few seconds after main engine cutoff. Holding the propellants in the bottom of the tanks, following engine cutoff on this direct ascent mission, was not attempted or required. Actually, the mixing and splashing of the liquid residuals throughout the tank cools the ullage and favorably depresses the pressure rise rate. The average pressure rise rate after engine cutoff was 1.19 psi per minute in the hydrogen tank and 0.274 psi per minute in the oxygen tank.

Predicted and actual tank ullage pressure histories during the final Centaur retromaneuver are shown in figure V-30. The pressure rise prior to start of tank blowdown (residual propellants forced out through the engines to provide retrothrust) was normal. At the start of retrothrust, the oxygen tank pressure was 25.2 psia and the hydrogen tank pressure was 20.6 psia. Initially, the propellant discharge was liquid or two-phase flow, and the volume of this liquid-gas discharge had little effect on reducing tank pressure. However, 30 seconds later, the liquid hydrogen residuals were depleted as evidenced by the rapid decrease in tank pressure due to a pure gas flow. The liquid oxygen residuals, however, were not depleted until 80 seconds after start of blowdown. At T + 1246.9 seconds, the retrothrust maneuver was terminated, the engine propellant valves were closed, and both the oxygen and hydrogen solenoid controlled vent valves were commanded from the closed to the normal regulating mode. The ullage pressures at this time had decreased to 20.2 and 14.1 psia in the oxygen and hydrogen tanks, respectively. A summary of the pneumatic tank pressurization data is given in table V-VII.

Engine and hydrogen peroxide control regulators. - The engine and hydrogen peroxide bottle control regulators maintained required system pressures throughout the flight. The engine controls regulator provided helium to the engine valves at a steady pressure of 460 psia. The hydrogen peroxide regulator maintained a nearly constant bottle pres-

TABLE V-VII. - CENTAUR PNEUMATIC SYSTEM DATA, AC-10

Parameter	Time, sec						
	Specification T - 10	Actual T - 10	Booster engine cutoff T + 142	Main engine start T + 251.7	Main engine cutoff T + 689.2	Start retro-thrust T + 996.9	End retro-thrust T + 1247
Engine control regulator output, psia	455 to 490	468	464	460	460	460	460
Hydrogen peroxide bottle regulator output, psia	312 to 330	320	320	306	306	305	305
Helium bottle pressure, psia	2615 to 2965	2763	2760	2500	2400	2380	2380
Helium bottle temperature, ^{o}F	90 (max)	69	67	53	48	46	44
Helium supply (4650-cu in. bottle), lb	----------	4.78	----	4.47	----	----	4.35
Insulation panel purge differential pressure, psid	0.03 (min)	0.17	----	----	----	----	----
Hydrogen ullage pressure, psia	19.7 to 22.0	20.5	20.2	19.8	14.7	20.6	14.1
Oxidizer ullage pressure, psia	29.2 to 32.3	30.3	30.3	38.5	23.8	25.2	20.2

sure of 306 psia. These pressures were well within the required control range. A summary of the regulator pressure data for various flight times is given in table V-VII.

Pneumatic purges. - The pneumatic purge system was controlled by ground support equipment to provide the necessary component conditioning prior to launch. The required helium environment during the prelaunch was maintained for a purge rate of 110 pounds per hour. This purge rate provided an insulation panel differential pressure of 0.17 psid, which was well above the minimum allowable of 0.03 psid required for launch. The pneumatic purge was switched from the ground to airborne system at T + 9.7 seconds by enabling blowdown of the airborne helium purge bottle. The purge then continued until the helium supply was depleted, by which time the vehicle had cleared the atmosphere.

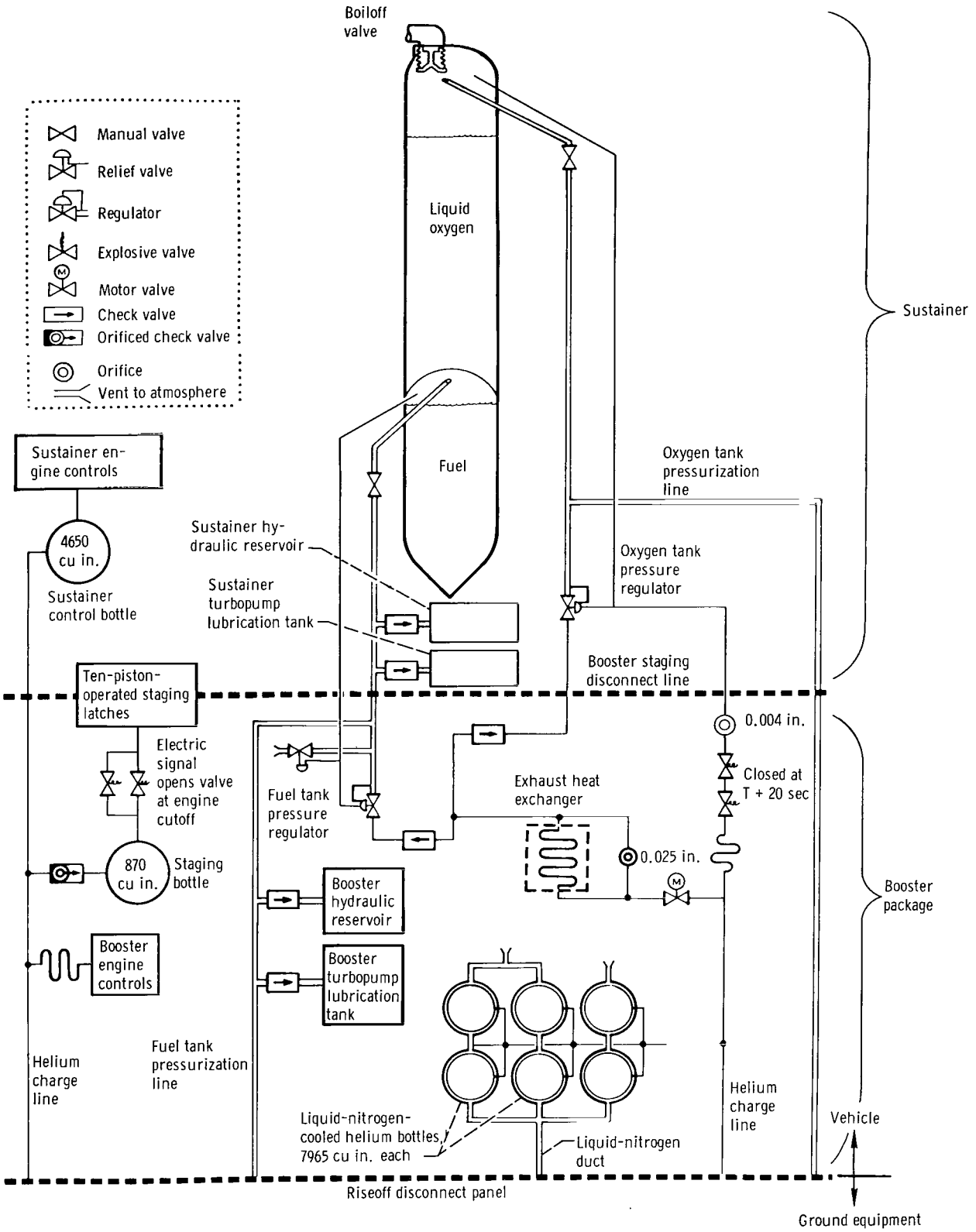

Figure V-24. - Atlas vehicle pneumatic system, AC-10.

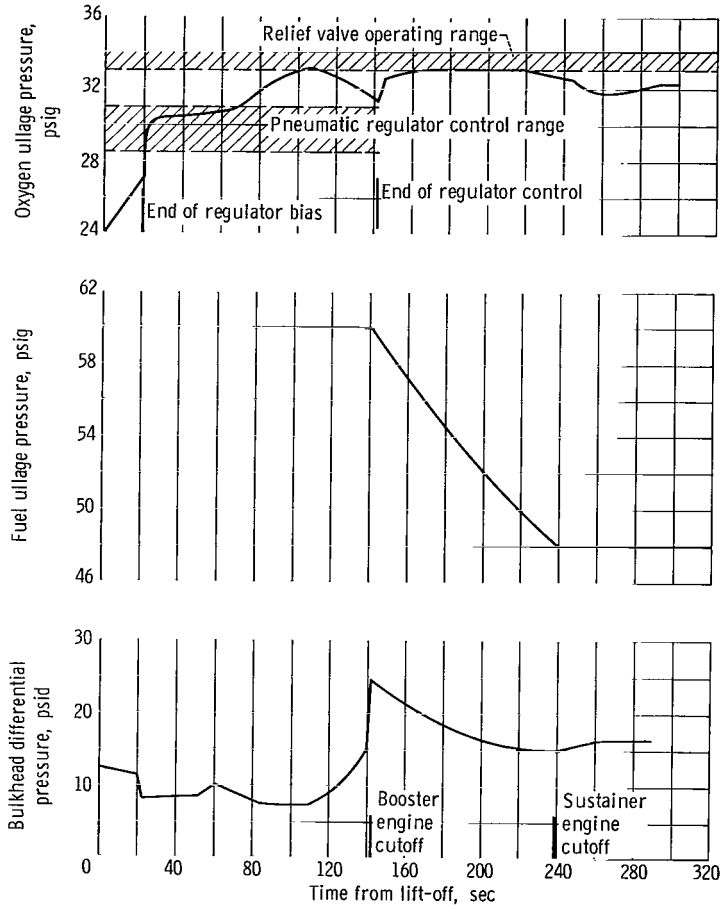

Figure V-25. - Atlas oxidizer and fuel tank ullage pressure, AC-10.

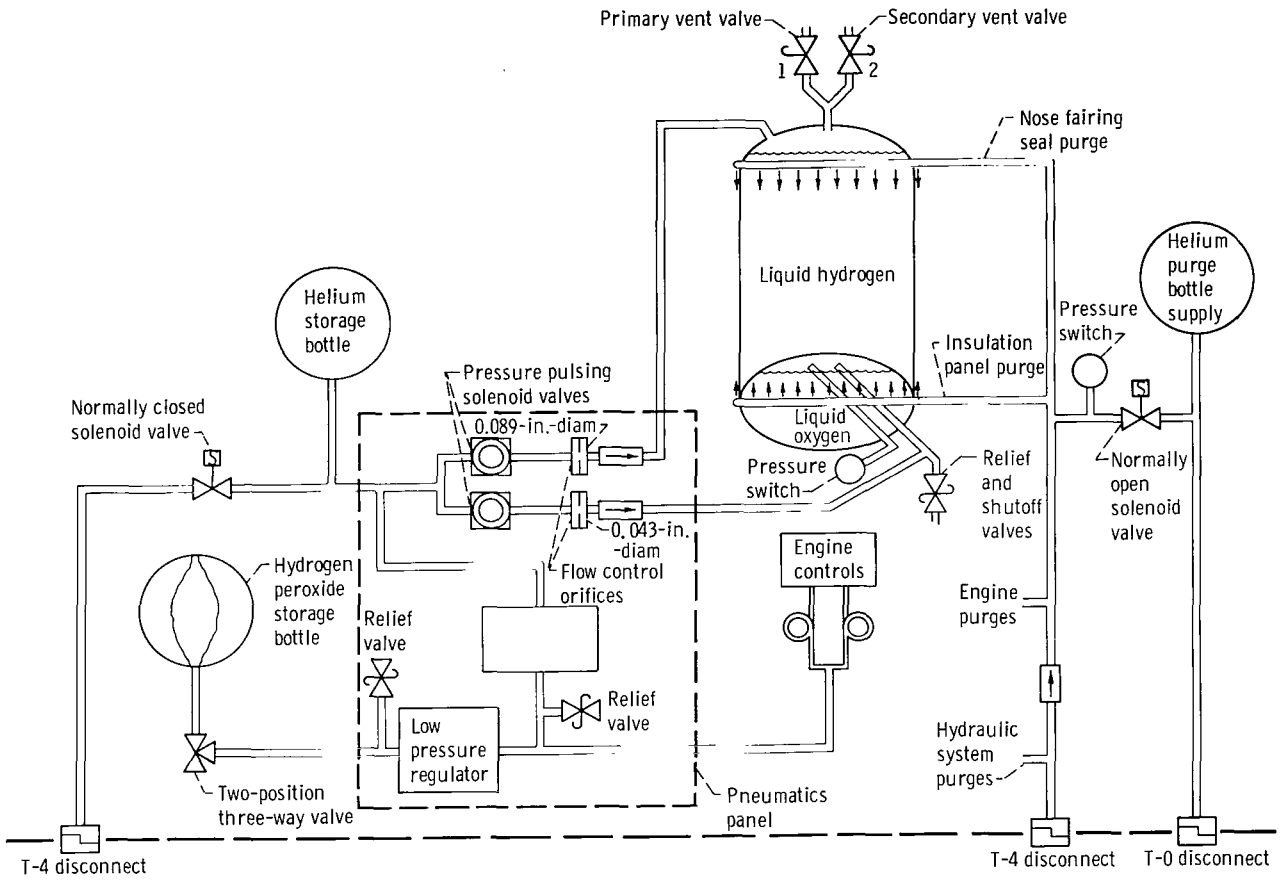

Figure V-26. - Centaur pneumatics system, AC-10. CD-9519

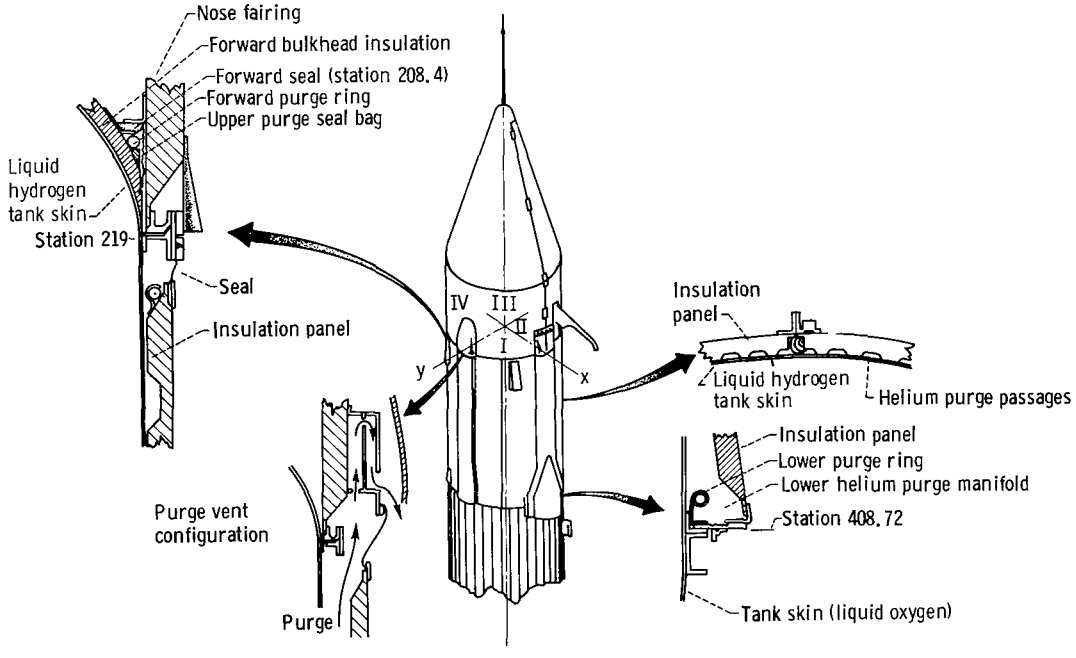

Figure V-27. - Helium purge and nose fairing jettison systems, AC-10.

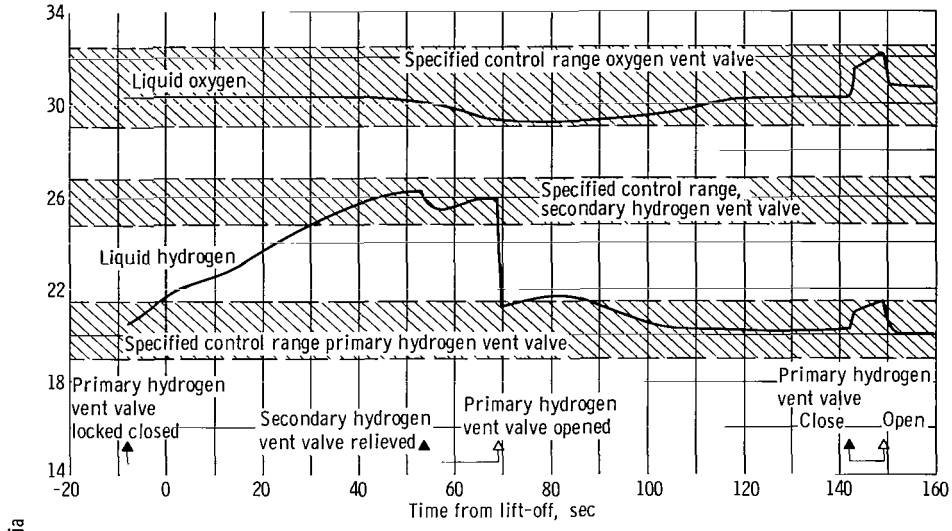

(a) Time, -20 to 160 seconds.

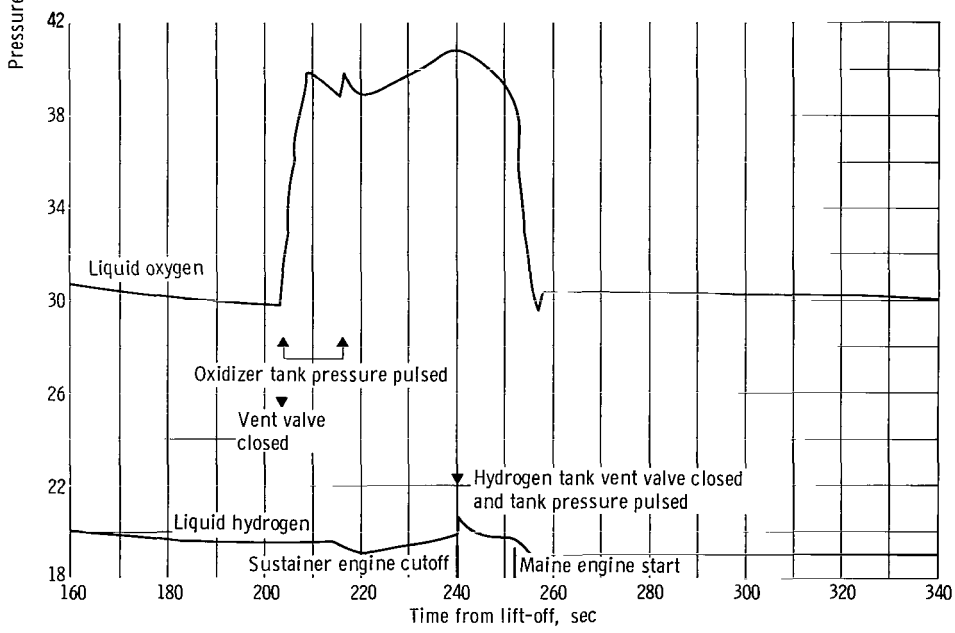

(b) Time, 160 to 340 seconds.

Figure V-28. - Centaur fuel and oxidizer tank ullage pressure histories, AC-10.

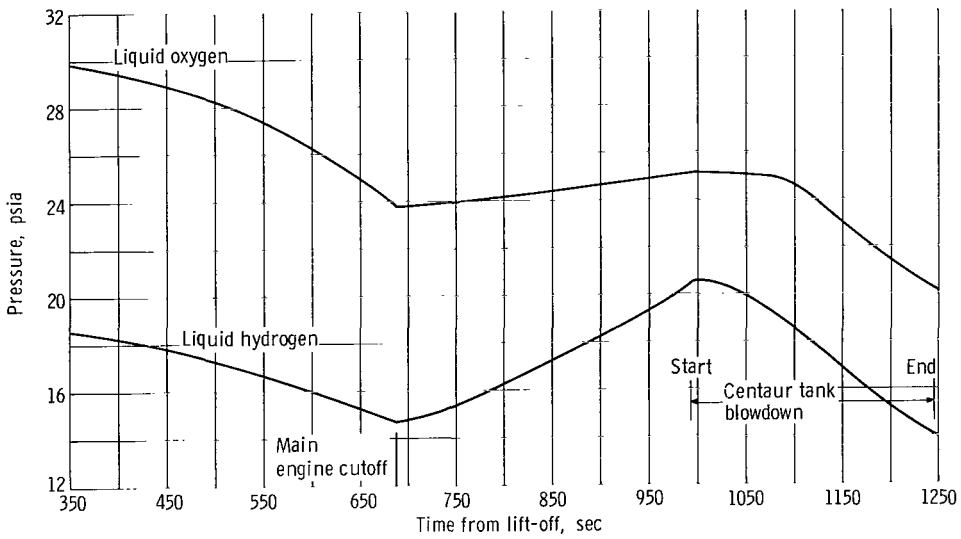

(c) Time, 350 to 1250 seconds.

Figure V-28. - Concluded.

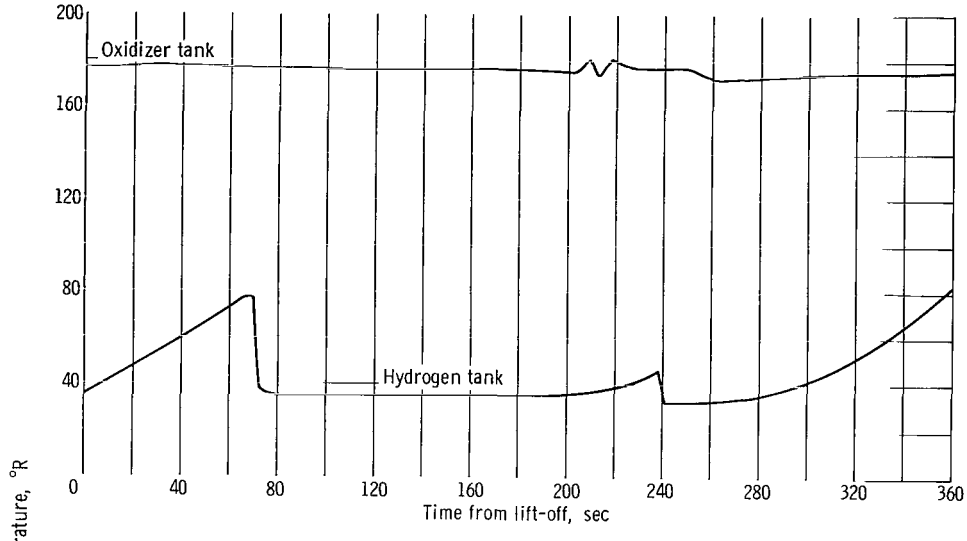

(a) Time, 0 to 360 seconds.

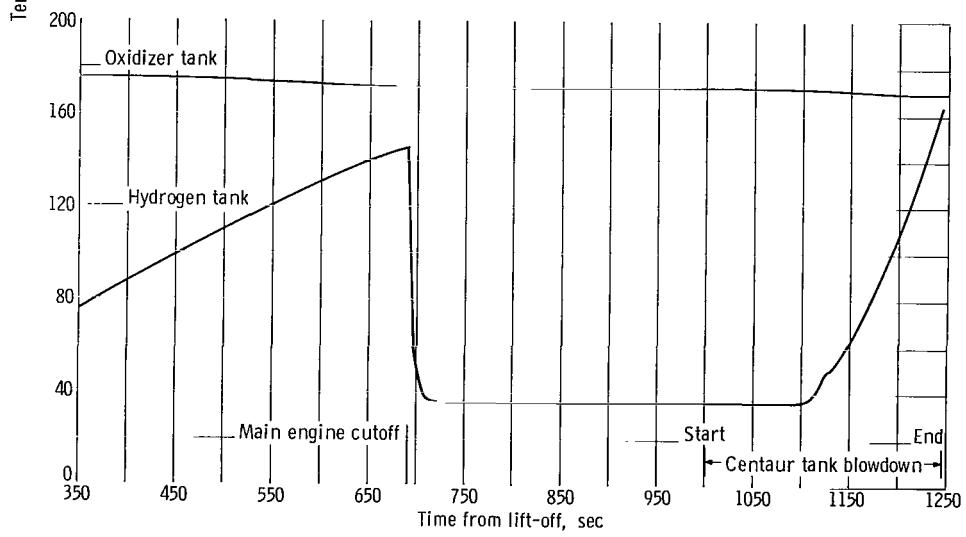

(b) Time, 350 to 1250 seconds.

Figure V-29. - Centaur fuel and oxidizer tank ullage temperatures, AC-10.

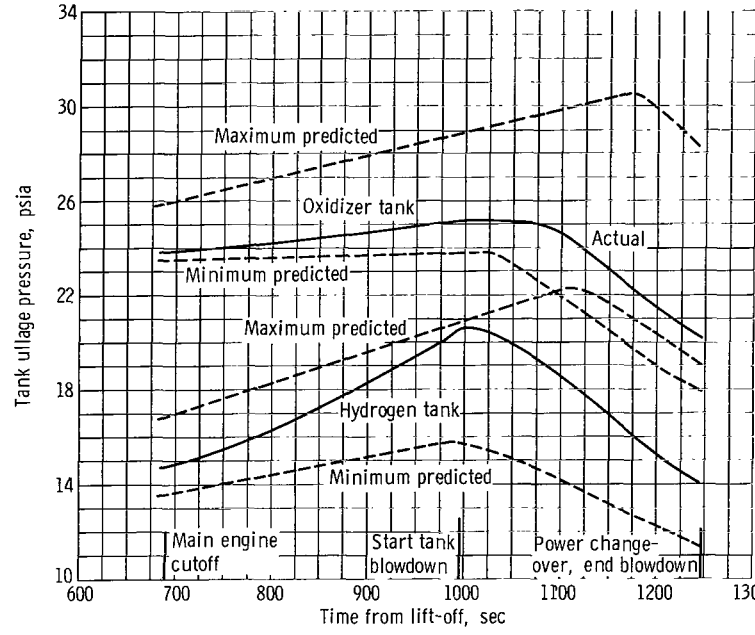

Figure V-30. - Centaur propellant tank ullage pressure profiles during retromaneuver, AC-10.

HYDRAULIC SYSTEMS

by Eugene J. Cieslewicz

Atlas

System description. - Hydraulic systems on the Atlas vehicle, as shown in figure V-31, were used to supply fluid power for operation of sustainer engine control valves, and for thrust vector control of the engines. Two separate systems were used, one for the booster stage and one for the sustainer stage.

The booster hydraulic system provided power solely for gimbaling the two thrust chambers. System pressure was supplied by a single pressure-compensated, variable-displacement pump driven off the engine turbopump. Additional components of the system included a safety relief valve, two pressure accumulators, and a reservoir. Engine gimbaling in response to flight control commands was effected by servocylinders providing separate pitch and yaw control for each thrust chamber. Maximum booster engine gimbal angle capability was $\pm 5^{\circ}$ in a conical pattern.

The sustainer stage used the same type hydraulic components. System requirements, however, were to provide power for sustainer engine control valves as well as gimbaling the sustainer and two vernier engines. The sustainer thrust chamber was gimbaled in pitch and yaw by two servocylinders and had a maximum displacement capability of $\pm 3^{\circ}$. The sustainer engine, however, was not enabled for thrust vector control until after booster staging. Vernier engine gimbaling was for roll control only during the Atlas sustainer flight phase, and the actuator limit travel was $\pm 70^{\circ}$.

System performance. - Hydraulic system pressures in both the booster and sustainer circuits, as shown in figure V-32, were stable and successfully maintained throughout the boost flight phase. The transition from ground to airborne hydraulic systems following engine ignition was normal. Pressures increased from about 1800 psia up to flight levels in less than 2 seconds. Starting transients produced a normal overshoot of about 10 percent with the pump discharge pressures stabilizing at 3140 psia in the booster circuit and 3110 psia in the sustainer circuit.

Engine gimbaling requirements during flight were generally less than 1° with one exception during the period of maximum dynamic pressure. At this time, maximum booster engine gimbal angles of about 3.6° were required in the pitch plane to correct for wind shear. For similar requirements in the yaw plane, the engine booster gimbal angles did not exceed 1.5°. These excursions were normal and were well within the engine gimbal limits of $\pm 5^{\circ}$.

Centaur

System description. - Two separate but identical hydraulic systems, one for each engine, as shown in figure V-33, were used on the Centaur stage to gimbal the engine thrust chambers for pitch, yaw, and roll control. Each system consisted of two servocylinders, high and low pressure pumps, reservoirs, accumulators, and relief valves for pressure regulation. Hydraulic pressure was provided by a constant-displacement vane-type pump driven off the liquid oxygen turbopump drive shaft. A secondary electrically powered recirculation pump was also used to provide low pressure for engine gimbaling requirements during prelaunch checkout, to aline the engines prior to main engine start, and for limited thrust vector control during the propellant tank blowdown portion of the Centaur retrothrust maneuver. Maximum engine gimbal capability was $\pm 3^{\circ}$.

System performance. - Performance of both hydraulic systems on the Centaur stage was satisfactory throughout the flight. Thermal conditioning of the system prior to launch was maintained by ambient helium purges and by operation of the low pressure recirculation pumps. The hydraulic manifold temperature at lift-off, as shown in figure V-34, was 66° F. This temperature was well above the minimum required limit of 20° F. During the Atlas flight phase, the system temperatures cooled only slightly to 62° F at time of main engine start. Then, with activation of the main pumps, the hydraulic manifold temperatures increased normally to 170° F at main engine cutoff.

Pressure supply and regulation were normal and supported all system requirements. At T + 239.4 seconds, the electrically driven hydraulic pumps were activated to provide low pressure hydraulic power for alining the engines prior to main engine start. System pressures, as shown in figure V-34, came up to 133 and 122 psia in the C-1 and C-2 hydraulic manifolds, respectively. At main engine start, with increasing turbopump speed the system pressures increased rapidly to flight levels of 1159 psia on the C-1 and 1130 psia on the C-2 engine system. Pressures were steady throughout the Centaur engine firing, although a slight decay amounting to about 2 percent was noted by main engine cutoff. This decay was not abnormal as pressures were within the required control limits of 1100 to 1180 psia.

After main engine cutoff, the hydraulic system was inactive until start of the propellant tank blowdown at T + 996.9 seconds. The electrically driven recirculation pumps were then turned on to provide low pressure hydraulic power for alining the engines and providing limited thrust vector control during the retrothrust blowdown maneuver. This limited control supplemented the primary hydrogen peroxide attitude control system and helped to reduce the duty cycle on these engines.

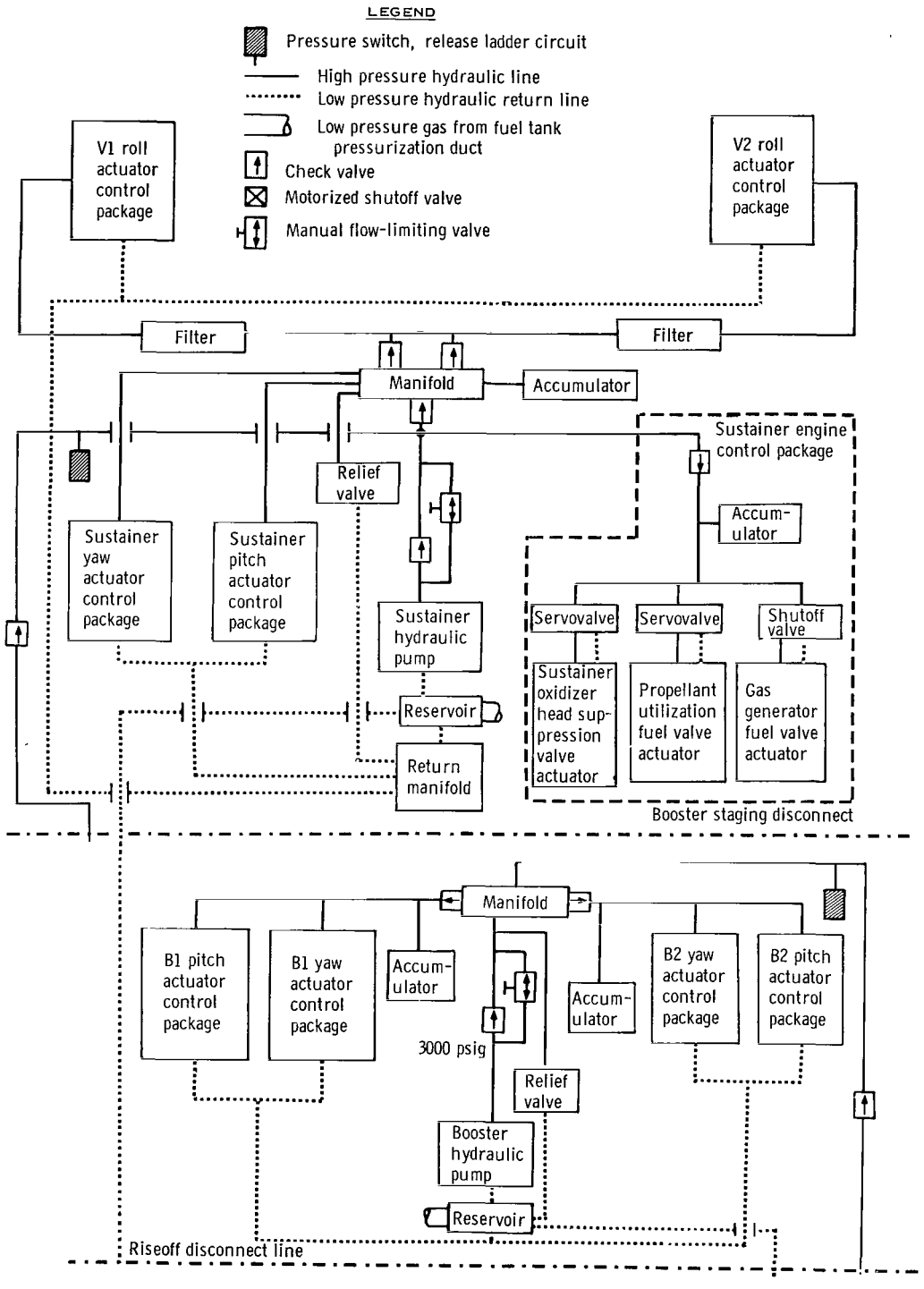

Figure V-31. - Atlas hydraulic system, AC-10.

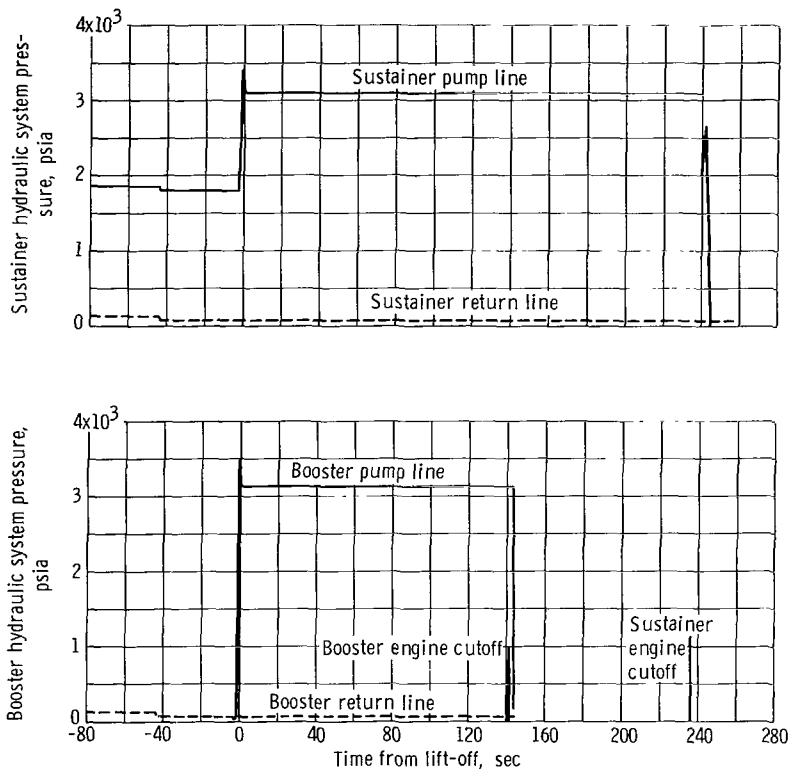

Figure V-32. - Atlas hydraulic system pressures, AC-10.

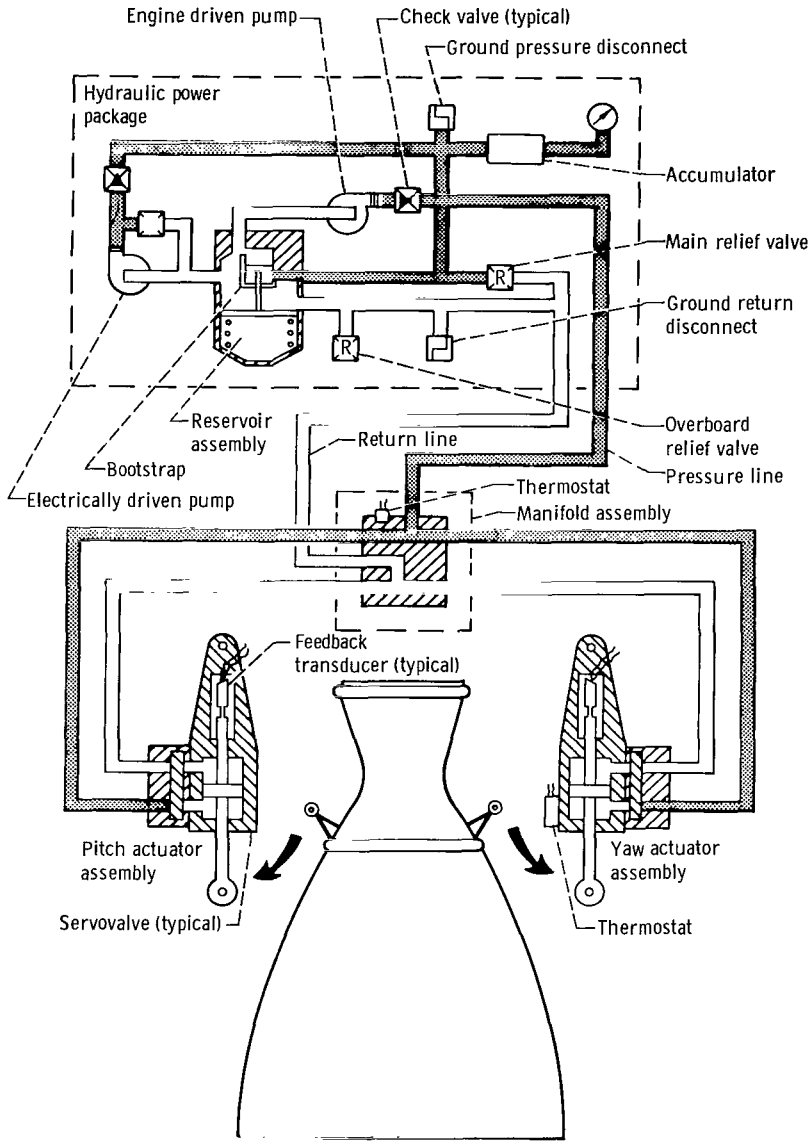

Figure V-33. - Centaur hydraulic system, AC-10. (System shown is typical for each engine.)

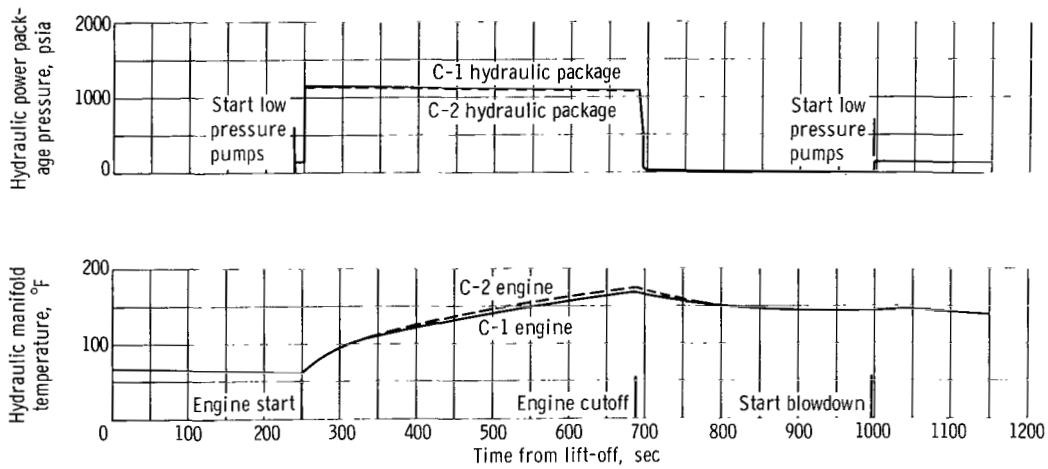

Figure V-34. - Centaur hydraulic system pressures and temperatures, AC-10.

ELECTRICAL SYSTEMS

by John P. Quitter, James Nestor, and John M. Bulloch

Power Sources and Distribution

Atlas system description. - The Atlas power requirements were supplied by one main missile battery, one telemetry battery, two range safety command batteries, and a 400-hertz rotary inverter. Transfer of the Atlas electrical load from external to internal battery power was accomplished by the main power changeover switch at T - 2 minutes.

Atlas system performance. - The Atlas main missile battery supplied the requirements of the dependent systems at near normal voltage levels. The battery voltage was 28.2 volts at lift-off, rising to 28.4 volts at sustainer engine cutoff. A small decline to 27.9 volts occurred after retrorocket firing.

The three batteries which supplied the telemetry and range safety command systems provided normal voltage levels throughout Atlas flight. The voltage at lift-off was 28.2 volts for the telemetry system, 28.9 volts for range safety command system 1, and 29.0 volts for range safety command system 2.

The Atlas rotary inverter, supplying the airborne 400-hertz power operated within established voltage and frequency parameters. The voltage at lift-off was 115.2 volts with a decline to 114.9 volts at end of data acquisition. The inverter frequency at lift-off was 402.5 hertz and rose to 403 hertz at the end of programmed Atlas flight. The gradual rise in frequency is typical for the Atlas rotary inverter and has been noted on earlier flights and during ground testing. The required difference of 1.3 to 3.7 hertz between Atlas and Centaur inverter frequencies was properly maintained to avoid generation of undesirable beat frequencies in the autopilot system. If a beat frequency occurred in resonance with the slosh or natural frequencies of the vehicle, false commands would be given to the autopilot resulting in possible degradation of vehicle stability.

Centaur system description. - The Centaur electrical power system consisted of a main missile battery, two range safety command batteries, two pyrotechnic batteries, a main power changeover switch, and a 400-hertz solid-state inverter. This inverter supplied 400 hertz power to the guidance, flight control, and propellant utilization systems.

Centaur system performance. - System operation was satisfactory throughout the flight. Transfer of the Centaur electrical load from external power to the internal battery was accomplished by the power changeover switch within 250 milliseconds. Transient voltages were small. The umbilical disconnects operated satisfactorily on command.

The main power battery voltage level at lift-off was 28.2 volts. It dropped to a low of 27.7 volts at main engine start then recovered to 28.2 volts during Centaur powered flight.

Comparison of the preflight battery load profiles with the actual AC-10 flight recorded

profile shows close correlation between sequential events. Battery current at lift-off was 46 amperes reaching a peak of 64 amperes at T + 240 seconds, as shown in the load profile (fig. V-35).

Both pyrotechnic battery voltages were 35.2 volts at lift-off (minimum specification limit is 34.7 V). Proper operation of the pyrotechnic batteries and relay system was verified by the successful jettison of the insulation panels and nose fairing.

Performance of the two range safety command batteries was satisfactory as verified by proper command receiver operation during launch and flight. The battery voltages were 32.1 and 32.3 volts, respectively, with the receivers in operation (minimum specification limit is 30 V).

The temperature of the staging disconnect was not monitored during the launch or flight. Temperature measurements obtained during propellant tanking tests showed that a warming gas provided adequate heating for proper operation of the disconnect.

The solid-state Centaur inverter operated satisfactorily throughout the flight. Telemetered voltage levels compared closely with values recorded during preflight testing. The inverter phase voltages at lift-off were as follows: phase A, 114.5 volts; phase B, 115.0 volts; and phase C, 115.0 volts. Only minor voltage changes occurred during flight.

The inverter frequency remained constant at 400.0 hertz throughout the flight. Inverter skin temperature was 100° F at T - 180 minutes and rose as expected to a high of 111.6° F at T - 60 minutes. Inverter temperature was monitored to verify that adequate cooling was present. Temperature rise of the inverter paralleled the rise in ambient temperature in the electronic compartment from 52° to 66° F. The inverter temperature decreased during propellant tanking to 94° F at lift-off. Flight temperature was not monitored because of satisfactory experience on earlier flights. Figure V-36 is included to show the marked dependence of inverter temperature on its changing environment due to propellant tanking and panel purging. Lift-off temperature of 94° F is 10° less than that noted at T - 0 during the tanking test. The difference is attributed to cool gas leaking through the nose fairing seal at station 208 (see fig. V-27).

Instrumentation and Telemetry

Atlas system description. - The Atlas telemetry system consisted of a single PAM/FM/FM unit, identified as RF 1, transmitting at 229.9 megahertz. The letter designation PAM refers to Pulse Amplitude Modulation, a technique of sampling data to allow better utilization of the data handling capacity of the telemetry system. The letter designation FM/FM (Frequency Modulation/Frequency Modulation) refers to the technique of frequency modulating a transmitter with the output of several subcarrier oscillators

TABLE V-VIII. - ATLAS MEASUREMENT SUMMARY, AC-10

Airborne systems	Number and type of measurement									
	Acceleration	Rotation rate	Current	Deflection	Pressure	Rate	Temperature	Voltage	Discrete	Total
Airframe	-	-	-	--	3	-	2	-	24	29
Range safety	-	-	-	--	--	-	-	3	1	4
Electrical	-	-	1	--	--	-	-	3	--	4
Pneumatic	-	-	-	--	7	-	2	-	--	9
Hydraulic	-	-	-	--	6	-	-	-	--	6
Axial acceleration	1	-	-	--	--	-	-	-	--	1
Propulsion	-	3	-	2	19	-	2	-	6	32
Flight control	-	-	-	11	--	3	-	2	12	28
Telemetry	-	-	-	--	--	-	1	-	--	1
Propellant	1	-	-	--	2	-	-	1	--	4
Total	2	3	1	13	37	3	7	9	43	118

which, in turn, have been frequency modulated by data signals. All operational measurements were transmitted by two antennas, one in each pod. Locations of ground and ship stations are shown in figure V-37. Telemetry coverage was continuous as shown in figure V-38.

Atlas system performance. - A summary of the 118 Atlas instrumentation measurement transmissions is given in table V-VIII. Of these measurements, the following five failures occurred:

(1) The angle-of-attack pressure transducers in the pitch and yaw planes operated satisfactorily; however, the nose cap angle of attack calibration measurement, by which dynamic pressure was to be obtained, was invalid. To compute angle of attack dynamic pressure was obtained from trajectory data.

(2) Three insulation panel breakwire measurements indicated "open" at shaped charge firing. These measurements should not indicate "open" until the panel has traveled 5 feet from the tank. It is presumed that debris from the shaped charge severed these three breakwires causing an open circuit.

(3) The transducer measuring Atlas thrust compartment temperature opened electrically at booster jettison. The period of interest for this measurement is the time up to booster jettison. The exact cause of the failure is unknown; however, it is probable that the staging sequence damaged the instrumentation harness or transducer. In addition to the preceding failures, the following measurements failed partially but yielded usable data:

(1) The transducer measuring main liquid oxygen valve position showed intermittent data from T + 35 to T + 42 seconds, from T + 65 to T + 112 seconds, and from T + 210 to

T + 220 seconds causing intermittent degradation of the data. This degradation is characteristic of discontinuities in the wiper arm circuit and has been observed on several previous Atlas flights.

(2) The transducers measuring sustainer hydraulic pump line and booster hydraulic pump discharge pressures exhibited intermittent degradation of data during the flight. This degradation is characteristic of discontinuities in the wiper arm circuit and was observed on previous flights.

(3) Quadrant II insulation panel separation measurement indicated anomalous behavior during the panel separation sequence. Normally, this measurement indicates a sustained electrical open circuit at that time. In this case, however, the circuit closed briefly and then reopened. It is hypothesized that the breakwire was momentarily disengaged by the shaped charge firing or by vibration as the panel separation started. Further movement may have caused momentary contact between the pin and socket of the breakwire, until final separation severed the breakwire completely.

Centaur system description. - For the AC-10 operational flight, Centaur telemetry consisted of one PAM/FM/FM unit transmitting at 225.7 megahertz. A block diagram of the Centaur telemetry system is shown in figure V-39. All measurements were transmitted by the Centaur telemetry antenna mounted on a ground plane atop the umbilical island. Figure V-40 shows the location of antennas on the Centaur.

Centaur system performance. - Reception was virtually continuous throughout the programmed flight to T + 5940 seconds with one exception. Range instrumentation ship General H. H. Arnold was unable to track the vehicle. The received signal was weak and no usable data were recorded. The two receiving stations, one uprange and one downrange of the Arnold, received data for the entire period except for 5 seconds from T + 775.5 to T + 780.5 seconds. Analysis before and after loss of signal indicates that no significant data were lost. Centaur telemetry coverage is shown in figure V-41.

A summary of the 140 Centaur instrumentation measurement transmissions is given in table V-IX. Of these measurements, the following failures occurred:

(1) The five thermocouples indicating attitude control engine chamber temperatures yielded qualitative data only because the original reference junction on the liquid oxygen sump was defective. Because of the inaccessibility of this reference, a new reference was located in the vicinity of the sump. However, since the actual temperature of this new reference was not known, the data from these five measurements were qualitative only.

(2) The A-3 attitude control engine temperature transducer became intermittent from T + 698 seconds to the end of the flight. The data suggest that the thermocouple may have had an intermittent ground within its metallic sheath.

(3) The thermocouple measurement on the A-4 attitude control engine was erratic throughout the flight.

(4) The signal indicating liquid hydrogen tank ullage pressure exhibited cyclic

TABLE V-IX. - CENTAUR MEASUREMENT SUMMARY, AC-10

Airborne systems	Number and type of measurement										
	Rotation rate	Current	Deflection	Vibration	Pressure	Frequency	Temperature	Voltage	Discrete	Digital	Total
Airframe	-	-	-	-	--	-	--	--	1	-	1
Range safety	-	-	-	-	--	-	--	2	5	-	7
Electrical	-	1	-	-	--	1	--	4	--	-	6
Pneumatic	-	-	-	-	5	-	3	--	2	-	10
Hydraulic	-	-	-	-	2	-	2	--	--	-	4
Guidance	-	-	-	-	--	-	1	18	3	1	23
Staging separation	-	-	1	-	--	-	--	--	--	-	1
Propulsion	4	-	-	-	13	-	13	--	8	-	38
Flight control	3	-	-	-	--	-	--	4	28	-	35
Propellant	-	-	2	-	--	-	--	2	--	-	4
Spacecraft	-	-	3	5	1	-	1	--	--	1	11
Total	7	1	6	5	21	1	20	30	47	2	140

variations as high as 4 percent (peak to peak) during the first 250 seconds of flight. This condition has been observed on previous flights and is believed to be caused by a boiloff and condensation cycle of liquid hydrogen in the sensing line. No data were lost as a result of this irregularity.

Tracking

System description. - The airborne tracking beacon was a C-band radar transponder providing real-time position and velocity data to the range safety tracking system impact predictor. The tracking system provided data for use by the Deep Space Network for acquisition of the spacecraft and for guidance and flight trajectory analysis. The airborne system included a lightweight transponder, circulator (to channel receiving and sending signals), power divider, and two antennas located on opposite sides of the tank. The locations of the Centaur antennas are shown in figure V-40. The ground and ship stations are shown in figure V-37.

System performance. - Overlapping coverage was obtained to main engine cutoff. The C-band ground station radars at Merritt Island and Grand Turk Island, however, experienced numerous disturbances of the angle track caused by balance point shifts attributed to the vehicle beacon antenna pattern. Balance point shifts result from radio-frequency phase front distortion in the signal propagated from the beacon and simulate a

fictitious (relative to true) target position. Radar reaction to this phenomenon is characterized by

(1) Pronounced nulls (usually) in the received signal strength

(2) Angle servoerror signals which indicate an off-target direction while the radar is still pointed properly

(3) Servocommands following item (2) which drive the antenna according to the fictitious target position

The Antigua station tracked to T + 690 seconds, at which time it abruptly lost track. The station had been committed to T + 729 seconds. Loss of track resulted from the instrumentation ship General H. H. Arnold overriding Antigua. The ship acquired the beacon at T + 690 seconds and attempted to track several times but could not hold it. Therefore, C-band radar coverage was not obtained between T + 690 and T + 1109. The Centaur was again acquired by the Ascension tracking station at T + 1109 seconds. Radar coverage is shown in figure V-42.

Flight Termination System (Destruct)

System description. - The Atlas and Centaur stages each contained independent vehicle-borne flight termination systems which were designed to function simultaneously on receipt of command signals from the ground stations. These systems included redundant receivers and batteries whose operation was entirely independent of the main vehicle power system. Block diagrams of these systems are shown in figures V-43 and V-44.

The Atlas and Centaur flight termination systems provide a highly reliable means of shutting down the engines only, or shutting down the engines and destroying the vehicle. When the vehicle is destroyed in the event of a flight malfunction, the tank is ruptured with a shaped charge, and the liquid propellants of the first and second stages are dispersed. In addition, the upper stage system has the capability to destroy the Surveyor spacecraft engine prior to spacecraft separation. These functions can be commanded by the range safety officer.

System performance. - The Atlas-Centaur-Surveyor range safety command systems were prepared to execute termination commands throughout the flight. Neither engine cutoff or destruct commands were sent by the range transmitters, nor were inadvertent commands generated at the vehicle. The command from Antigua to disable the range safety command system shortly after Centaur main engine cutoff was properly received and executed. Figure V-45 depicts ground transmitter utilization in supporting the flight termination system.

Signal strength at the Atlas and Centaur range safety command receivers was excellent throughout the flight as indicated by telemetry measurements. Telemetered data

indicated that both the Centaur receivers were deactivated at approximately T + 702 seconds thus confirming that the disable command was transmitted from the Antigua station. The Surveyor destructor, controlled by the upper stage receivers, was also deactivated when the command to disable the range safety command system was sent from Antigua.

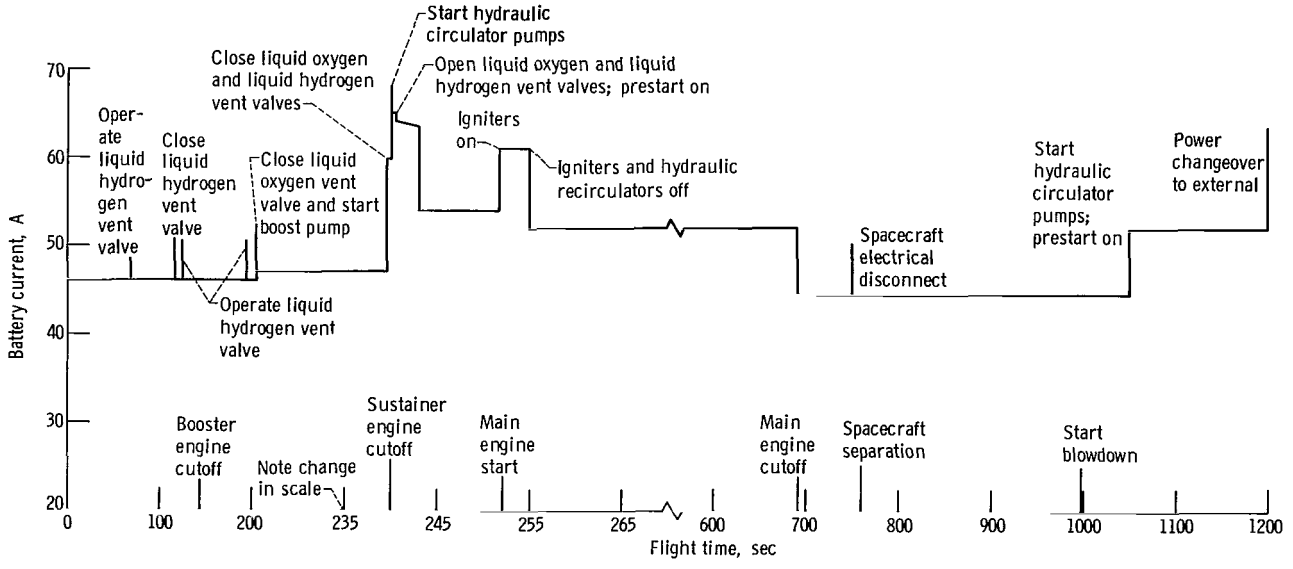

Figure V-35. - Centaur main battery load profile, AC-10.

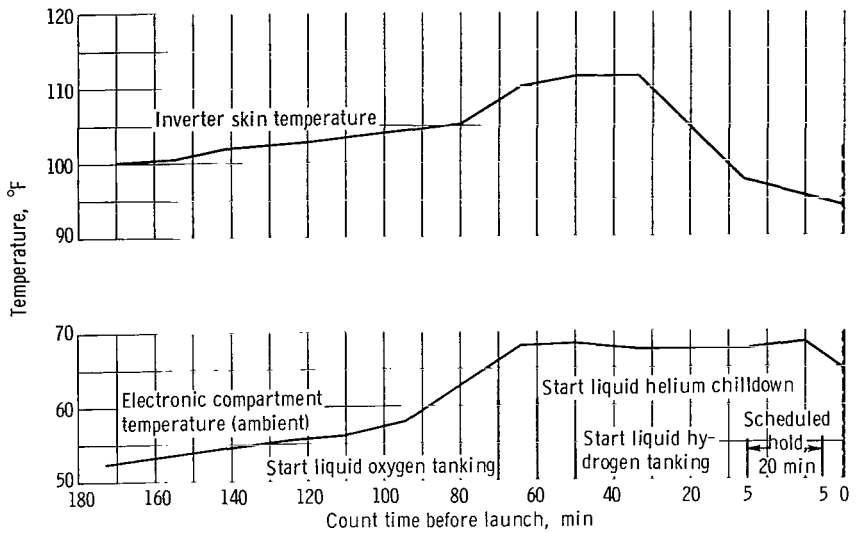

Figure V-36. - Centaur inverter and electronic compartment temperatures, AC-10.

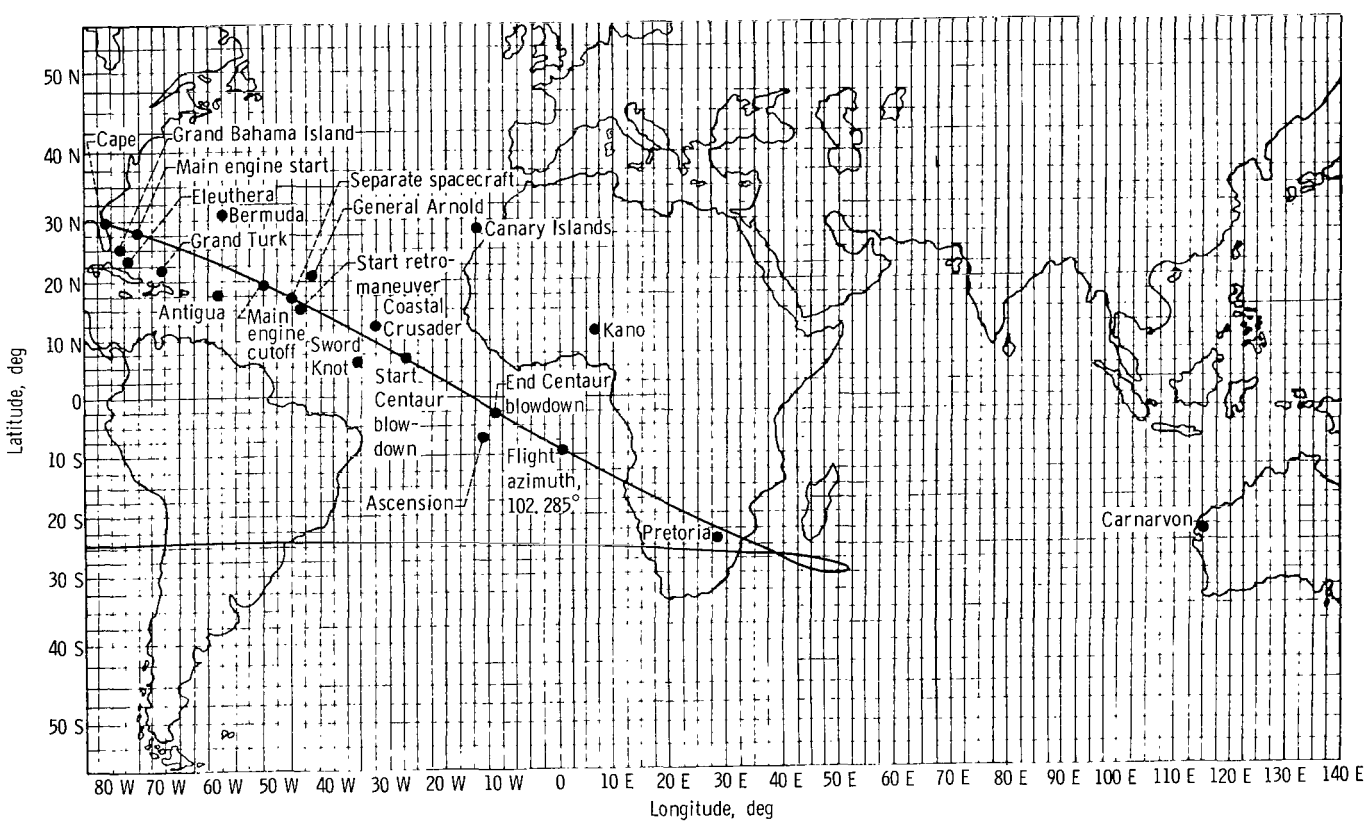

Figure V-37. - Tracking station location and vehicle trajectory Earth track, AC-10/SC-1.

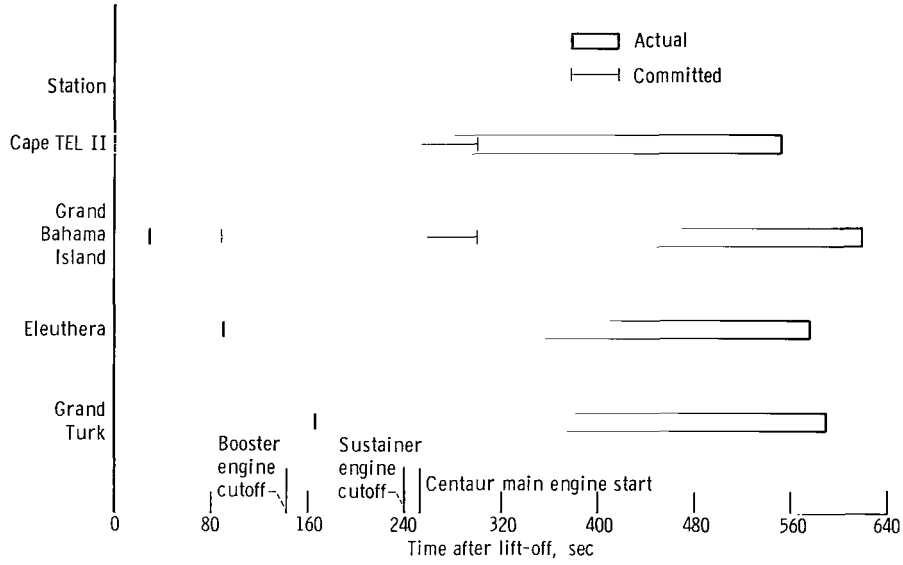

Figure V-38. - Atlas telemetry coverage, AC-10. Eleuthera and Grand Turk stations were not committed but tracked for best obtainable data.

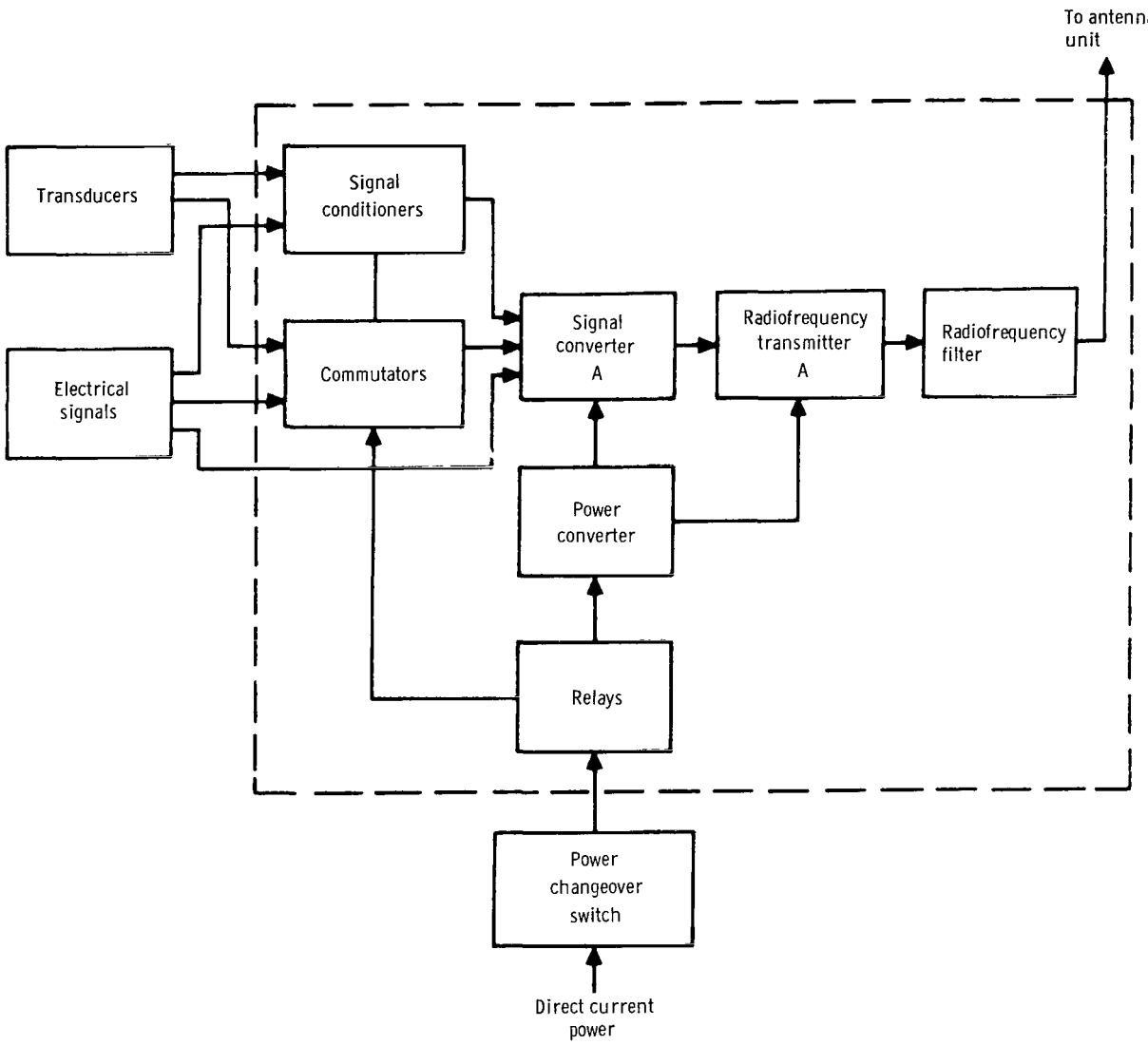

Figure V-39. - Centaur telemetry system block diagram, AC-10.

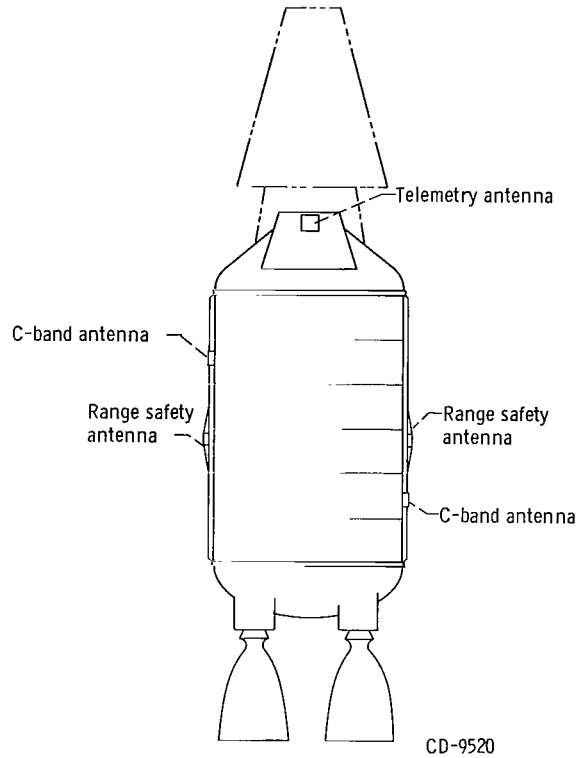

Figure V-40. - Location of Centaur antennas, AC-10.

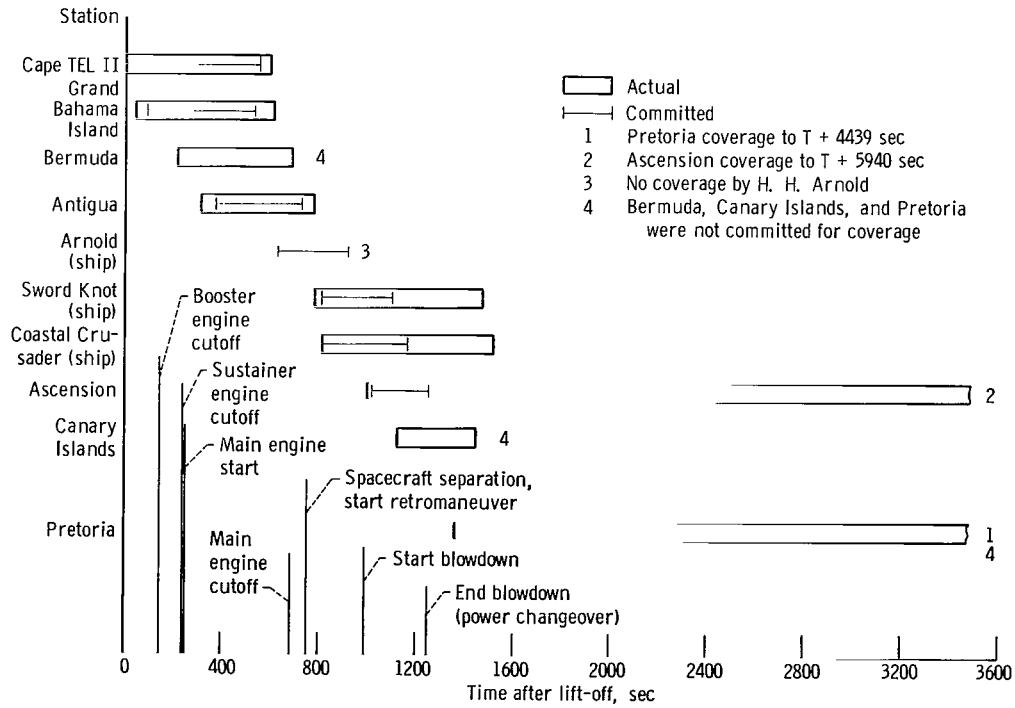

Figure V-41. - Centaur telemetry coverage, AC-10.

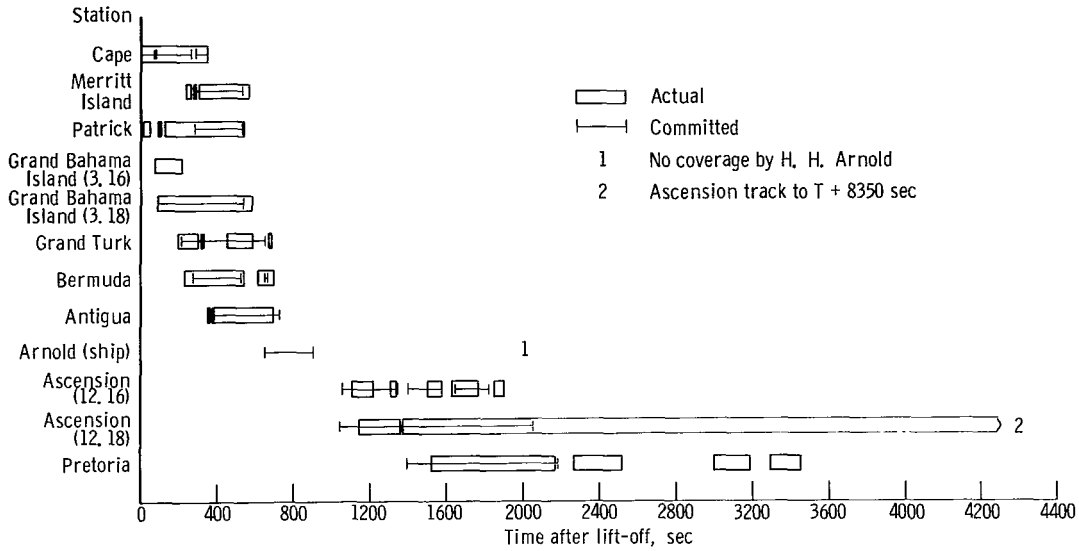

Figure V-42. - C-band radar coverage (automatic beacon track only), AC-10.

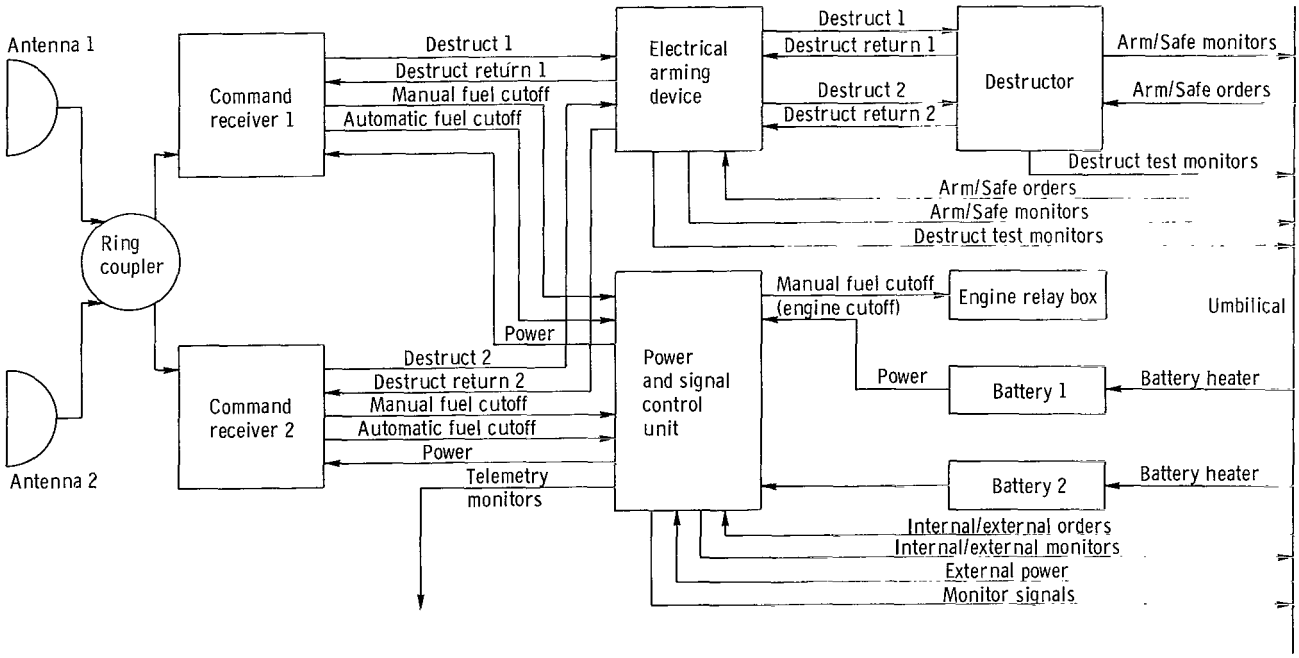

Figure V-43. - Atlas flight termination system block diagram, AC-10.

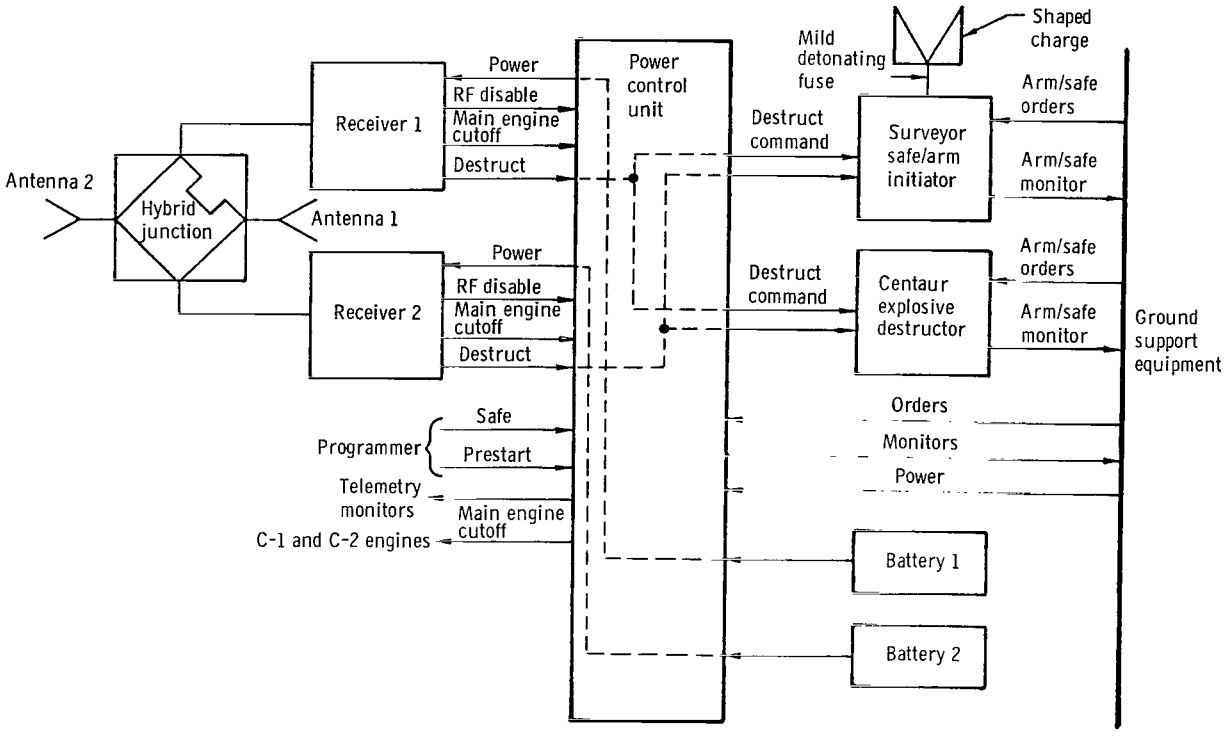

Figure V-44. - Centaur flight termination system block diagram, AC-10.

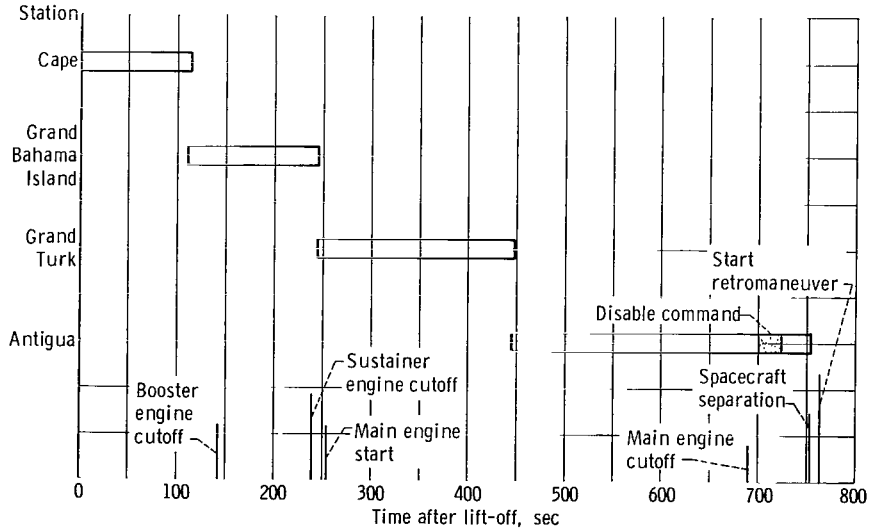

Figure V-45. - Range safety command system transmitter coverage, AC-10.

VEHICLE STRUCTURES

by Robert C. Edwards, Theodore F. Gerus, and Dana H. Benjamin

System Description

Vehicle structures include the basic Atlas and Centaur tanks and all bolt-on and jettisonable hardware attached. The Atlas and Centaur propellant tanks provided the primary vehicle structure. Both stages used thin wall pressure stabilized tank sections of monocoque construction. These propellant tanks had a minimum pressure requirement for various periods of flight in order to maintain structural stability. The structural capability of the tank as a pressure vessel limited the maximum allowable pressure in the propellant tanks.

Vehicle Structural Loads

Centaur tank pressure criteria. - The maximum allowable and minimum required tank pressures were predicted based on the maximum design flight loads being imposed on the vehicle. Appropriate factors of safety were also included. The AC-10 tank pressure profiles during the flight are compared with the maximum allowable and minimum required tank pressures in figure V-46. The areas of the tank structure which determine the maximum allowable and minimum required tank pressures during different phases of the flight are described in figure V-47.

The liquid oxygen tank pressure was of greatest concern at booster engine cutoff at which time it approached most closely the maximum design allowable. The maximum allowable liquid oxygen tank pressure was 33.0 psia at booster engine cutoff, whereas the actual AC-10 liquid oxygen tank pressure as shown in figure V-46(a) was 30.3 psia. The minimum required liquid oxygen tank pressure was not a critical factor during any period of flight.

The liquid hydrogen tank pressure reached a value closest to the allowable design maximum just prior to the primary hydrogen vent valve being opened at T + 69.3 seconds. The maximum allowable pressure was 25.0 psia plus the nose fairing internal pressure. At T + 69.3 seconds, the nose fairing internal pressure was 3.0 psia; thus, the maximum allowable liquid hydrogen tank pressure was 28.0 psia. This pressure is determined by the hoop stress capability of the forward bulkhead conical section. The actual liquid hydrogen tank pressure at this time was 26.0 psia.

The minimum required liquid hydrogen tank pressure was of primary importance at the following times: prelaunch, launch, primary hydrogen vent valve opening (T + 69.3 sec), and nose fairing jettison:

(1) Prior to launch, the insulation panel pretensioning imposed local bending stresses on the liquid hydrogen cylindrical skin. The minimum required liquid hydrogen tank pressure at this time was 19.0 psia; the actual tank pressure was 20.5 psia.

(2) During the launch phase (T - 0 to T + 10 sec), the payload imposed compression loads on the forward bulkhead due to inertia and lateral vibration. The minimum required liquid hydrogen tank pressure was 19.5 psia at T + 0; at this time the actual tank pressure was 21.6 psia.

(3) Just after the primary hydrogen vent valve was opened at T + 69.3 seconds the inertia and bending compression loads were critical at station 409.6 on the cylindrical skin. The minimum required liquid hydrogen tank pressure was 20.3 psia. The tank pressure at this time was 21.3 psia.

(4) At nose fairing jettison, the nose fairing exerted inboard radial loads at station 219. The minimum required tank pressure at this time was 18.5 psia; the tank pressure was 19.5 psia.

The maximum and minimum differential pressures between the liquid oxygen and liquid hydrogen tank were limited by the strength of the Centaur intermediate bulkhead. The liquid oxygen tank pressure must always be greater than the liquid hydrogen tank pressure for stability (to prevent bulkhead reversal), and maximum pressure differential was limited by the bulkhead material strength.

The desirable minimum differential pressure across the intermediate bulkhead was 2.0 psi. Before the primary hydrogen vent valve was opened at T + 69.3 seconds, the actual differential pressure across the intermediate bulkhead was 3.3 psi. The maximum allowable differential pressure across the intermediate bulkhead was 23.0 psi. During step pressurization of the liquid oxygen tank, the actual differential pressure was 21.0 psi at T + 238 seconds.

Atlas tank pressure criteria. - The Atlas intermediate bulkhead differential pressure, as shown in figure V-48, remained well above the minimum allowable of 2.0 psi throughout the critical lift-off period when the Atlas liquid oxygen mass was subjected to longitudinal oscillations. Thereafter, the bulkhead differential pressure varied between a minimum of 7.0 psi at T + 100 seconds and a maximum of 23.8 psi at booster engine cutoff. The design flight loads on the Atlas liquid oxygen tank were critical in bending between T + 60 and T + 80 seconds. Controlled tank pressures during that time, as shown in figure V-49, were above the minimums required for resisting the maximum design flight loads. The minimum differential between required and actual pressures occurred at T + 80 seconds when the liquid oxygen tank pressure was 33.5 psia and the minimum allowable was 31.8 psia. The maximum allowable liquid oxygen pressure was most closely approached at T + 70 seconds. At this time, the tank pressure was 36.2 psia; the allowable maximum pressure was 39.3 psia.

Quasi-steady-state load factors. - The longitudinal load factor buildup, a maximum

value of 5.68 g's, was reached at booster engine cutoff which was within the ±3 σ range (5.62 to 5.78 g's).

Atlas launcher transients. - The AC-10 launcher was instrumented to monitor the effect of the launcher on the vehicle acceleration and on the booster fuel staging valve installation on the Atlas. Launcher kick strut peak loads measured on AC-10 were slightly lower than on the previous AC-8 flight (28 000 lb against 30 000 lb). Peak-to-peak longitudinal oscillations, however, were slightly higher although still acceptable (0.8 g compared with 0.6 g for AC-8). The higher peak acceleration probably resulted from a difference in phasing between the existing vehicle oscillations and the kick strut loads. Holddown cylinder pressure decay was within specification. Fuel staging valve poppet clearance was a minimum at the time of kick strut second peak load and was 1.70 inches, well within allowable limits. Fuel manifold strut loads were similar to those seen on AC-8 and never exceeded 20 percent of the ultimate values.

Vehicle Dynamic Loads

The Atlas-Centaur launch vehicle may receive dynamic loading from several sources. These loads fall into three major categories: (1) external loads, such as aerodynamic and acoustic loads; (2) loads due to transients, such as engines starting and stopping and separation transients; and (3) loads due to dynamic coupling between major systems.

Previous flights of the Atlas-Centaur had shown that these loads were within the structural limits. For this flight, an operational one, only a limited number of flight measurements of dynamic loads and local spacecraft vibrations were made. However, these few data indicate accurately the structural loading of the vehicle. The response indicated by the data taken at fixed locations, and using the analytical model which has been set up, permits computation of the dynamic loads which occur throughout the vehicle. The measurement instruments and the parameters measured are tabulated as follows:

Measurement instrument	Parameter measured
Low-frequency range accelerometer	Launch vehicle longitudinal vibration
Centaur pitch rate gyro	Launch vehicle pitch plane vibration
Centaur yaw rate gyro	Launch vehicle yaw plane vibration
Spacecraft accelerometer	Spacecraft vibrations
Engine gimbal angles	Vehicle aerodynamic loads
Angle of attack	Vehicle aerodynamic loads

Launch vehicle longitudinal vibrations, as measured on the Centaur forward bulkhead, are shown in figure V-50. The frequency and amplitude of the vibrations measured on this flight are compared with three other representative flights.

Launch vehicle longitudinal vibrations were excited during launcher release (see previous discussion, Atlas launcher transients, p. 82). The amplitude and frequency of these vibrations were near those oberved during other flights. Calculations using the analytical model show that Atlas intermediate bulkhead pressure fluctuations were the most significant effects produced by the launcher induced longitudinal vibrations. The pressure fluctuations computed were 5.8 psi; since the steady-state bulkhead differential pressure measured at this time was 9.8 psi (see fig. V-48), the minimum differential pressure was 4.0 psi. The minimum differential pressure across the bulkhead allowed for this flight (which includes an allowance for errors) was 2.0 psi.

During Atlas flight, between T + 72 and T + 125 seconds, intermittent longitudinal vibrations of 0.10 g, at a frequency range of 11 to 15 hertz, were observed on the payload. These vibrations are believed to be caused by dynamic coupling between structure, engines, and propellant lines (commonly referred to as POGO). The level and frequency of the vibrations are similar for the four vehicles shown in figure V-50, because the vehicle configuration has not changed from flight to flight. These vibrations at the amplitudes measured do not produce significant vehicle loads (see ref. 4).

During booster engine thrust decay, short duration transient longitudinal vibrations of 1.7 g's at a frequency of 80 hertz were observed. The analytical models did not indicate significant structural loading due to this transient.

During the boost phase of flight, the vehicle vibrates in the pitch and yaw axes as an integral unit at all its natural frequencies. Previous analyses and tests have defined these natural frequencies or modes and the shapes which the vehicle assumes when the modes are excited. The rate gyros on the Centaur, which sense the local rate of change of slope, were used as instruments to sense the level of these modes. The maximum first mode excitation was seen in the pitch plane at T + 135 seconds (fig. V-51). The level was about 6 percent of the allowable deflection. The maximum second mode excitation was seen in the yaw plane at T + 40 seconds (fig. V-52). The yaw level was about 23 percent of the allowable deflection.

Vehicle bending moments were computed by using computed angle of attack, engine gimbal data, vehicle weights, and vehicle stiffnesses. Angles of attack were calculated by using two differential pressures measured on the nose fairing and the total pressure obtained from a trajectory reconstruction. Computed angles of attack and gimbal angles are shown in figures V-53 to V-56. Predicted values are shown for comparison. Gimbal capability ratio is defined as engine gimbal angle required divided by engine gimbal angle total capability. The difference between actual and predicted values of angles of attack and gimbal angles are within the expected dispersion values for all significant

TABLE V-X. - SINGLE AMPLITUDE SHOCK AND VIBRATION LEVELS DURING AC-10 FLIGHT

Spacecraft accelerometer location	Flight events									
	Launch		Booster engine cutoff		Booster jettison		Insulation panel jettison		Nose fairing jettison	
	Frequency, Hz	Acceleration g's	Frequency, Hz	Acceleration g's	Frequency, Hz	Acceleration g's	Frequency Hz	Acceleration g's	Frequency, Hz	Acceleration g's
Retromotor attachment 1, z-axis sensitivity	6 (low) 140 (high)	0.38	11	0.8	Off scale 600	Off scale ~10 to 12	[a]700	10	32	1.4
Retromotor attachment 2, z-axis sensitivity	6.7 (low) 250 (high)	0.57 1.76	11	0.8	(b)	(b)	(b)	(b)	(b)	(b)
Retromotor attachment 3, z-axis sensitivity	6 (low) 250 (high)	0.51 1.76	(b)	(b)	600	8	(b)	(b)	(b)	(b)
Foot accelerometer, station 130, radial sensitivity	250	4.95	(b)	(b)	(b)	(b)	[a]550	10	(b)	(b)
Accelerometer on spacecraft	200	1.27	(b)	(b)	(b)	(b)	(b)	(b)	18	0.875

Spacecraft accelerometer location	Flight events								Frequency band of channel, Hz
	Atlas-Centaur separation		Main engine start		Main engine cutoff				
	Frequency, Hz	Acceleration g's	Frequency, Hz	Acceleration g's	Frequency, Hz	Acceleration g's			
Retromotor attachment 1, z-axis sensitivity	[a]600	12	20	0.38	33	1.1			790
Retromotor attachment 2, z-axis sensitivity	[a]550	8.5	20	0.397	(b)	(b)			330
Retromotor attachment 3, z-axis sensitivity	(b)	(b)	20	0.12	(b)	(b)			330
Foot accelerometer, station 130, radial sensitivity	(b)	(b)	(b)	(b)	(b)	(b)			330
Accelerometer on spacecraft	(b)	(b)	(b)	(b)	33	1.85			330

[a]Shock level.

[b]Not sampled because of time sharing between accelerometers.

times in flight. The differences between B1 and B2 engine gimbal angles at the same time are believed to be a result of the thermal effects. Expected angles of attack and gimbal angles were calculated by using upper wind data obtained from a weather balloon released at T + 9 minutes. The balloon was released to obtain upper wind information as close to flight time as possible for a postflight evaluation.

The vehicle bending moments computed were added to axial load equivalent moments and moments resulting from random dispersions. The most significant dispersions considered were launch vehicle performance uncertainties, vehicle center-of-gravity offset, and wind gusts. The total equivalent predicted bending moment was divided by the bending moment allowable to obtain the structural capability ratio, as shown in figure V-57. The structural capability ratio shown in figure V-57 is greatest between T + 50 and T + 90 seconds because of high aerodynamic loads during this period. The maximum structural capability ratio of 0.90 was computed by using predicted axial loads and moments due to random dispersions. Since the angles of attack and gimbal angles measured in flight were within the expected dispersion values, it can be assumed that structural capability ratio did not exceed 0.90.

Local shock and vibrations were measured by five spacecraft accelerometers. Accelerometer data were carried by two telemetry channels. One telemetry channel carried one accelerometer continuously, and the second channel carried four accelerometers, sharing time between accelerometers. Because of time sharing between accelerometers, some short duration transients were not measured.

A summary of the most significant shock and vibration levels is shown in table V-X. The steady-state vibration levels were highest near lift-off as expected. An analysis of the data indicates that the levels were well within spacecraft qualification levels. Shock loads were measured by the spacecraft accelerometers during transients. The maximum level of the shock loads (10.0 g's) occurred at Atlas-Centaur separation and insulation panel jettison.

A comparison between shock levels measured during Atlas-Centaur separation on AC-6 and AC-10 is shown in table V-XI. Shock levels on AC-10 were about the same as those measured on AC-6.

TABLE V-XI. - COMPARISON OF AC-6 AND AC-10 MAXIMUM SHOCK LEVELS

Spacecraft accelerometer location	Event	Single amplitude,[a] maximum g's	
		AC-6	AC-10
Retromotor attachment 1, z-axis sensitivity	Atlas-Centaur separation	9.5	12
Retromotor attachment 2, z-axis sensitivity	Atlas-Centaur separation	12.5	8.5
Retromotor attachment 3, z-axis sensitivity	Atlas–Centaur separation	12.5	Not measured
Retromotor attachment 1	Insulation panel jettison	9.5	10.0
Retromotor attachment 2	Insulation panel jettison	11.2	Not measured
Retromotor attachment 3	Insulation panel jettison	11.0	Not measured

[a]Frequencies at these mark events are in the range from 600 to 700 Hz.

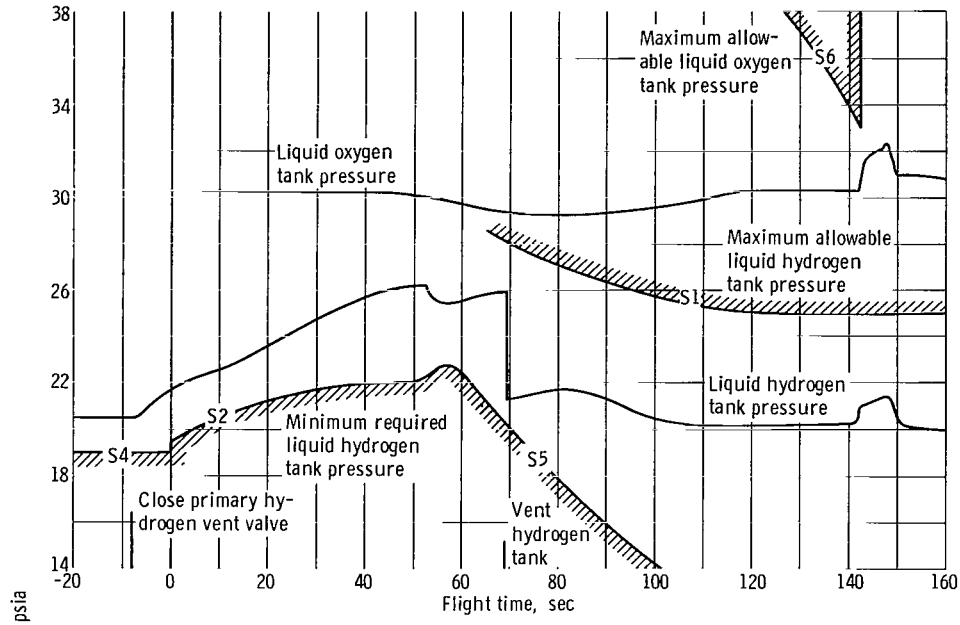

(a) Time, T - 20 to T + 160 seconds.

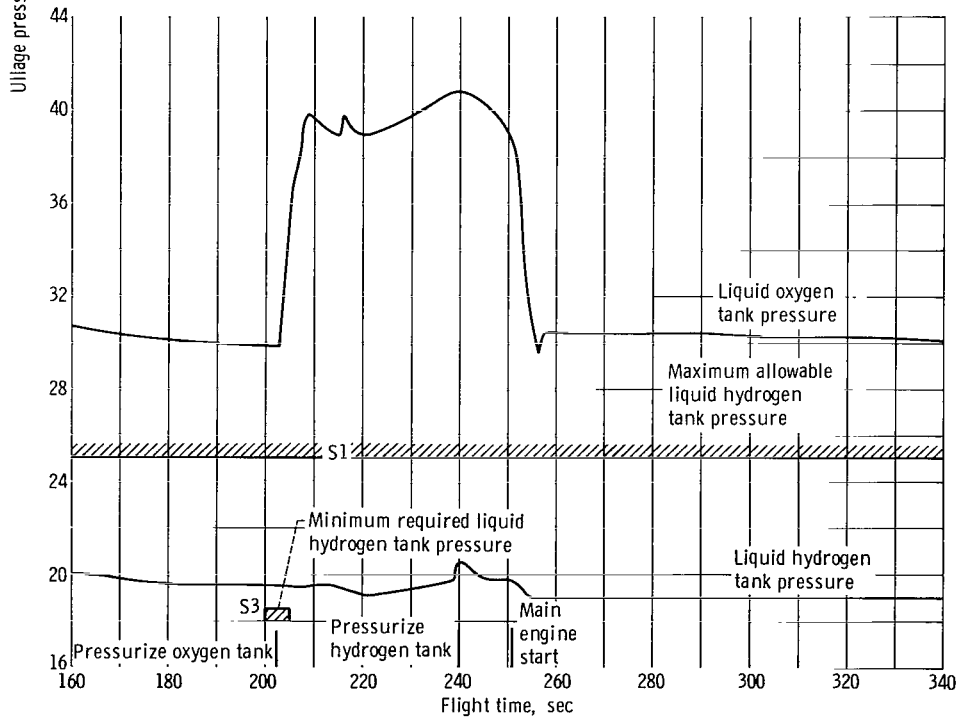

(b) Time, T + 160 to T + 340 seconds.

Figure V-46. - Centaur fuel and oxidizer tank ullage pressures, AC-10. (S1, S2, etc., are defined in fig. V-47.)

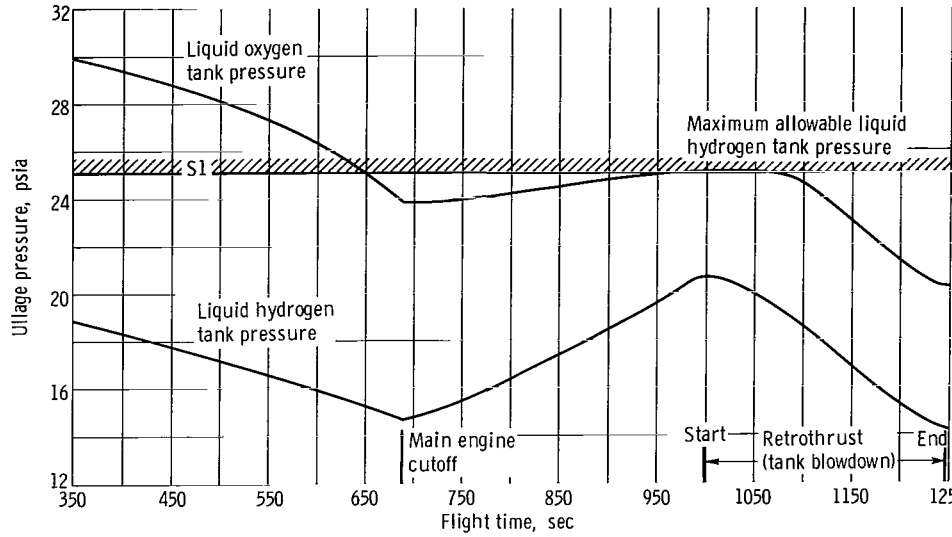

(c) Time, T + 350 to T + 1250 seconds.

Figure V-46. - Concluded.

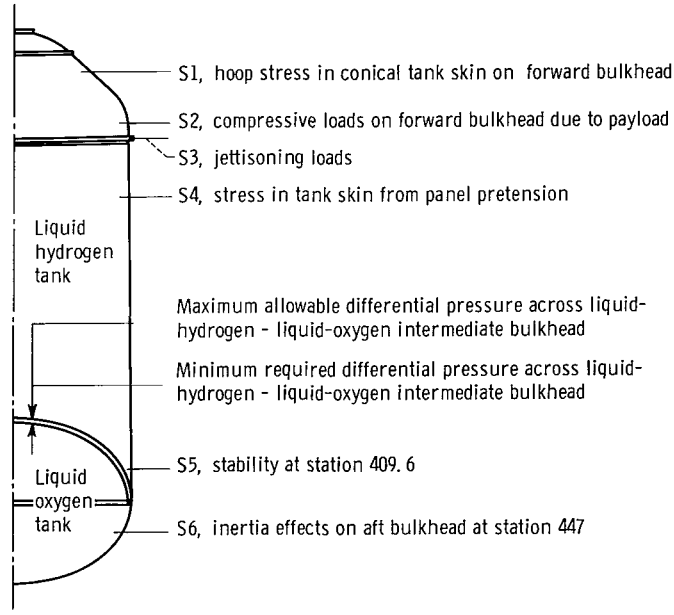

Figure V-47. - Tank areas which determined allowable pressures, AC-10.

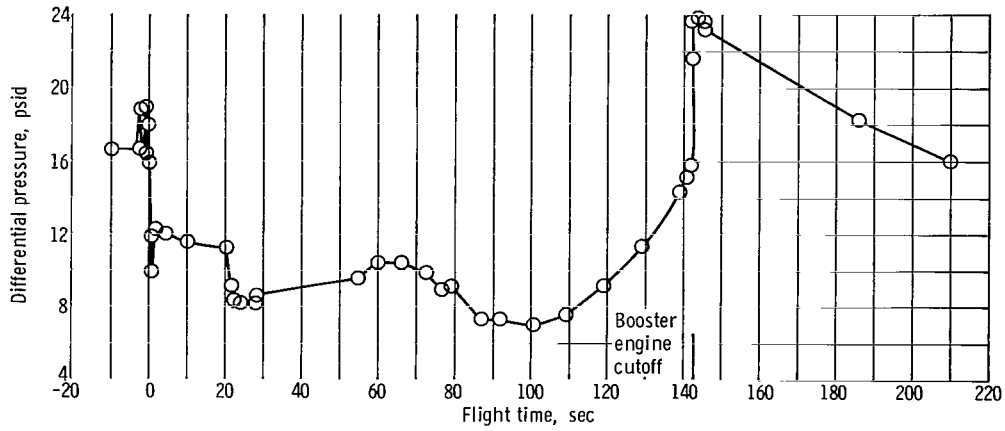

Figure V-48. - Atlas intermediate bulkhead differential pressure, AC-10.

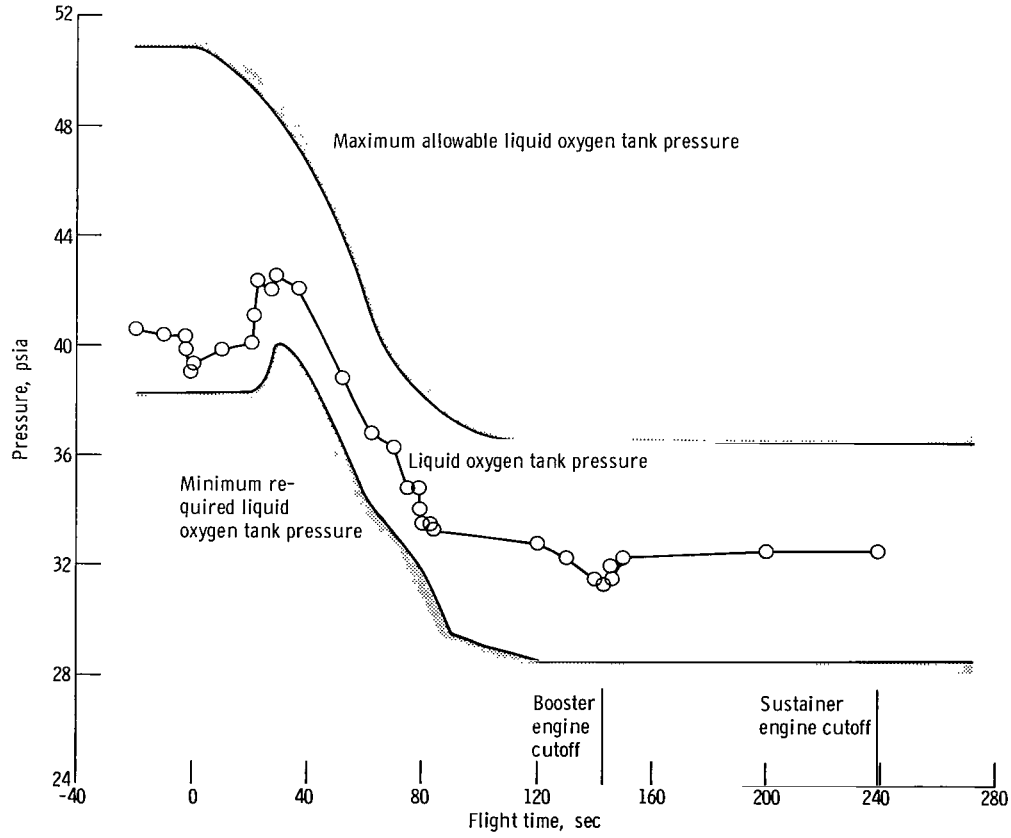

Figure V-49. - Atlas liquid oxygen tank ullage pressure, AC-10.

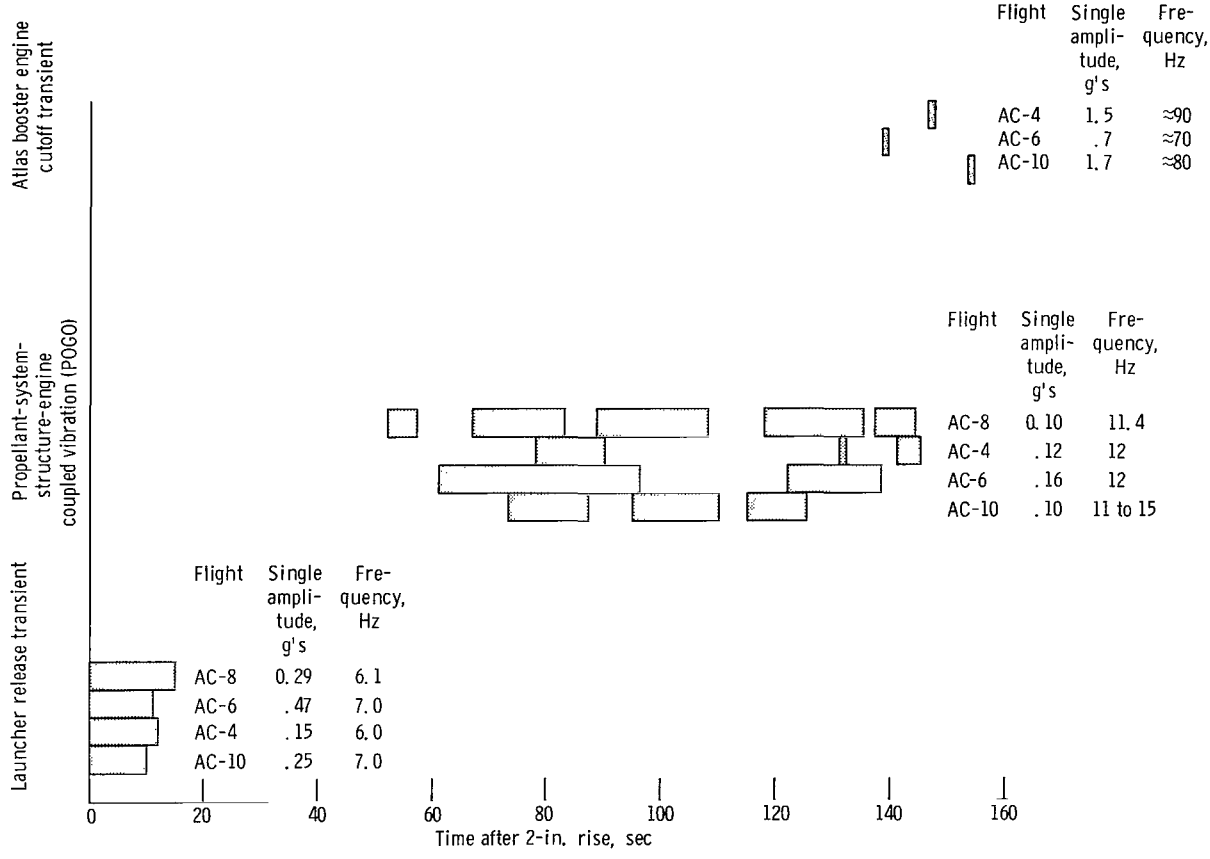

Figure V-50. - Longitudinal vibrations for Atlas-Centaur flights. (Length of bars indicates duration of vibration.)

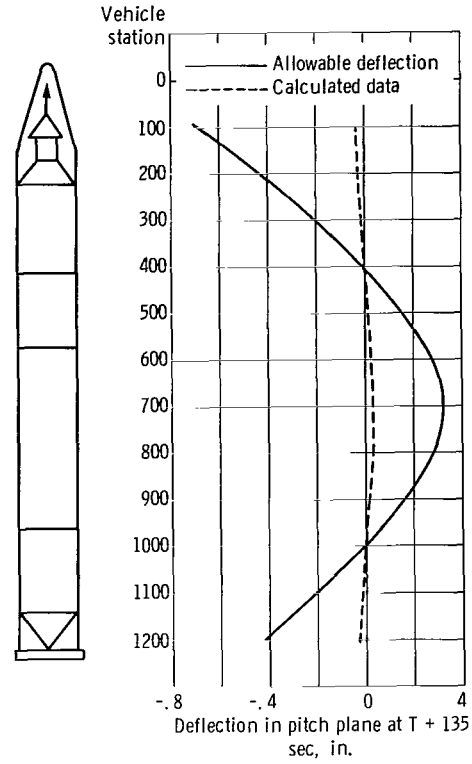

Figure V-51. - Maximum pitch plane first bending mode amplitudes, AC-10.

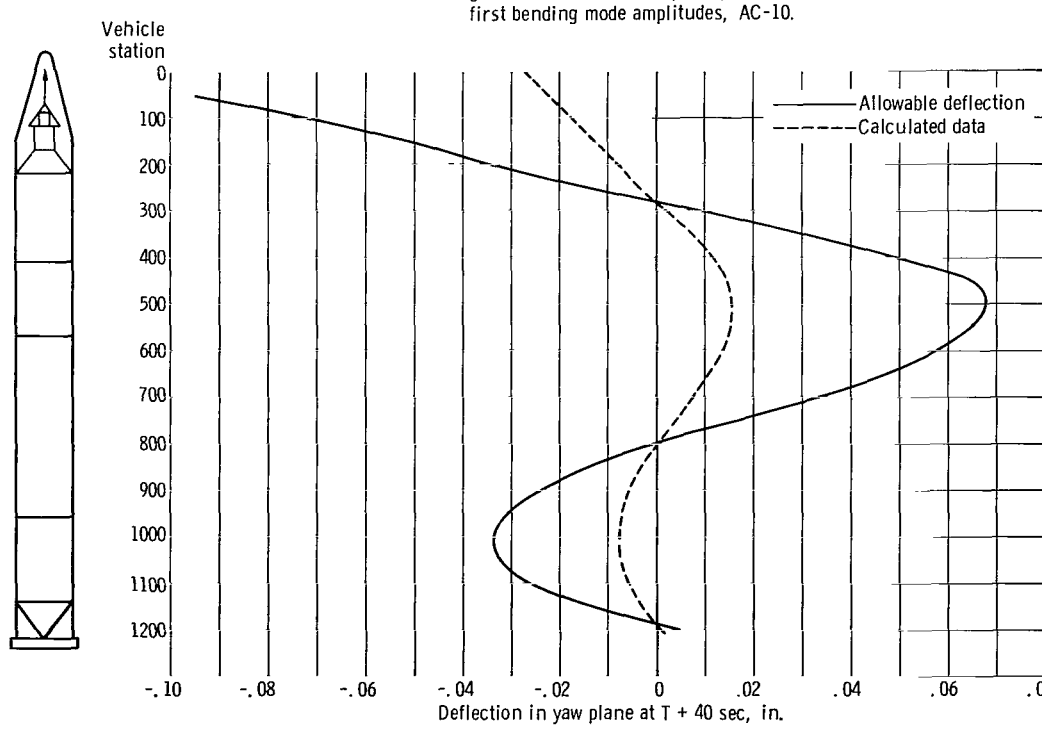

Figure V-52. - Maximum yaw plane second bending mode amplitudes, AC-10.

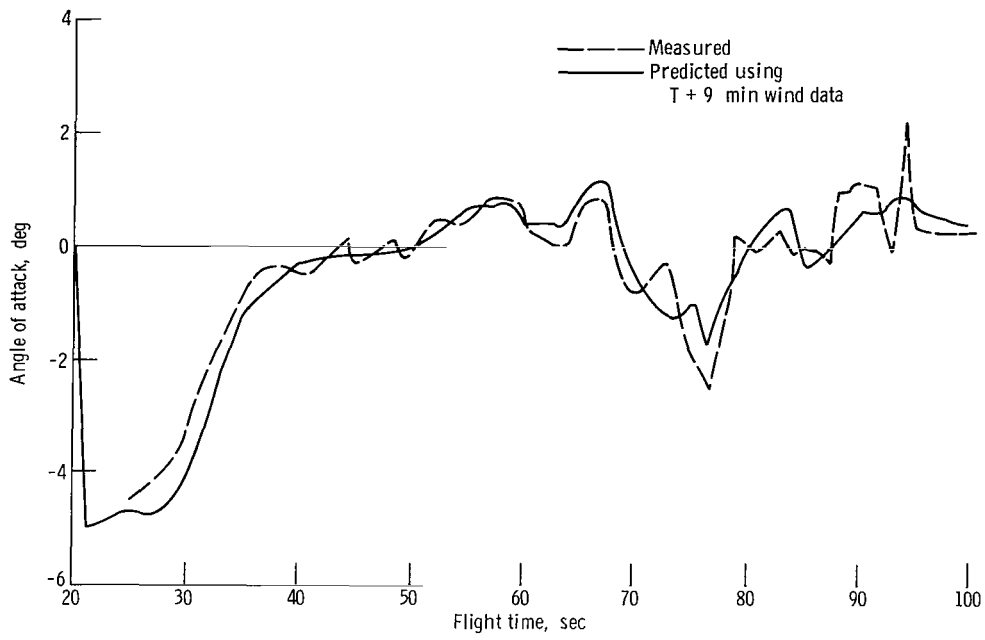

Figure V-53. - Pitch angles of attack, AC-10.

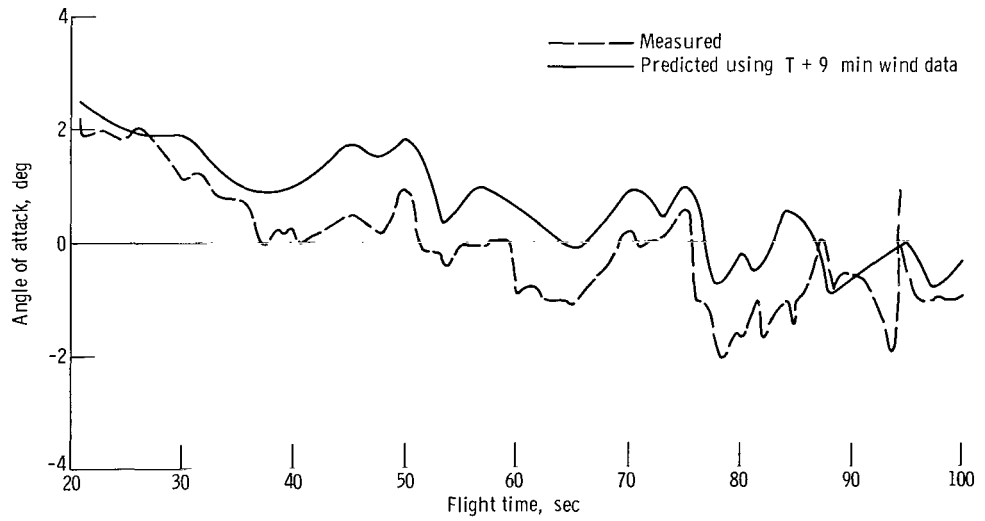

Figure V-54. - Yaw angles of attack, AC-10.

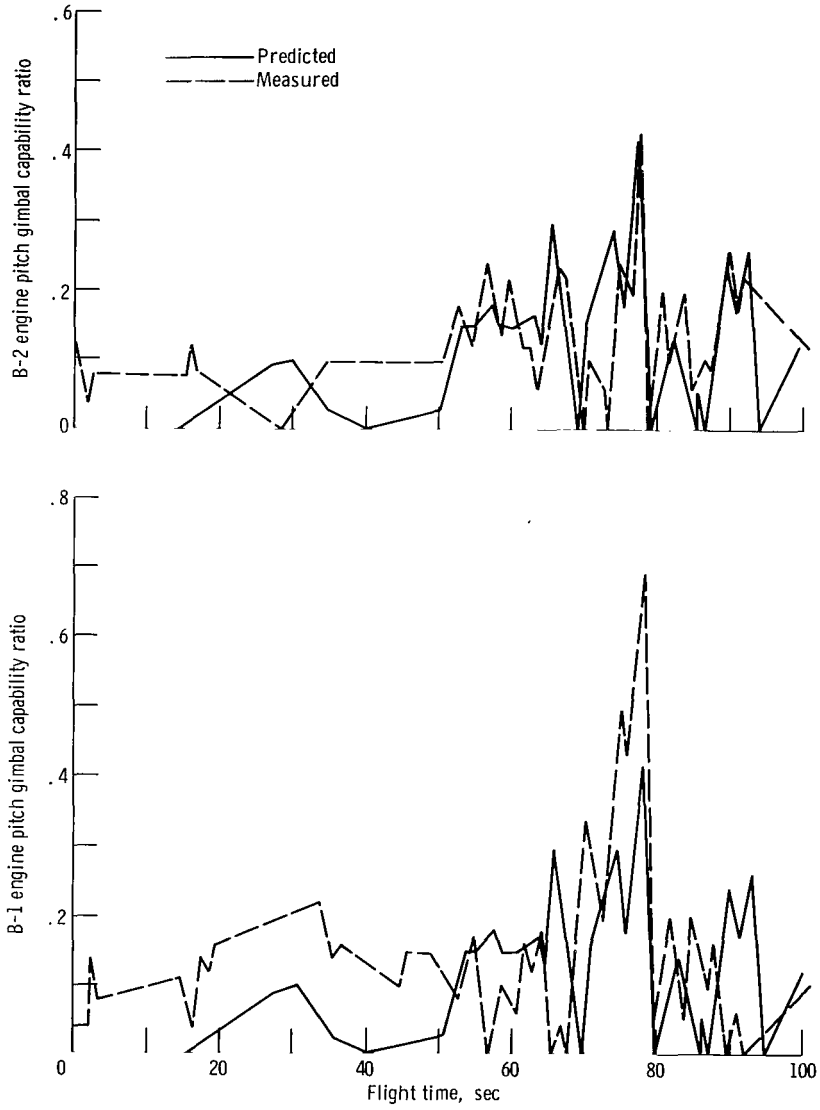

Figure V-55. - Atlas booster engine pitch gimbal capability ratio, AC-10.

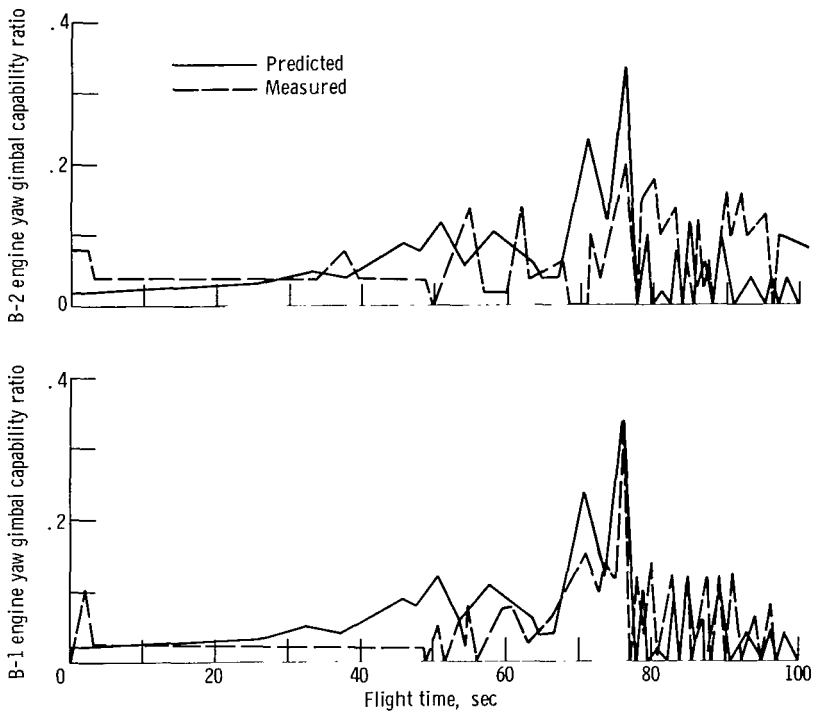

Figure V-56. - Atlas booster engine yaw gimbal capability ratio, AC-10.

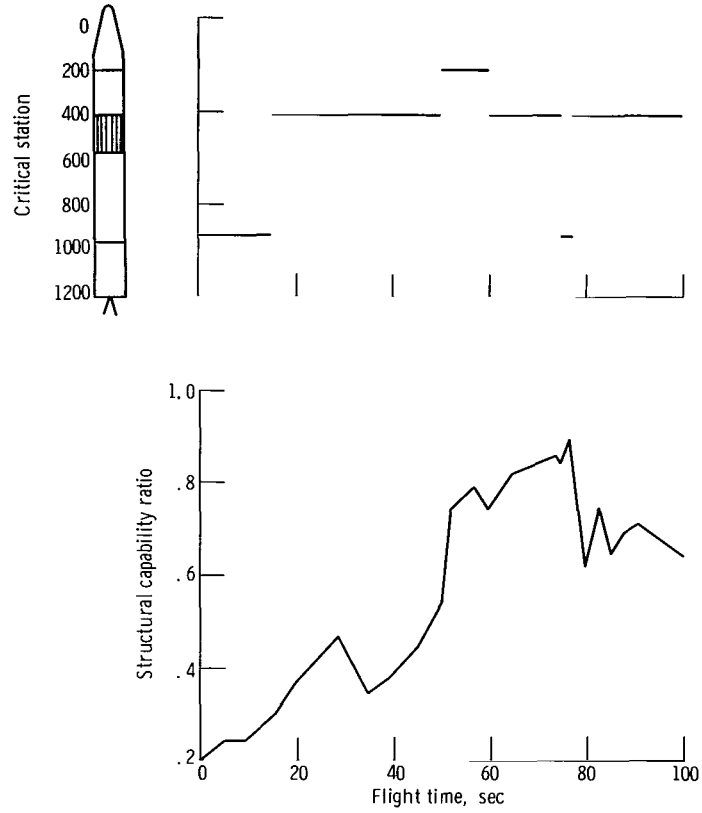

Figure V-57. - Maximum predicted structural capability ratio (total equivalent predicted bending moment)/(bending moment allowable) and critical station, AC-10.

SEPARATION SYSTEMS

by Thomas L. Seeholzer

System Description

The Atlas-Centaur vehicle required the separation of stages and certain jettisonable structures during the launch phase. Systems were required for (1) insulation panel separation, (2) nose fairing separation, (3) Atlas-Centaur separation, and (4) spacecraft separation.

Four insulation panels were separated by a flexible linear shaped charge located at the forward, aft, and logitudinal seams. Each panel was jettisoned about two interstage adapter hinge points (fig. V-58). After shaped charge firing, the panels were forced to rotate about the hinge points by (1) center-of-gravity offset, (2) in-flight purge pressure, and (3) elasticity of the panels due to hoop tension. After approximately 45^{o} of rotation, the panels jettisoned free from the Centaur vehicle.

Nose fairing jettison was accomplished by nitrogen gas powered thrustors located at the forward end of the fairings, one in each cone half. The thrustors, when fired, forced the fairing halves to pivot outboard around their respective hinge points. After approximately 35^{o} of rotation, the fairings separated from the Centaur vehicle. Prior to thrustor actuation, the aft circumferential connection to the Centaur tank was severed by firing a flexible linear shaped charge (fig. V-59), and the nose fairing split line was opened by release of eight pyrotechnically operated pin puller latches.

Atlas-Centaur separation, as shown in figure V-60, was accomplished by a flexible linear shaped charge which cut the interstage adapter circumferentially near its forward end. The Atlas and interstage adapters were then separated from Centaur by retrorockets which fired approximately 0.1 second later. The spacecraft was separated from Centaur by three pyrotechnically operated pin puller latches mounted on the forward payload adapter, as shown in figure V-61. Separation force was provided by three mechanical spring assemblies, each having a 1-inch stroke, which were mounted adjacent to each separation latch on the forward adapter.

System Performance

Insulation-panel separation. - A review of the flight data indicated that all four panels separated and jettisoned normally. Twenty-four breakwires were attached to the insulation panel hinge arms and the interstage adapter to record panel separation, as shown in figure V-62. Eight breakwires, one on each hinge, recorded panel separation after a

35^{o} panel rotation, and eight additional breakwires recorded panel separation after a 0.5-inch displacement of hinge arm from hinge pin. For normal jettison, the 35^{o} breakwires break first while hinge arms are engaged on hinge pins. The 0.5-inch breakwires break after the panels have separated from the hinge pins. In addition, eight break-corner breakwires were installed on each aft corner of the insulation panels to determine if the panels fail during jettison. The breakwire data verified that panels did not break or come out of the hinges prematurely.

Nose fairing separation. - Separation of the nose fairing occurred at T + 202.8 seconds. There was a slight transient in the vehicle roll rate at this time, but it did not produce any detrimental effects. As expected, no pressure buildup in the payload compartment occurred at nose fairing thrustor bottle actuation (fig. V-63).

Atlas-Centaur separation. - Vehicle staging was initiated by firing of the linear shaped charge at T + 241.3 seconds which severed the interstage adapter at station 413. The retrorockets mounted around the aft end of the Atlas fired approximately 0.1 second later to decelerate the booster. Accelerometer data indicated that all eight retrorockets ignited.

The critical motion was in pitch as there was less radial clearance between the interstage adapter and the Centaur in the y-z plane. The gyros indicated an apparent rotation in the pitch plane of 0.03^{o} between the two stages as the Atlas cleared the Centaur. The resulting vertical motion at the separation plane was approximately 0.3 inch, which represents the lowest level of pitch motion yet observed during staging. All the flight data indicated that a positive clearance existed between stages during separation.

The steering gyros mounted on the Atlas indicated that it rotated about its yaw axis approximately 0.18^{o} at the time it cleared the Centaur. This rotation created a lateral displacement at the forward end of the interstage adapter of 1.8 inches.

Spacecraft separation. - Centaur-Surveyor separation occurred at T + 756.9 seconds. Data from extensometers on separation spring assemblies indicated that all three separation latches actuated within 2 milliseconds of each other. The three jettison spring assemblies were calibrated, as shown in figure V-64. These springs operated normally during flight and yielded approximately identical data for stroke against time, as shown in figure V-65. The separation was normal producing no significant spring induced angular rate in the spacecraft.

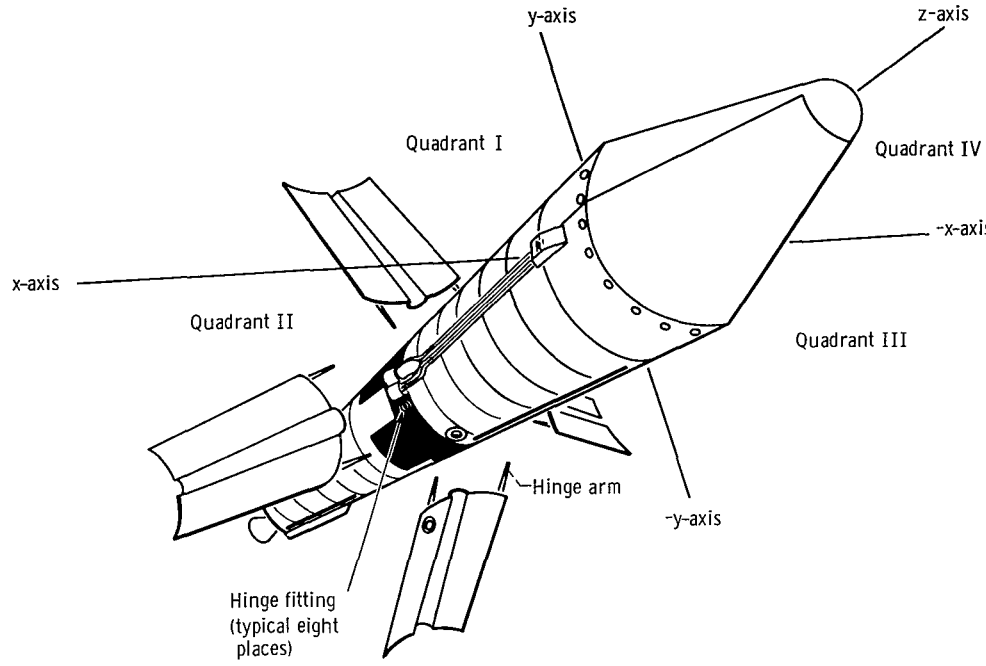

Figure V-58. - Jettisonable insulation panel system, AC-10.

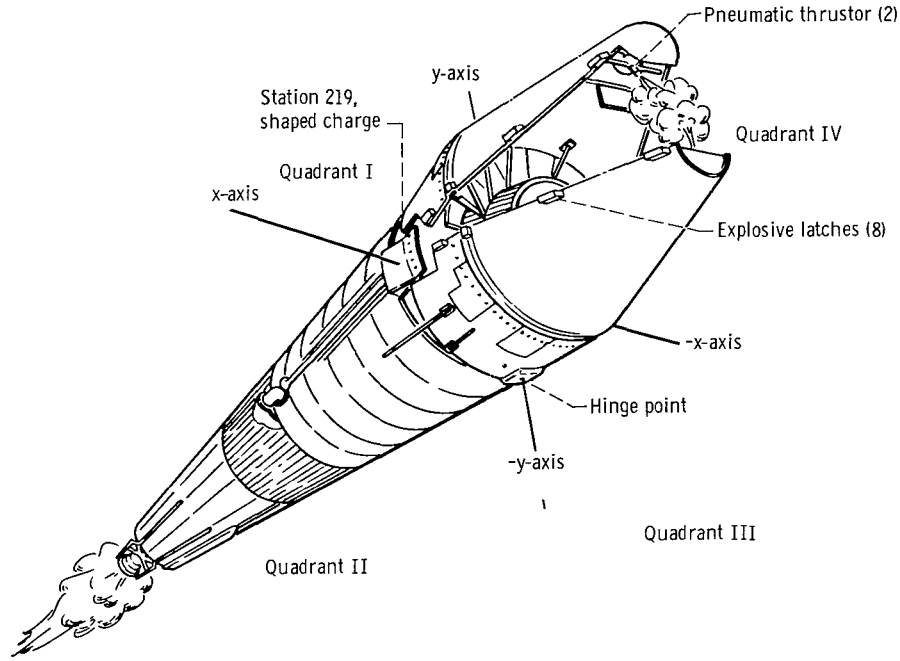

Figure V-59. - Surveyor nose fairing jettison, AC-10.

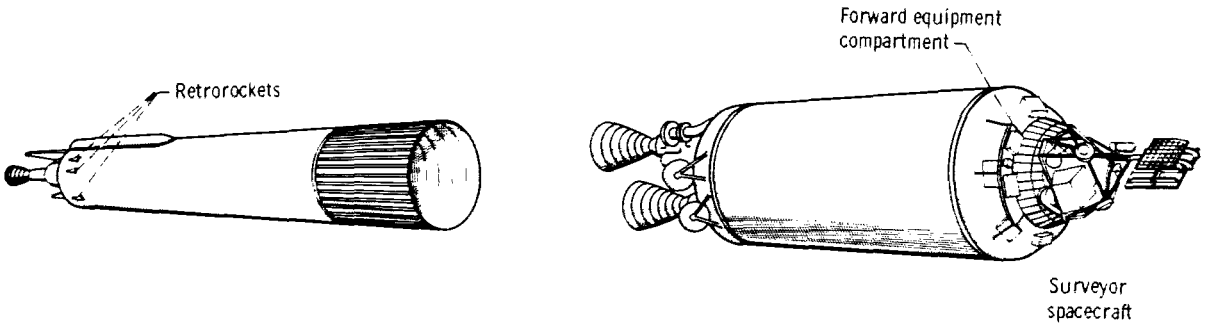

Figure V-60. - Atlas-Centaur separation, AC-10.

CD-9521

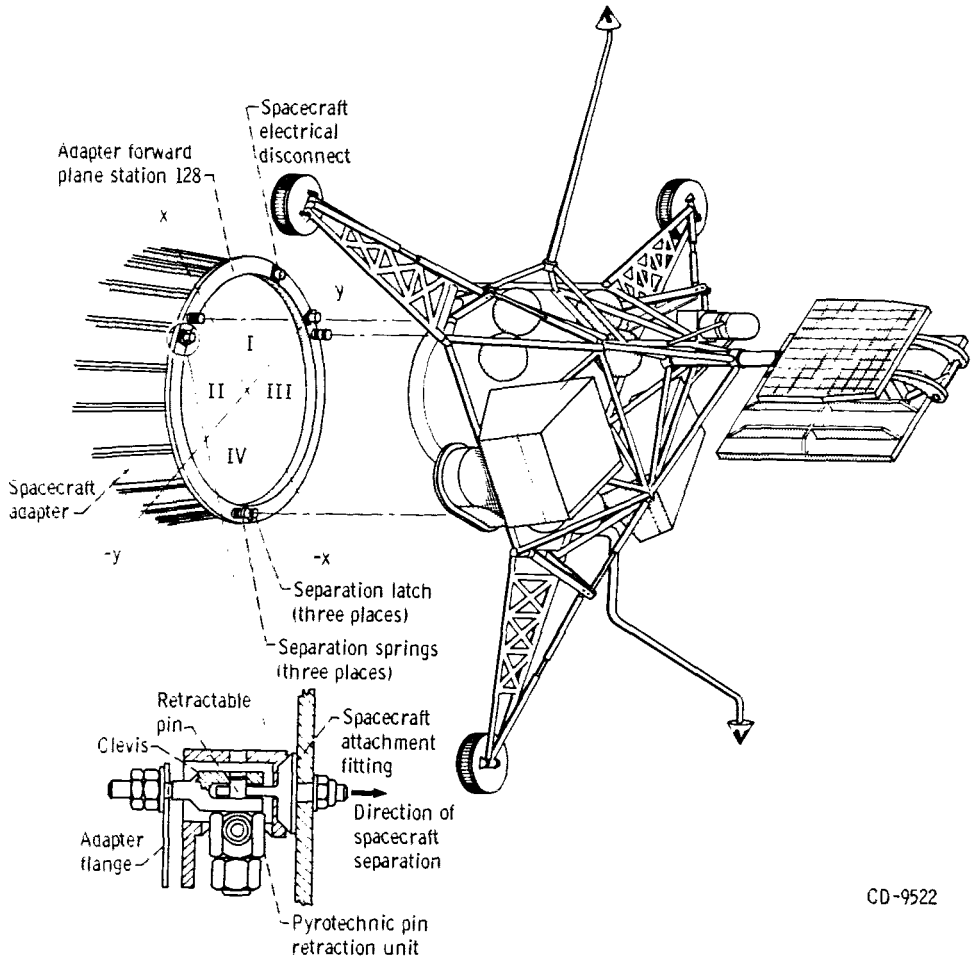

CD-9522

Figure V-61. - Centaur-Surveyor separation, AC-10.

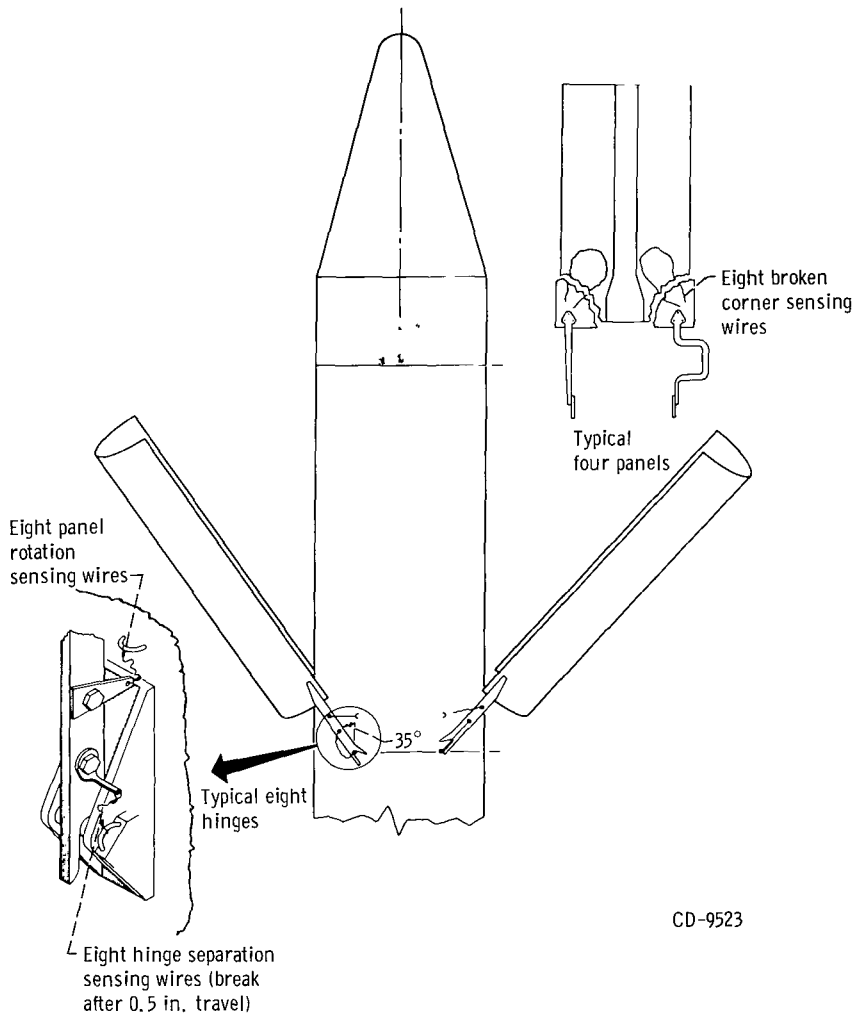

Figure V-62. - Insulation panel breakwire locations, AC-10.

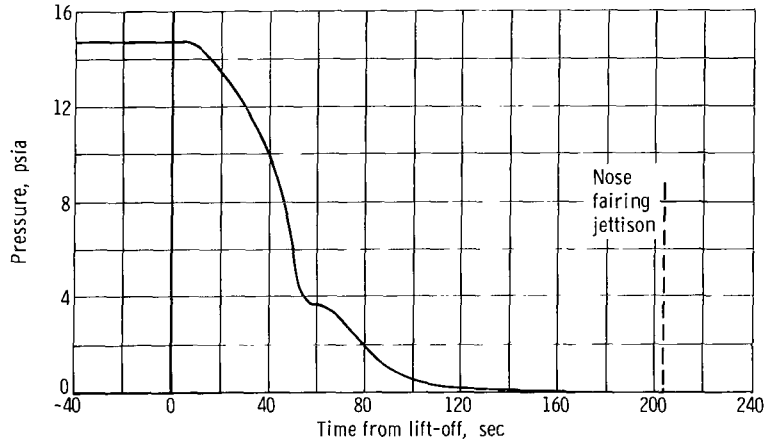

Figure V-63. - Payload compartment pressure, AC-10.

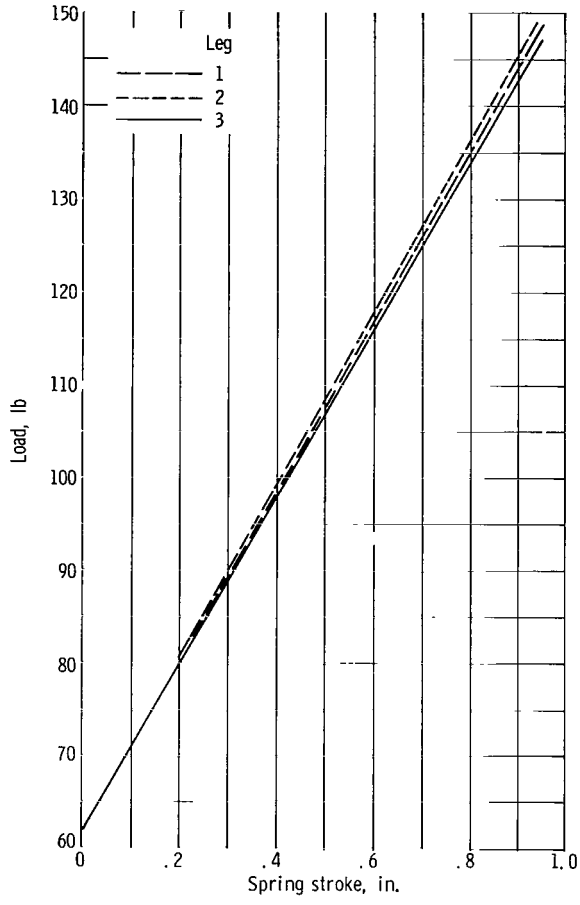

Figure V-64. - Surveyor jettison spring calibration at Eastern Test Range, AC-10.

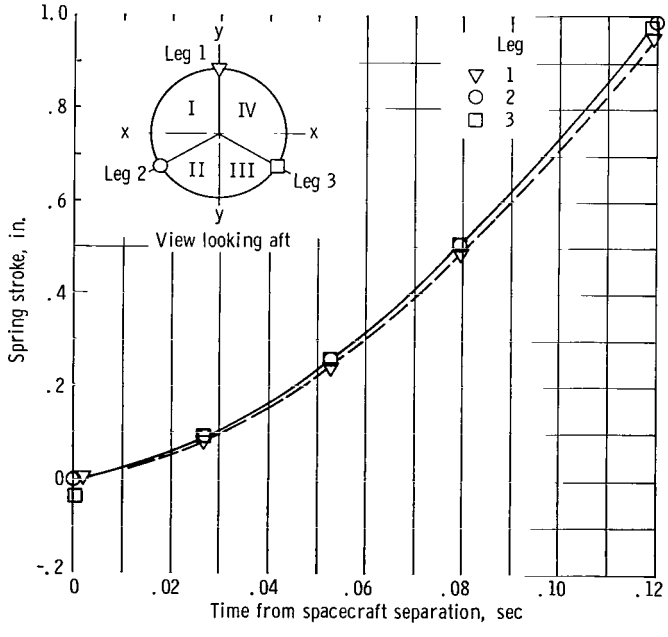

Figure V-65. - Centaur-Surveyor separation spring assemblies, AC-10.

GUIDANCE AND FLIGHT CONTROL SYSTEMS

by Donald F. Garman, William J. Middendorf, Edward R. Ziemba,
and Theodore W. Porada

The functions of the guidance and flight control systems were to stabilize, control, and sequence flight events of the Atlas-Centaur vehicle from lift-off through completion of the Centaur retromaneuver after spacecraft separation. These functions were accomplished by using a self-contained inertial guidance system in the Centaur stage and individual flight control systems in the Atlas and Centaur stages. The objective was to guide the launch vehicle to the injection point and establish the required launch vehicle velocity necessary to place the Surveyor spacecraft in a lunar transfer orbit. The systems had the capability to compensate for trajectory dispersions resulting from thrust misalinement, winds, and performance variations in Atlas and Centaur. Capability existed for either a direct ascent or a parking orbit ascent to the injection point. A direct ascent mission was used for the AC-10 flight. Three modes of operation for stabilization and control of the launch vehicle were used. These modes were rate stabilization, open loop control, and closed loop control. These modes are shown in simplified block diagram form in figure V-66, and the time periods of each mode are shown in figure V-67.

The purpose of the rate stabilization mode was to maintain the vehicle with near zero rotational rates about the vehicle pitch, yaw, and roll axes. This was done by sensing rotational rates with rate gyros (one for each axis) and gimbaling the engines or using the hydrogen peroxide attitude control system after Centaur main engine cutoff to counter any vehicle angular rates. This mode was used only for short periods of time after Atlas-Centaur separation and after Centaur main engine cutoff.

The open loop control mode was accomplished by combining the rate gyro information with displacement information. Rate integrating gyros (one each for pitch, yaw, and roll axes) were used to provide a reference attitude from which vehicle angular displacement was measured. Engine gimbaling provided directional thrust which resulted in vehicle movement to zero-out the displacement difference angle. The reference attitude was programmed to vary in discrete steps as a function of time. This commanded the vehicle to go from a vertical toward a horizontal attitude and also to roll the vehicle to the required launch azimuth angle. This is called open loop control since there was no method to measure the actual angles through which the vehicle rotated and compare it to the commanded angles. The open loop control mode was used only during Atlas booster phase of flight.

Closed loop control was accomplished by combining the rate gyro information with displacement information from the guidance system. This displacement position in-

formation was the difference between desired position and actual or measured position. The term "closed loop control" denotes this method of operation where the error signal is generated by the difference between the desired or command signal and the measured output of the system. Closed loop control was used during Atlas sustainer and Centaur phase of flight. This type of control was used for only two axes, pitch and yaw. During Atlas sustainer phase, the roll displacement information was provided by the Atlas rate integrating gyro. During the Centaur phase of flight, the roll axis was stabilized only by the rate gyro information. Figure V-68 is a simplified diagram of the guidance and flight control systems interface showing the summation points for the three different modes of operation.

The sequencing of flight events was another shared function between the flight control systems and the guidance system. Shared is used in the sense that one system could initiate a period of performance, such as main engine start and another system could terminate that period of performance, such as main engine cutoff. Table V-XII lists the main events commanded by these systems and identifies the system that originated the discrete command for the flight event.

TABLE V-XII. - GUIDANCE AND FLIGHT CONTROL SYSTEMS

SHARED DISCRETE COMMANDS, AC-10

Event	Originating source of discrete command
Guidance to flight condition	Guidance launch equipment
Enable Atlas flight control system	42-in.-rise umbilical ejection
Start roll program	Atlas flight control
Start pitch program	Atlas flight control
Booster engine cutoff	Guidance
Start guidance steering	Atlas flight control
Sustainer engine cutoff	Atlas flight control
Atlas-Centaur separation	Atlas flight control
Centaur main engine start	Centaur flight control
Start guidance steering	Centaur flight control
Accept a main engine cutoff command	Centaur flight control
Main engine cutoff	Guidance
Separate spacecraft	Centaur flight control
Provide retromaneuver steering vector	Guidance
Start guidance steering	Centaur flight control
Calibrate telemetry on	Guidance
Calibrate telemetry off	Guidance
Centaur power to external	Centaur flight control

The following sections are organized to present the description and performance of each system in the order of (1) guidance system, (2) Atlas flight control system, and (3) Centaur flight control system.

Guidance System

System description. - The AC-10 Centaur guidance system was an inertial system which was completely independent from ground control after entering flight condition approximately 7 seconds before lift-off of the vehicle. The guidance system performed the following functions:

(1) Measured vehicle acceleration in fixed inertial coordinates

(2) Computed vehicle velocity, actual present position, and steering signals

(3) Determined time of discrete events

A simplified block diagram of the guidance system is shown in figure V-69.

Inertial measuring units: The function of measuring vehicle acceleration was accomplished by the following three units of the five units which comprise the complete quidance system:

(1) Inertial platform unit contained the gimbal assembly, gyros, and accelerometers

(2) Pulse rebalance, gyro torquer, and power supply unit contained the electronics associated with the accelerometers

(3) Platform electronics unit contained the electronics associated with the gyros

The remaining two units, the navigation computer and the signal conditioner, are discussed later in this section.

A platform assembly with four gimbals provided a three-axis coordinate system with a redundant fourth axis. The gimbals were used to isolate the inner or azimuth gimbal from movements of the vehicle airframe. A gimbal diagram is shown in figure V-70. The four gimbals allowed complete rotation of all three vehicle axes about the platform without gimbal lock. Gimbal lock is a condition where two axes coincide and 1 degree of freedom is lost. The inertial components, three gyros, and three accelerometers, were mounted on the azimuth gimbal. A gyro and an accelerometer were mounted as a pair with the input axes of each pair parallel. These gyro-accelerometer pairs were also alined on three mutually perpendicular (orthogonal) axes corresponding to the three axes of the platform.

The three gyros used were the single-degree-of-freedom, floated-gimbal, rate-integrating types. Each of the three axes of the platform was controlled by a gyro, the only function of which was to maintain that axis fixed in inertial space. Control was provided by inputing the gyro signal to a servoamplifier. The output of the amplifier controlled a direct drive gimbal torque motor. Since the inner gimbals were fixed to an

inertial reference and the outer gimbal was fixed to the vehicle, the angles between the gimbals were used for an analog transformation of steering signals from inertial coordinates to a vehicle coordinate system. The analog transformation was accomplished by resolvers, mounted between gimbals, which produced the sine and cosine functions of the gimbal angles.

The three accelerometers used were the single axis, viscous damped, and hinged pendulum types. The accelerometer associated with each axis measured the change in vehicle velocity along that axis as positive or negative pulses depending on an increase or decrease in vehicle velocity. The accelerometer and its associated electronics were designed so that each rebalance pulse, necessary to center the hinged pendulum, represented a unit of change in velocity of approximately 0.1 foot per second. These pulses of incremental velocity were then routed to the navigation computer unit for further processing to provide the outputs of the guidance system.

During launch countdown the inertial measuring units were alined and calibrated for initial conditions. The azimuth axis of the platform, to which the desired flight trajectory was referenced, was established by ground based optical alinement equipment. The remaining two axes of the platform were alined to the local vertical by using two appropriate accelerometers. The platform was then controlled to center the outputs of these accelerometers which alined the platform to the local vertical. Each gyro was calibrated for constant torque drift rate and mass unbalance along the input axis. The accelerometers were calibrated for misalinement of input axes, and the scale factor and zero bias offset of each accelerometer was determined. These prelaunch determined constants were stored in the navigation computer for use during flight.

Navigation computer unit: The navigation computer unit was a serial, binary, digital machine with a magnetic drum memory. The memory drum had a capacity of 2816 words (25 bits per word) of permanent storage, 256 words of temporary storage, and six special purpose tracks. The permanent storage was prerecorded and could not be altered by the computer. The temporary storage track was the working storage of the computer. The incremental velocity pulses from the accelerometers were the information inputs to the navigation computer. The operation of the navigation computer was controlled by a program prerecorded in the permanent memory of the computer. This program allowed the computer to perform three basic operations which are described by the prelaunch equations, navigation equations, and guidance equations.

The prelaunch equations established the initial conditions for the navigation and guidance equations to begin navigating and guiding at approximately 7 seconds prior to lift-off. This conditioning included selecting a reference trajectory, inserting launch pad values of position, and setting various navigation and guidance functions to predetermined initial values.

The navigation equations computed present velocity and present position. The present

(current) velocity was determined by algebraically summing the incremental velocity pulses from the accelerometers and then performing an integration on the computed velocity to determine present position. Corrections for the calibrated gyro and accelerometer constants were also made during the velocity and position determination to improve the navigation accuracy. As an example, the velocity information derived from the accelerometer data was adjusted to compensate for the accelerometer scale factors and zero offset biases that were measured during the launch countdown. The direction of the velocity vector was also adjusted to compensate for the gyro constant torque drift rates that were measured in the launch countdown.

The function of the guidance equations was to guide the vehicle to the required point in space for injection into the desired lunar trajectory. The guidance equations used were of the modified "velocity-to-be-gained" type. These guidance equations only required as inputs present position, present velocity, and the trajectory injection requirements. The equations were "modified" to optimize other mission constraints. Based on the modified-velocity-to-be gained concept, steering signals were generated to guide the vehicle along an optimized flight path from the present position to the desired injection conditions. Using the guidance equations, the navigation computer initiated five discrete commands: (1) booster engine cutoff, (2) backup start Centaur timer, (3) Centaur main engine cutoff, (4) calibrate telemetry on, and (5) calibrate telemetry off. The booster and backup start Centaur timer discrete commands were issued when the measured vehicle acceleration equaled a predetermined value. The Centaur main engine cutoff discrete command was issued when the computed vehicle energy (using measured vehicle velocity) equaled the orbital energy required for injection into the lunar trajectory. The telemetry discrete commands were issued on predetermined fixed time intervals from the backup sustainer discrete command.

Signal conditioner unit: The signal conditioner unit was the link between the guidance system and the vehicle telemetry system. The signals in the guidance system required modification and scaling to match the input range of the telemetry system.

System performance. - The overall performance of the AC-10 guidance system (designated MGS #12B) was excellent with no discrepancies or anomalies noted.

System accuracy: The guidance system performed within the expected limits. Data from 15 hours and 17 minutes of tracking information indicated that the midcourse correction required 20 hours after injection to impact the designed target point would have been 3.8 meters per second (miss only) or 6.4 meters per second (miss plus time of flight).[1]

[1]These values of 3.8 m/sec (miss only) or 6.4 m/sec (miss plus time of flight) are the accuracy values at the time of injection. These are not to be confused with the actual midcourse correction which was selected after spacecraft separation by the mission director (Jet Propulsion Laboratory) to optimize fuel residuals and other mission related parameters. (See section IV. SURVEYOR TRANSIT PHASE and/or ref. 2.)

These midcourse corrections were well within the specified accuracy requirement of not requiring a Surveyor midcourse correction in excess of 50 meters per second. Trajectory perigee was designed to be 90±5 nautical miles. The actual perigee was 91.3 nautical miles.

The overall injection velocity error was caused by three main sources: (1) an error in the prediction of engine shutdown impulse, (2) an error due to the computational techniques used and influenced by the actual trajectory flown, and (3) an error related to the accuracy of the guidance system. The components of the overall injection error are shown in the following table:

Error	Miss only, m/sec	Miss plus time of flight, m/sec
Engine shutdown impulse	6.07	11.02
Computer program	1.02	1.66
Guidance hardware	1.60	2.94
Total error (vector summation)	3.8	6.4

The engine shutdown impulse error vector was in a direction almost directly opposed to the guidance hardware and computer program error vector which resulted in a cancellation effect producing a small total injection error.

The landing conditions for which the computer program was designed and the landing conditions which would have been achieved had no midcourse correction maneuver been made, are listed in the following table:

Landing conditions	Designed	No midcourse correction
Selenographic latitude	3.25° S	11.42° S
Selenographic longitude	43.83° W	54.17° W
Unbraked impact velocity	2662.0 m/sec	2664.2 m/sec
Flight time to Moon	2 days	2 days
	14 hr	14 hr
	58 min	48 min
	27.3 sec	0.2 sec

These data reflect a projected miss of the designed target of about 216 nautical miles, an impact velocity error of 2.2 meters per second, and a flight time difference of 10 minutes, 27.1 seconds early.

Hardware performance: The navigation computer issued the Atlas booster engine cutoff discrete at T + 142.04 seconds. Acceleration of the vehicle at the time of booster cutoff discrete was 5.68 g's which was within the expected range of 5.62 to 5.78 g's. The Centaur main engine cutoff discrete was issued about 1 millisecond early and is within the uncertainty band of the computational technique that was used. All other aspects of computer performance were satisfactory, as demonstrated by the extremely small injection error contributed by the computer program. After booster engine cutoff + 4 seconds, the guidance steering signals were enabled. At this time, normal pitch and yaw corrections were made. Minor pitch and yaw motions, which occurred at Atlas-Centaur separation, were damped out rapidly. Negligible steering commands were observed during Centaur burn, which indicated that the thrust vector was properly alined with the desired velocity vector.

The four platform gimbal servoloops indicated satisfactory performance throughout the flight. Gimbal 1 (azimuth) and 2 (roll) oscillated at a frequency of about 2 hertz from the time of transfer to internal power until the end of the flight. Gimbal 1 oscillations were the largest and were equivalent to a platform displacement of about 5 arc-seconds peak to peak. These oscillations appeared to be unrelated to vehicle dynamics and have been observed on previous vehicles during ground testing of other missile guidance sets. There appeared to be no detrimental effect on vehicle performance resulting from these oscillations. Other low frequency oscillations (0.2 to 2.0 Hz) which were noted on all four gimbals appeared to be the result of vehicle dynamics. From T - 7 seconds and on, the predicted gyro drift was analytically compensated for by the guidance equations. On prior flights, the gyros were torqued to compensate for their predicted drift. The injection accuracy of this flight demonstrated the validity of the technique of analytical compensation.

Data from the accelerometers and the associated electronics indicated satisfactory performance of these components throughout the flight.

Flight Control Systems

Atlas system description. - The Atlas flight control system provided the primary functions required for vehicle stabilization, control, execution of guidance steering signals, and electronically timed switching sequences.

The Atlas flight control system comprised the following principal units:

(1) The displacement gyro unit consisted of three single-degree-of-freedom, floated,

rate-integrating-type gyros. These gyros were mounted to the vehicle airframe in an orthogonal triad configuration alining the input axis of a gyro to its respective vehicle axis of pitch, yaw, or roll.

(2) The rate gyro unit contained three single-degree-of-freedom, floated, rate gyros. These gyros were mounted in the same manner as the displacement gyro unit.

(3) The servoamplifier unit contained electronics to sum signals algebraically, amplify, and accept feedbacks signals of engine position.

(4) The programmer unit contained an electronic timer, arm-safe switch, power switches, the fixed pitch program, and circuitry to set the roll program from launch ground equipment.

During the Atlas booster phase, pitch and yaw open loop control was accomplished by gimbaling the booster engines. Roll open loop control was accomplished by gimbaling the vernier engines in roll and differential gimbaling of booster engines in yaw. During the Atlas sustainer phase, roll open loop control was achieved by differential gimbaling of the vernier engines; pitch and yaw closed loop control was provided by gimbaling the sustainer engine.

At 42-inch rise + 1 second, a roll rate of 0.2 degree per second was commanded to rotate the vehicle from the azimuth of the launcher to the azimuth required for the flight trajectory. At T + 15 seconds, the roll program was disabled and a pitch program initiated. One of four available seasonal pitch program kits had been selected and installed months prior to launch. These programs allowed a choice in the vehicle pitch trajectory to compensate for expected seasonal differences in upper atmosphere winds. The pitch program was a timed sequence of pitch rates which were designed to control the vehicle during ascent through the atmosphere with acceptable aerodynamic heating conditions and at near zero angle of attack.

The functions performed by the Atlas flight control system to stabilize and control the vehicle were previously discussed in this section. Also, discussed previously were the issuance of discrete commands that had a shared relation to commands issued by the guidance system. In addition to these "shared" commands, many other timed discrete commands were issued by this system.

Atlas system performance. - The flight control system performed satisfactorily throughout the Atlas phase of flight. The control corrections required because of vehicle disturbances were well within the control system capability. Table V-XIII summarizes the analysis of flight disturbances. The transient response resulting from each flight event was evaluated in terms of amplitude, frequency, and duration as observed on rate gyro data. In this table, the percent control capability at the time of each disturbance is also listed. The percent control capability is the amount of engine gimbal angle used with respect to the total engine gimbal angle capability available. The control capability shown in the table V-XIII includes that necessary for correction of the vehicle disturbance and

TABLE V-XIII. - VEHICLE DYNAMIC RESPONSE TO FLIGHT DISTURBANCES, AC-10

Event	Flight time, sec	Measurement	Rate gyro amplitude (peak to peak), deg/sec	Transient frequency, Hz	Transient duration, sec	Required percent control capability
Lift-off transients 42-in. rise	T + 0.96	Pitch	1.12	0.67	2	16
		Yaw	1.04	.67	4	6
		Roll	1.52	No fundamental frequency		6
Maximum aerodynamic loads	Data reviewed for maximum rates between T + 70 and T + 80	Pitch	1.52	0.67	10	71
		Yaw	1.12	.5	10	28
		Roll	.4	1	10	28
Booster engine cutoff	T + 142.0	Pitch	2.08	5	2.2	16
		Yaw	.6	5	2.2	9
		Roll	.8	3.5	2	9
Booster engine jettison	T + 145.1	Pitch	0.72	2.5	0.5	24
		Yaw	3.36	.77	3	61
		Roll	2.96	.833	3	16
Start guidance steering	T + 150.0	Pitch	1.28	1.67	1.5	48
		Yaw	1.36	.833	4	38
		Roll	.72	.833	5	4
Insulation panel jettison	T + 176.2	Pitch	0.64	10	0.8	10
		Yaw	.4	5	2	2
		Roll	1.44	4	1	4
Nose fairing jettison	T + 202.8	Pitch	1.92	20	1	10
		Yaw	.32	12.5	.3	1
		Roll	1	1.67	1	4
Sustainer engine cutoff	T + 234.4	Pitch	Smooth separation - no noticeable transients			
		Yaw				
		Roll				

the capability used for steady-state requirements, such as gimbal angle required to execute the pitch program.

The programmer was started at 42-inch rise which occurred at approximately T + 0.96 second. The roll error was near zero by T + 2 seconds using 6 percent of the control capability. At T + 2 seconds, an estimated roll rate of 0.24 degree per second was sensed, indicating the roll program had been initiated. The errors in pitch and yaw approached zero by T + 4 seconds using 6 percent of the control capability. The pitch

program was observed to start at T + 15.4 seconds with a pitch rate of -0.56 degree per second.

During a 10-second period around T + 75 seconds, aerodynamic forces required the maximum control response in pitch, yaw, and roll. During this period of maximum aerodynamic loading, 71 percent of the control capability was required to overcome both steady-state and transient loading. For the aerodynamic conditions based on the T + 9 minute balloon data, the maximum predicted control requirement for both steady-state and transient disturbances was 68 percent.

The booster engines were cut off at T + 142.04 seconds. The rates imparted to the vehicle by the transients were damped out in 2.2 seconds using a maximum of 11 percent of the sustainer engine gimbal capability. The booster engines were jettisoned at T + 145.04 seconds. The rates imparted to the vehicle by booster jettison required a maximum of 36 percent of the total control capability to stabilize the vehicle.

Prior to the sustainer portion of flight, the Atlas flight control system provided the vehicle displacement reference. At T + 150.04 seconds, the Centaur guidance system was used as the displacement reference. The new displacement command resulting from the change in reference required 23 percent of the total control capability. The maximum vehicle rate during this change was 1.36 degrees per second peak to peak. The vehicle stabilized on the new reference within 5 seconds.

Insulation panels and nose fairings were jettisoned at T + 175.84 seconds and T + 202.76 seconds, respectively. The maximum vehicle transient observed due to these disturbances was a peak-to-peak pitch rate of 1.92 degrees per second. The maximum control capability used to overcome the jettison forces was 4 percent.

Sustainer engine cutoff occurred at T + 239.38 seconds. Atlas-Centaur separation was smooth with no noticeable transients.

Centaur system description. - The Centaur flight control system provided primary functions required for vehicle stabilization and control during Centaur powered flight, for execution of guidance steering signals, and to provide timed switching sequences for programmed flight events. A simplified block diagram of the Centaur flight control system is shown in figure V-71.

The Centaur flight control system comprised the following principal units:

(1) The rate gyro unit contained three single-degree-of-freedom, floated, rate gyros with electronics for channel selection and signal amplification. These gyros were mounted to the vehicle in an orthogonal triad configuration alining the input axis eye of the gyro to its respective vehicle axis eye of pitch, yaw, or roll.

(2) The servoamplifier unit contained the threshold and logic circuitry for the hydrogen peroxide engines and the required electronics to control the main engine actuators.

(3) The electromechanical timer unit contained a 400-hertz synchronous motor which provided the time reference. The motor drove a mechanical arrangement of shafts and

cams which activated switch contacts. The switches were used as control inputs for the auxiliary electronics unit.

(4) The auxiliary electronics unit contained logic, relay switches, transistor power switches, power supplies, and an arm-safe switch. Signals from these devices then controlled sequencing of other subsystems. The arm-safe switch electrically isolated the pyrotechnic devices and valve actuators from control switches.

Vehicle steering during Centaur powered flight was by thrust vector control through gimbaling of the two main engines. There were two actuators for each engine to provide pitch, yaw, and roll control. Pitch control was accomplished by moving both engines in the pitch plane. Yaw control was accomplished by moving both engines in the yaw plane, and roll control was accomplished by differentially moving the engines in the yaw plane. Thus, the yaw actuator responded to an algebraically summed yaw-roll command. By controlling the direction of thrust of the main engines, the flight control system maintained the flight of the vehicle on a trajectory directed by the guidance system.

After main engine cutoff, control of the vehicle was maintained by the flight control system using selected constant thrust hydrogen peroxide engines in an "on-off" mode of operation. This was accomplished by threshold and logic circuitry within the flight control system responding to rate and displacement signals.

The functions performed by the Centaur flight control system to stabilize and control the vehicle were previously discussed in this section. Also, discussed was the issuance of discrete commands that had a shared relation to commands issued by the guidance system. In addition to these "shared" commands many other timed discrete commands were issued.

Centaur system performance. - The Centaur flight control system performance was satisfactory throughout the flight. Vehicle stabilization and control were maintained at all times, and all flight programmer discrete events were executed at the required times.

The Centaur timer was started at sustainer engine cutoff (T + 239.38 sec) by a discrete from the Atlas programmer. Appropriate commands were issued for pressurizing the hydrogen tank, centering the Centaur engines, engine prestart and cooldown, and main engine start. Vehicle rates sensed in pitch, yaw, and roll were mild during staging and did not exceed 1.5 degrees per second.

Main engine start was commanded at T + 250.86 seconds. Rates due to engine start transients were not greater than 2.73 degrees per second and were corrected by gimbaling the engines less than 1°. When guidance steering was admitted to the Centaur flight control system 4 seconds after engine start, the vehicle attitude was 1.0° nose high and 4.0° nose right of the desired steering vector. This difference was corrected within 4 seconds.

Vehicle steady-state rates during main engine firing were essentially zero in yaw and roll. Pitch rates in response to closed loop control did not exceed 0.20 degree per

second. Approximately 60 seconds prior to main engine cutoff, the pitchdown rate decreased as the vehicle approached the desired orbital injection conditions, and the guidance velocity-to-be-gained terms approached zero.

Rates imparted to the vehicle due to engine cutoff transients were mild, indicating a small differential impulse. Maximum disturbance rate was 0.76 degree per second in roll. Coincident with main engine cutoff, closed loop control was terminated. The hydrogen peroxide attitude control system was activated, and these engines fired only if vehicle rates exceeded 0.2 degree per second. Vehicle disturbances were almost negligible and the hydrogen peroxide attitude control engines fired only 3 percent of the time.

After Centaur main engine cutoff, the timer issued commands to prepare the spacecraft for separation, and all required commands were issued properly. At T + 756.91 seconds, the hydrogen peroxide attitude control system was deactivated for 5 seconds, and the spacecraft was successfully separated from Centaur. The hydrogen peroxide attitude control system was deactivated during this time to preclude collision of the Centaur vehicle with the spacecraft.

The retromaneuver was initiated at T + 762.0 seconds when the Centaur was commanded to turn approximately 180^{o} to the negative of the injection guidance steering vector. Simultaneously, the attitude control system was activated and began a negative pitch, positive yaw maneuver toward the new vector. Approximately half way (90^{o}) through the turnaround, two of the 50-pound hydrogen peroxide engines were commanded to fire to provide 100 pounds thrust for 20 seconds as planned. Guidance gimbal resolver data indicated that the vehicle turned through 161^{o} in approximately 104 seconds to the new vector. The total angle and the turnaround time were within the expected dispersions.

At T + 997 seconds, the engine prestart valves were opened to allow the residual propellants to blow down through the main engines. Coincident with the start of this blowdown, the engine thrust chambers were gimbaled to aline the thrust vector through the vehicle center of gravity. Thrust from the propellant blowdown provided adequate separation between the Centaur and Surveyor spacecraft. Separation distance at the end of 5 hours was 1054 kilometers. This was more than three times the required separation distance to prevent the Surveyor star sensor from acquiring the reflected light of Centaur rather than the star Canopus.

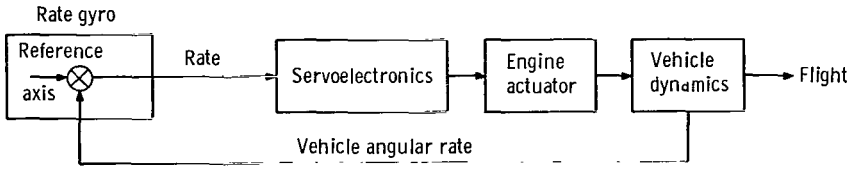

(a) Rate stabilization.

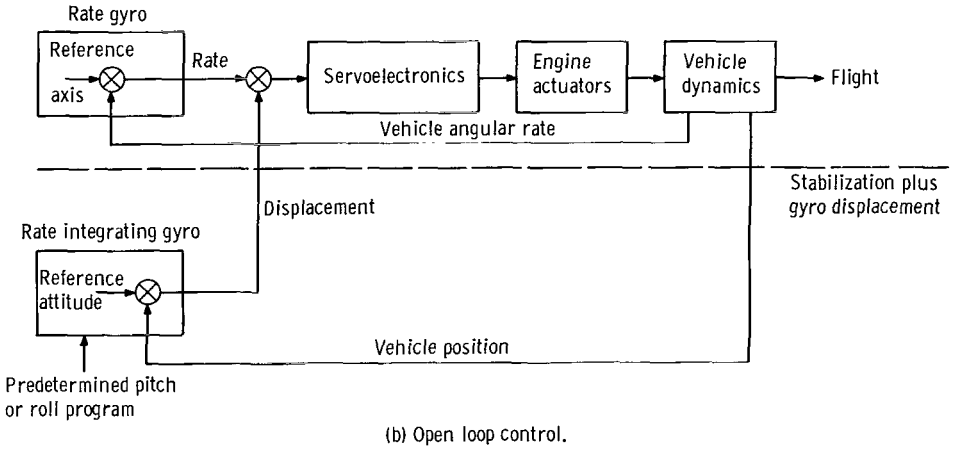

(b) Open loop control.

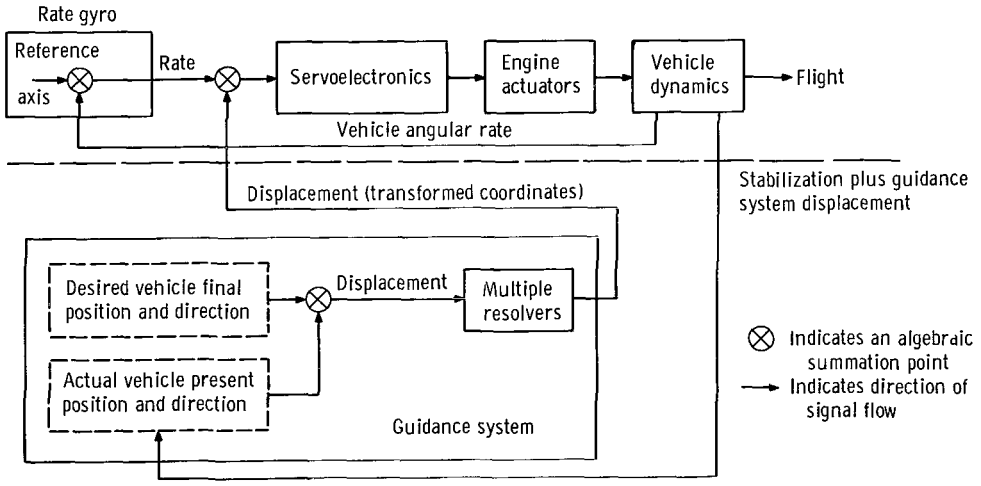

(c) Closed loop control.

Figure V-66. - Guidance and flight control modes of operation, AC-10.

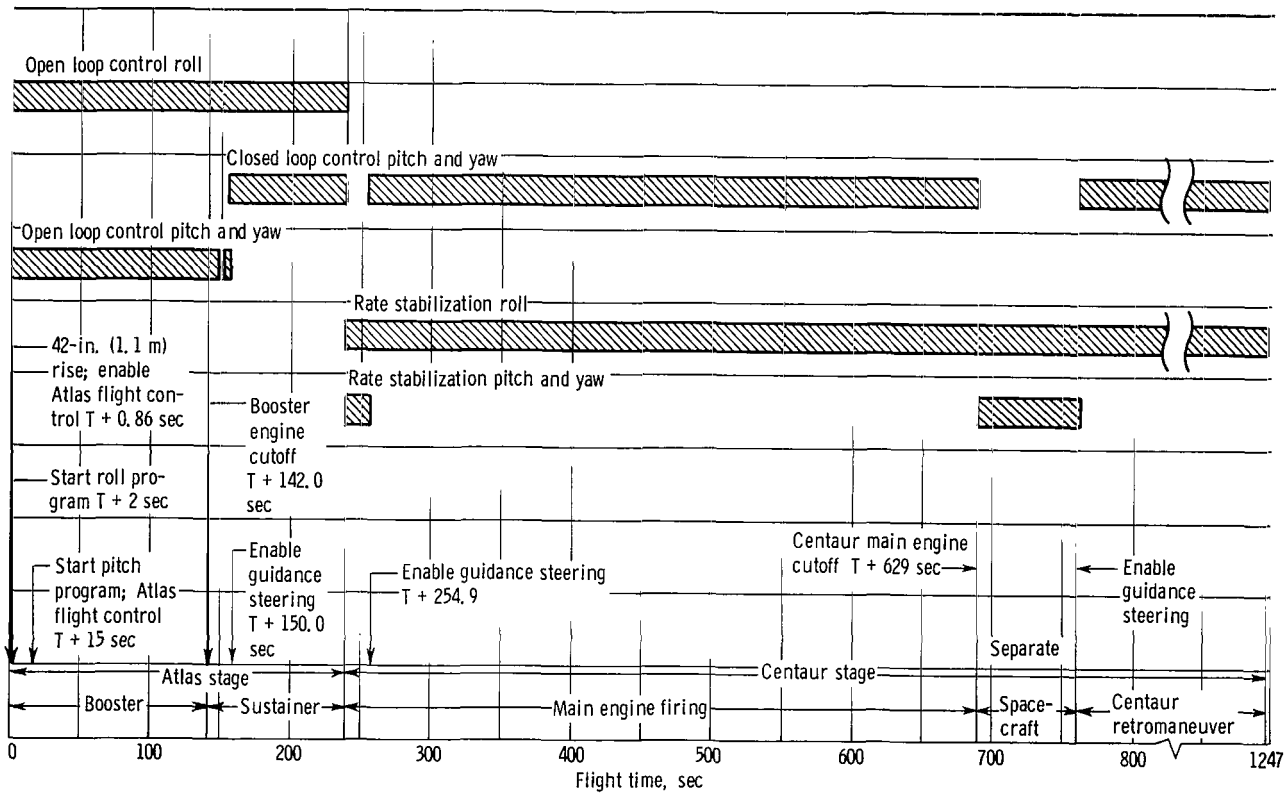

Figure V-67. - Guidance and flight control modes of operation, AC-10.

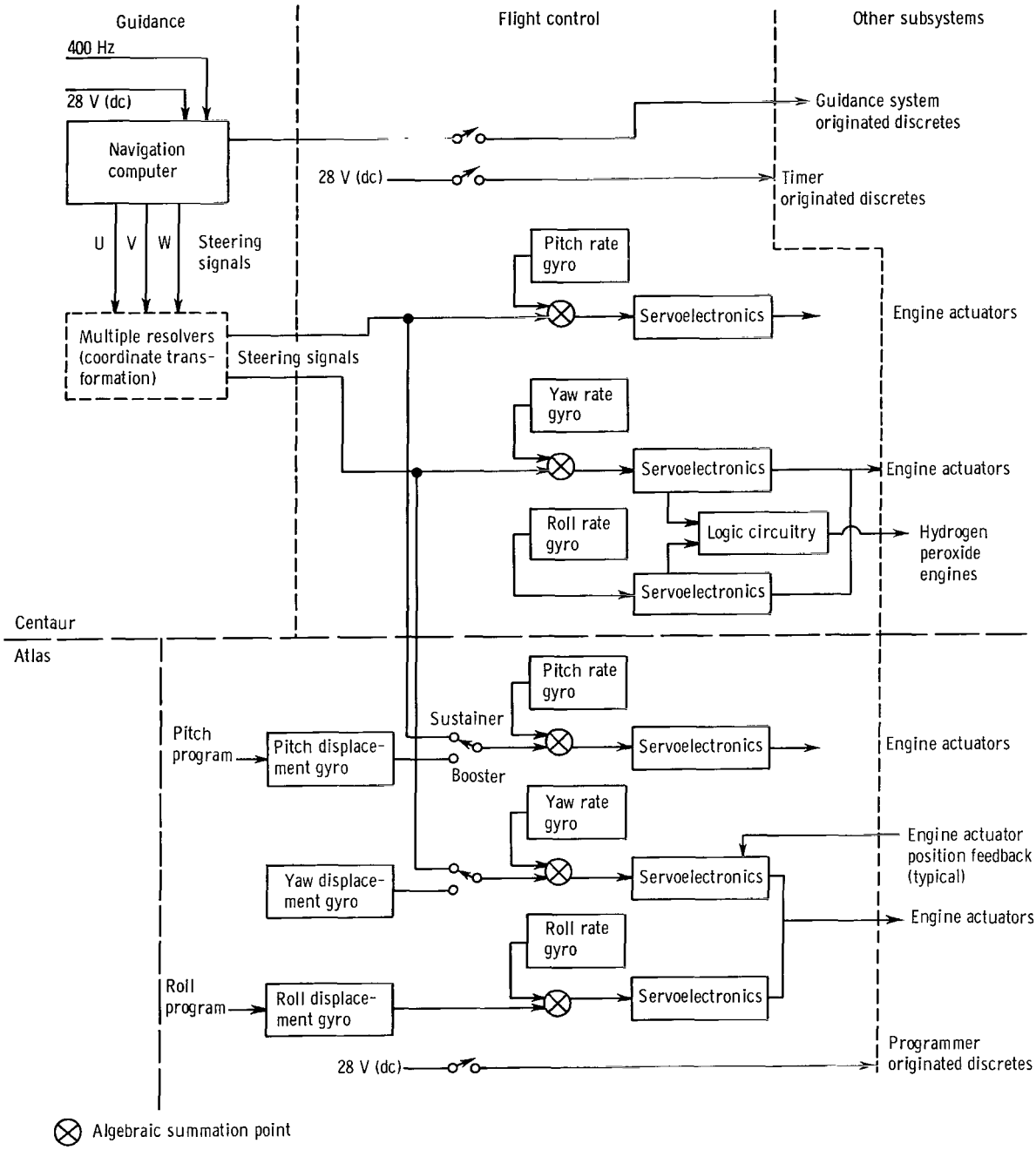

Figure V-68. - Simplified guidance and flight control systems interface, AC-10.

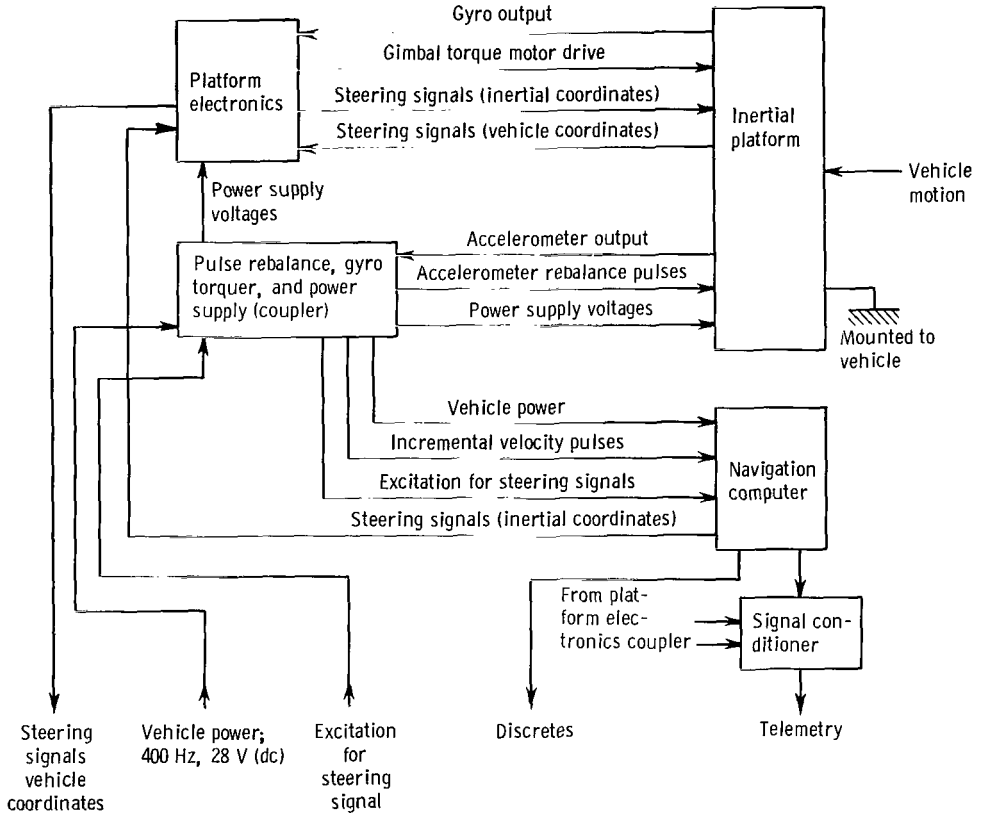

Figure V-69. - Simplified block diagram of Centaur guidance system, AC-10.

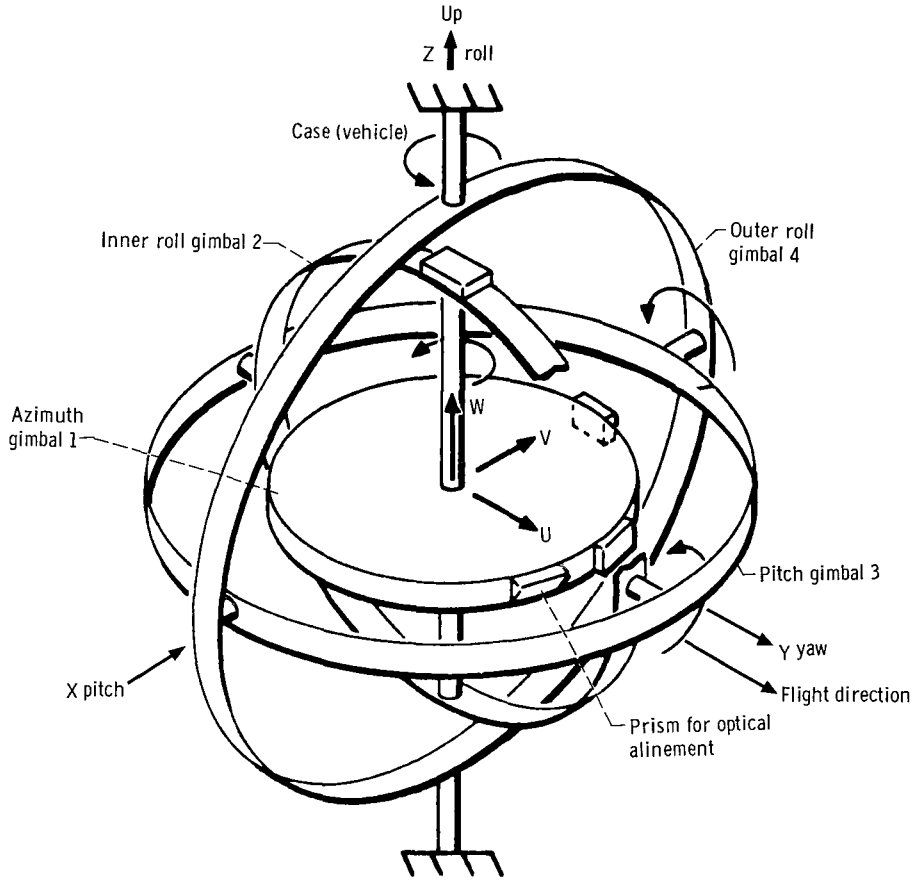

Figure V-70. - Gimbal diagram, AC-10. Launch orientation: inertial platform coordinates, U, V, and W; vehicle coordinates, X, Y, and Z.

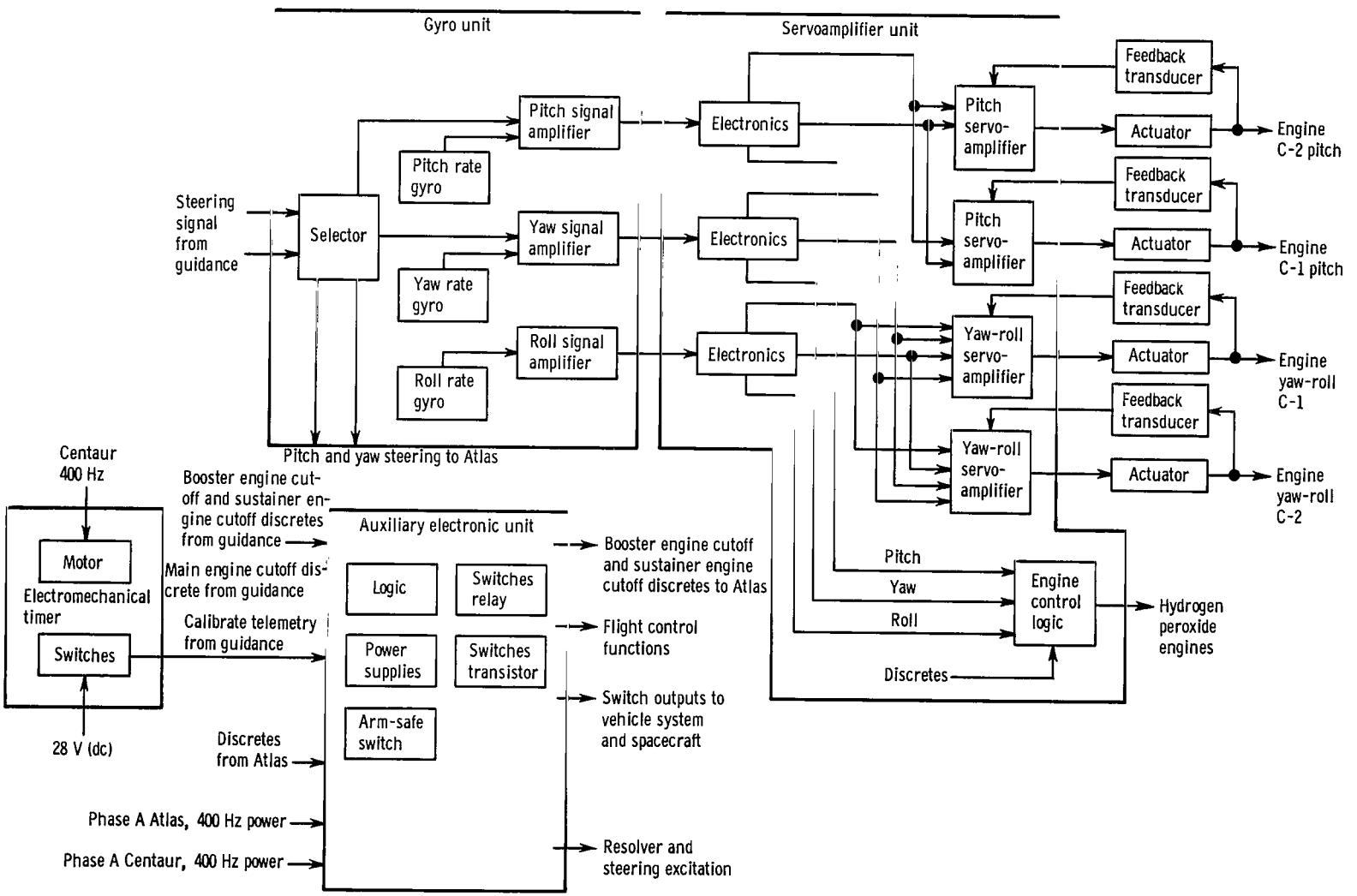

Figure V-71. - Centaur flight control system, AC-10.

APPENDIX A

SUPPLEMENTAL FLIGHT, TRAJECTORY, AND PERFORMANCE DATA

by John J. Nieberding

POSTFLIGHT VEHICLE WEIGHT SUMMARY

The postflight weight summary for the Atlas-Centaur vehicle AC-10 with the Surveyor spacecraft SC-1 is given in tables A-I and A-II.

TABLE A-I. - ATLAS POSTFLIGHT VEHICLE WEIGHT SUMMARY

	Weight, lb
Booster jettison weight:	
Booster dry weight	6 172
Booster residuals	1 126
Unburned lubrication oil	31
Total	7 329
Sustainer jettison weight:	
Sustainer dry weight	5 402
Sustainer residuals	1 461
Interstage adapter	1 025
Unburned lubrication oil	17
Total	7 905
Ground expendables:	
Fuel (RP-1)	548
Liquid oxygen, oxidizer	1 835
Lubrication oil	3
Exterior ice	50
Liquid nitrogen in helium shrouds	140
Pre-ignition gaseous oxygen loss	450
Total	3 026
Flight expendables:	
Main impulse (RP-1)	75 648
Main impulse oxygen	171 594
Helium panel purge	6
Oxidizer vent loss	15
Lubrication oil	171
Total	247 434
Total Atlas weight at lift-off:	
Booster jettison	7 329
Sustainer jettison	7 905
Flight expendables	247 434
Total	262 668

TABLE A-II. - CENTAUR POSTFLIGHT VEHICLE WEIGHT SUMMARY

	Weight, lb
Basic hardware:	
Body group	972
Propulsion group	1 194
Guidance group	314
Control group	140
Pressurization group	139
Electrical group	268
Separation equipment	78
Flight instrumentation	274
Miscellaneous equipment	133
Total	3 512
Centaur flight expendables:	
Main impulse hydrogen	4 982
Main impulse oxygen	24 793
Inflight chilldown hydrogen	24
Inflight chilldown oxygen	33
Booster phase vent hydrogen	40
Booster phase vent oxygen	42
Sustainer phase vent hydrogen	18
Sustainer phase vent oxygen	30
Hydrogen peroxide, boost pumps	49
Helium, tank pressurization	1
Total	30 012
Jettisonable hardware:	
Nose fairing	1 964
Insulation panels	1 174
Ablated ice	50
Total	3 188

	Weight, lb
Centaur residuals:	
Liquid hydrogen, trapped	72
Liquid oxygen, trapped	68
Liquid hydrogen, burnable	58
Liquid oxygen, burnable	131
Gaseous hydrogen	83
Gaseous oxygen	164
Hydrogen peroxide, retromaneuver	18
Hydrogen peroxide, trapped	5
Hydrogen peroxide, reserve	60
Helium	4
Ice	12
Total	675
Ground expendables:	
Hydrogen gas, ground boiloff	22
Oxygen gas, ground boiloff	24
Total	46
Total Centaur weight at lift-off:	
Basic hardware	3 512
Centaur residuals	675
Centaur flight expendables	30 012
Jettisonable hardware	3 188
Total	37 387
Combined launch vehicle lift-off weight:	
Atlas	262 668
Centaur	37 387
Spacecraft	2 193
Total	302 248

ATMOSPHERIC SOUNDING DATA

Ambient Pressure and Temperature

The atmospheric conditions at the launch site were measured by Rawinsonde runs on the day of launch. The actual data shown were measured at 0950 hours eastern standard time. Profiles of measured temperature and pressure are compared with values predicted on the basis of seasonal June weather. Temperature data, as shown in figure A-1, were nearly normal to an altitude of 7.6 nautical miles. Above this altitude, the actual temperatures averaged 5.5^{o} higher than predicted. However, this variation is not significant. The measured pressures, as shown in figure A-2, were in close agreement with the predicted values at all altitudes.

Atmospheric Winds

Wind speed and azimuth data as a function of altitude are compared with the usual June winds data in figures A-3 and A-4. Wind azimuth is the direction in which the wind is blowing. Notable discrepancies existed between the predicted and actual maximum wind speeds at altitudes up to about 9 nautical miles. A maximum wind speed of 65 feet per second was predicted at an altitude of 16.2 nautical miles, but a maximum of 108 feet per second was encountered at a height of 7.1 nautical miles. A significant variation from the predicted wind azimuths was present to an altitude of approximately 10 nautical miles. The measured azimuths below this altitude averaged about 60^{o} from North compared with predicted values of about 130^{o} from North. At higher altitudes, the agreement between predicted and actual wind azimuths was good.

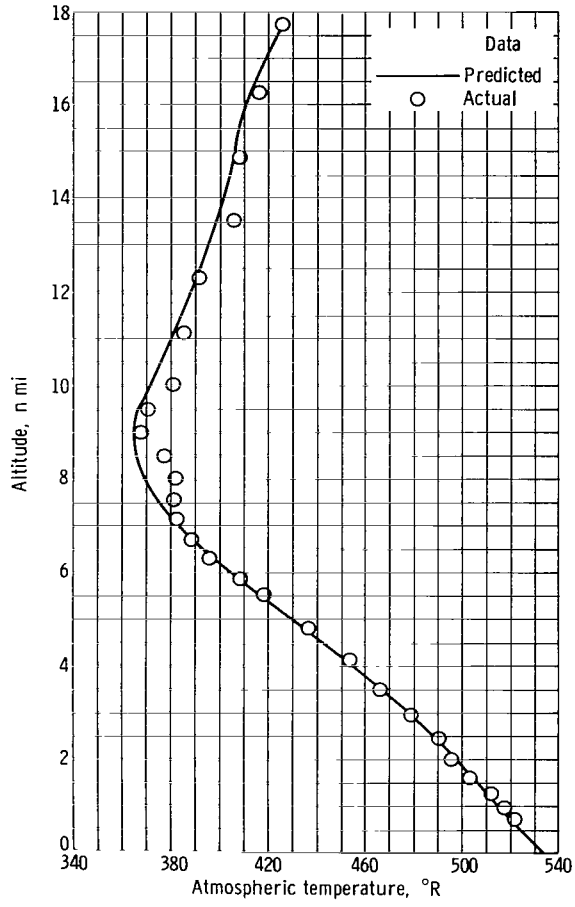

Figure A-1. - Altitude as function of temperature, AC-10.

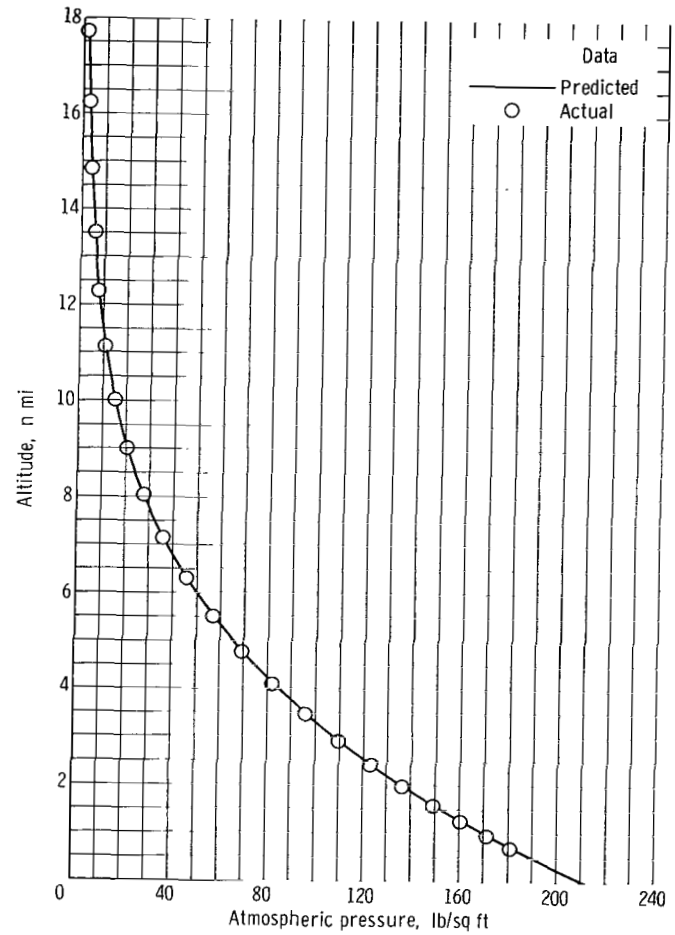

Figure A-2. - Altitude as function of pressure, AC-10.

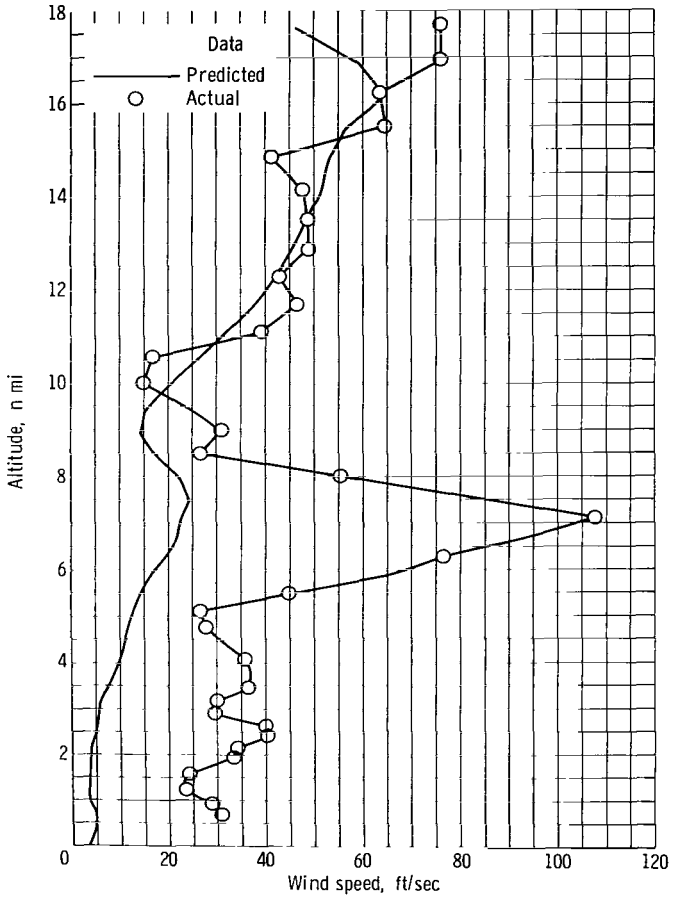

Figure A-3. - Altitude as function of wind speed, AC-10.

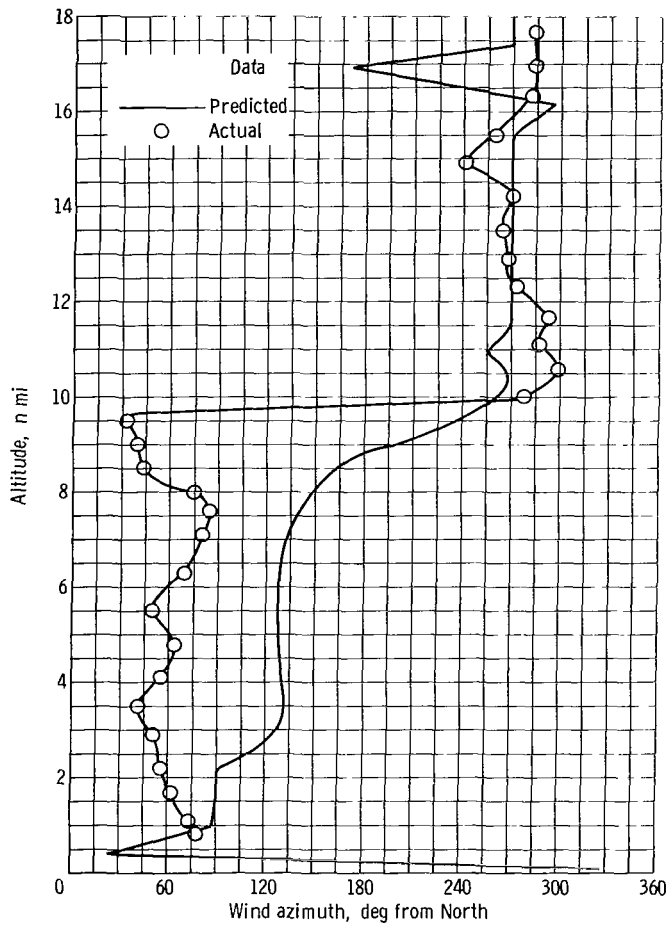

Figure A-4. - Altitude as function of wind direction, AC-10.

SURVEYOR LAUNCH WINDOWS

Launch opportunities established for the AC-10 flight in May and June of 1966 are shown in figure A-5. The countdown for the launch was normal, and there were no unscheduled holds. Data transmission problems with the tracking range were encountered during the count; however, they were cleared and did not delay the count. Lift-off occurred within the first second of the launch window (14:14). The launch azimuth was 102.285°. Figure A-5 shows how launch azimuth increases as the window approaches its closing time. If the vehicle had been launched at 15:27 (window closing time) instead of 14:41, the launch azimuth at this closing time would have been 115° instead of 102.285°. The maximum launch azimuth allowed by range safety restrictions is 115.0°.

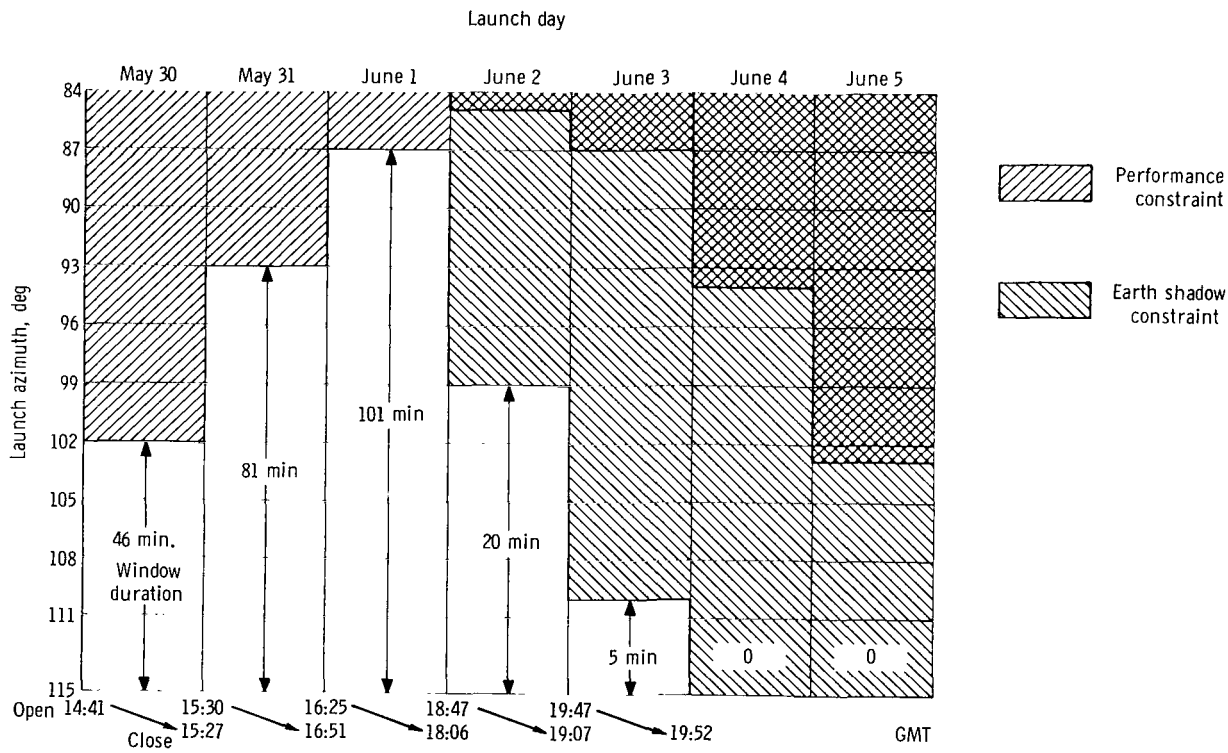

Figure A-5. - Surveyor launch window design for May/June 1966 launch window.

FLIGHT EVENTS RECORD

The major flight events during the AC-10 flight are listed in table A-III. Programmer times, when given, are for those flight events sequenced and commanded by an in-flight timer. Preflight times are based on the best estimate of the flight sequence for the actual flight azimuth. Actual times listed are the measured times of the given flight

TABLE A-III. - FLIGHT EVENTS RECORD, AC-10

Event	Programmer time, sec	Preflight time, sec	Actual time, sec
Guidance flight mode acceptance		T - 8.0	T - 8.50
Programmer start; 2-in. rise		T + 0.0	T + 0.00
Initiate roll program		T + 2.0	T + 2.00
Initiate pitch program		T + 15.0	T + 15.00
Unlock liquid hydrogen vent valve		T + 69.0	T + 69.30
Booster engine cutoff (BECO)	BECO	T + 142.5	T + 142.04
Jettison booster package	BECO + 3.1	T + 145.6	T + 145.14
Jettison insulation panels	BECO + 34	T + 176.5	T + 175.84
Unlatch nose fairing	BECO + 60.5	T + 203.0	T + 202.26
Fire thrustor bottles	BECO + 61	T + 203.5	T + 202.76
Start Centaur boost pumps	BECO + 62	T + 204.5	T + 203.70
Sustainer engine cutoff; vernier engine cutoff; start Centaur Programmer (SECO/VECO)	SECO	T + 239.7	T + 239.38
Start hydraulic recirculating pump	SECO + 0.5	T + 240.2	T + 239.88
Separate (first and second stage)	SECO + 1.9	T + 241.6	T + 241.31
Prestart	SECO + 3.5	T + 243.2	T + 242.40
Centaur main engine start (MES)	SECO + 11.5	T + 251.2	T + 250.90
Centaur main engine cutoff (MECO)	MECO	T + 683.9	T + 689.21
Centaur MECO backup (MBU)	MES + 446	T + 697.2	T + 696.90
Preseparation arming signal; extend landing gear	MBU + 18	T + 715.2	T + 715.50
Unlock omniantennas	MBU + 28.5	T + 725.7	T + 725.30
High power transmitter	MBU + 49	T + 746.2	T + 746.40
Electrical disconnect	MBU + 54.5	T + 751.7	T + 751.40
Spacecraft separation	MBU + 60	T + 757.2	T + 756.93
Begin Centaur reorientation maneuver	MBU + 65	T + 762.2	T + 762.00
Start Centaur lateral thrust	MBU + 105	T + 802.2	T + 802.00
End Centaur lateral thrust	MBU + 125	T + 822.2	T + 822.00
Start Centaur tank blowdown	MBU + 300	T + 997.2	T + 997.00
End Centaur tank blowdown	MBU + 550	T + 1247.2	T + 1247.00
Energize power changeover	MBU + 550	T + 1247.2	T + 1247.00

events. Timers for given sequences are enabled at one of four flight discretes, namely, BECO, SECO, MES, or MBU:

Booster engine cutoff (BECO): guidance cutoff command when vehicle acceleration reaches 5.7±0.08 g's; start timer for sequencing Centaur insulation panel and nose fairing jettison, start Centaur boost pumps, and pressurize oxidizer tank

Sustainer engine cutoff (SECO): usable propellant depletion cutoff command; start timer for Centaur main engine start sequences

Centaur main engine start (MES)

Centaur main engine cutoff (MECO): guidance cutoff command when vehicle attains orbital injection velocity

Centaur MECO backup (MBU): programmer start of timer for sequencing spacecraft separation and Centaur retromaneuver

TRAJECTORY DATA

Mach Number and Dynamic Pressure

Mach Number and dynamic pressure data for the AC-10 flight are given in figure A-6. These data were calculated from range tracking measurements and atmospheric soundings taken at the time of launch. The agreement between flight measurements and expected values of dynamic pressure was good except for the time interval between T + 74 and T + 80 seconds. Even in this interval, every actual data point can be correlated to within 1 pound per square foot of its predicted value if known dispersions in atmospheric temperature and pressure, and vehicle relative velocity (air speed) are considered.

Deviations of these three parameters from their predicted values caused the dynamic pressure dispersions between T + 74 and T + 80 seconds. The average deviation between preflight and in-flight temperature measurements was highest during approximately the same time interval (see fig. A-1). But at some times within this interval, actual temperatures did agree with predictions while dynamic pressures did not. Consequently, temperature variations do not appear to be the chief cause of the dynamic pressure dispersions. Relatively slight disagreement between measured and predicted atmospheric pressures during flight occurred at nearly all times. Atmospheric pressure dispersions were not limited to the interval between T + 74 and T + 80 seconds even though the major disagreements in dynamic pressure did fall between these times. Therefore, it is not likely that variations in atmospheric pressure were the chief cause. The in-flight deviation of relative velocities from predicted values followed a pattern characteristic of this particular 6-second interval only. Thus, it is probable that dispersions in relative velocities were the chief contributor to the variations of dynamic pressure.

This variation of actual relative velocity from predicted values appears to be related to the large discrepancies between preflight and in-flight values of wind speed and wind azimuth. Every point between T + 74 and T + 80 seconds occurs within the time interval when the wind speed deviated most from predictions (see figs. A-3 and A-9). During the same interval, the wind azimuths varied from their preflight values in such a way that the resultant vehicle relative velocities were lower than expected. This pattern of low velocities occurred only during this interval. Dynamic pressure is defined as $1/2(\rho v^2)$ where ρ is the atmospheric density and v is the vehicle relative velocity (air speed). Consequently, lower than predicted velocities yield lower than predicted dynamic pressures. At T + 76 seconds, the velocity disagreement was greatest. At this time, an altitude of 7.1 nautical miles, the maximum deviation in wind speed occurred. At this time, the dynamic pressure experienced its maximum deviation of 51 pounds per square foot lower than predicted.

Predicted and measured values of Mach number were in good agreement at all points on the curve.

Axial Load Factor

Axial load factor for the Atlas Centaur powered flight phase is shown in figure A-7. A plot of axial load factor is equivalent to a plot of thrust acceleration in g's. Agreement between preflight and actual data was good. Even though the actual data were somewhat lower than expected during approximately the last 200 seconds of Centaur burn, this dispersion was well within the 3σ tolerances.

A flattening of the curve occurs between about T + 54 and T + 58 seconds. This interval of constant acceleration reflects the severe vehicle perturbations undergone when the vehicle approached and surpassed Mach 1 (see fig. A-6). The curve abruptly drops, as expected, from 5.68 to 1.13 g's at booster engine cutoff. Approximately 3 seconds later, a slight upward jump reflects the sudden loss of the booster weight. Additional rises can be seen at insulation panel and nose fairing jettison. At sustainer engine cutoff, the curve again drops sharply. It then increases uniformly from Centaur main engine start to Centaur shutdown at T + 689.2 seconds.

For approximately the last 200 seconds of Centaur burn, the actual data were slightly lower than predicted. A possible cause was the lower than expected thrust (see section V. LAUNCH VEHICLE SYSTEM ANALYSIS). Actual data were not available past T + 597 seconds.

Inertial Velocity

Inertial velocity data for the flight is presented in figure A-8. The actual and predicted results show good agreement. Abrupt changes in the vehicle total acceleration, the slope of the inertial velocity curve, can be seen to coincide with the sharp changes in thrust acceleration (axial load factor, see fig. A-7). Because the thrust acceleration was lower than expected for approximately the last 200 seconds of Centaur burn, the inertial velocities in this interval also were lower than predicted. The lower than predicted thrust could not accelerate the vehicle to the velocity expected at any given time. The maximum deviation from preflight values occurred at T + 684 seconds, approximately 5 seconds before Centaur main engine cutoff. At this time, the actual velocity was about 770 feet per second low. The velocity dispersion reduced to 350 feet per second lower than expected at T + 686 seconds. The cause of the velocity dispersions is ex-

plained in the discussion of altitude as a function of time. No actual data were available after T + 686 seconds.

Altitude and Range

Altitude as a function of time and altitude as a function of ground range are shown in figures A-9 and A-10. The Earth trace or ground track of the vehicle subpoint, latitude as a function of longitude, is given in figure A-11. With few exceptions, the in-flight and preflight data agree well on all three curves.

On the curve for altitude as a function of time, at times near Centaur main engine cutoff (T + 689.2 sec) the measured altitudes were higher than predicted. These higher altitudes were necessary to compensate for the lower than expected inertial velocities in the same time interval (see fig. A-8). Since the low inertial velocities were present, higher altitudes were needed to ensure that the vehicle would reach the required mission energy at main engine cutoff. The maximum altitude dispersion was approximately 12 800 feet at about T + 684 seconds. This maximum deviation was expected at T + 684 seconds, because at this time the inertial velocity experienced its greatest deviation from predictions (see fig. A-8). Figure A-9 also shows that the altitude was decreasing when the vehicle was injected into the lunar transfer trajectory at main engine cutoff. This result is expected for any flight with a negative injection true anomaly (see table A-IV).

TABLE A-IV. - CENTAUR AND SURVEYOR ORBITAL PARAMETERS, AC-10

Parameter	Centaur (after retrothrust)	Surveyor (at spacecraft separation)
Time from lift-off, sec	1375.9	756.9
Greenwich mean time, hr	1503:55.9	1453:37.0
Earth relative velocity, ft/sec	31 120	34 655
Apogee altitude, n mi	236 939	333 575
Perigee altitude, n mi	91.2	91.3
Injection energy, C_3, $(km/sec)^2$	-1.72	-1.26
Semimajor axis, n mi	124 552	170 277
Eccentricity	0.971615	0.979238
Inclination, deg	30.05	30.05
True anomaly, deg	49.89	-2.45
Period, days	12.4	20.4
Longitude, deg	3.97 West	47.86 West
Latitude, deg	7.561 South	17.592 North

The in-flight data curves for altitude as a function of ground range and latitude as a function of longitude (figs. A-10 and A-11) agreed well with preflight estimates.

Orbital Parameters

The spacecraft-computed orbital elements for conditions at spacecraft separation are given in table A-IV. Similar data are also given for the Centaur stage but for the time after Centaur retromaneuver.

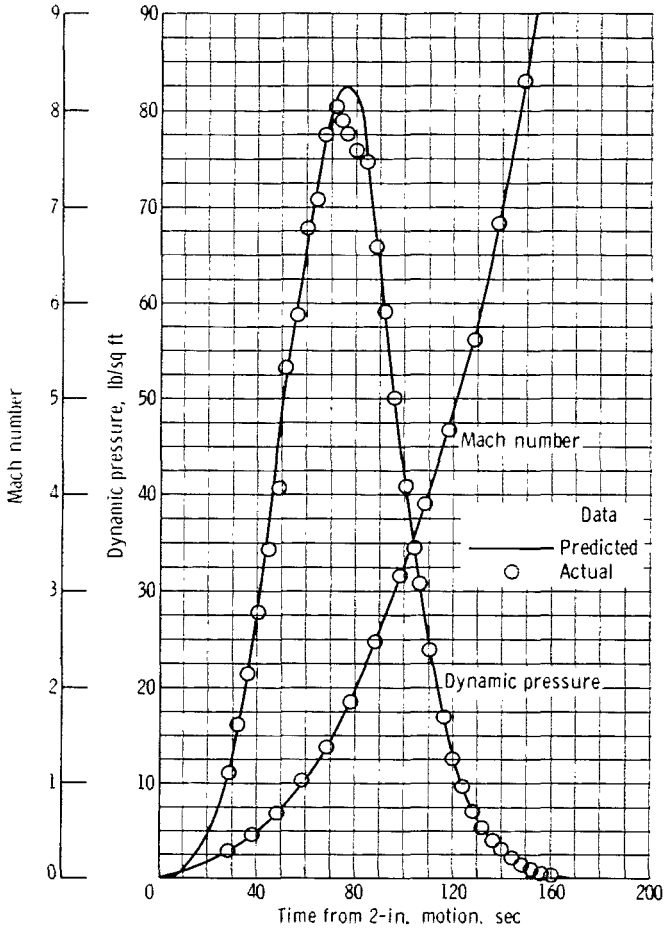

Figure A-6. - Dynamic pressure and Mach number as function of time, AC-10.

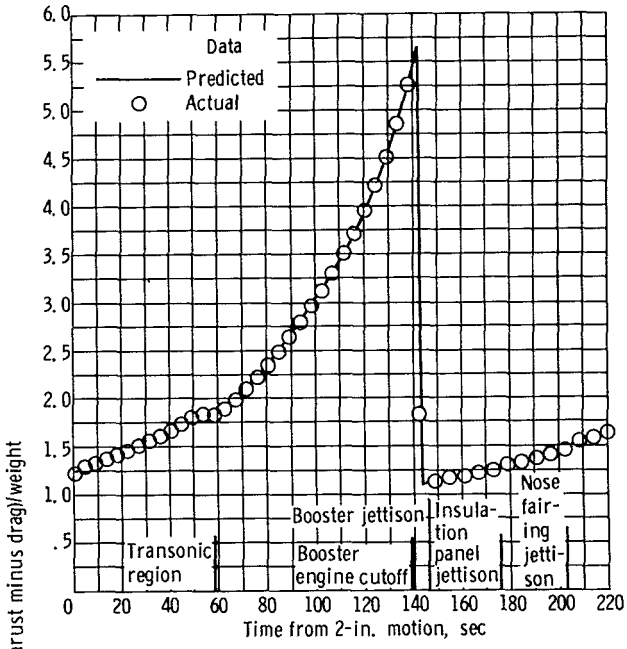

(a) Time, 0 to 240 seconds.

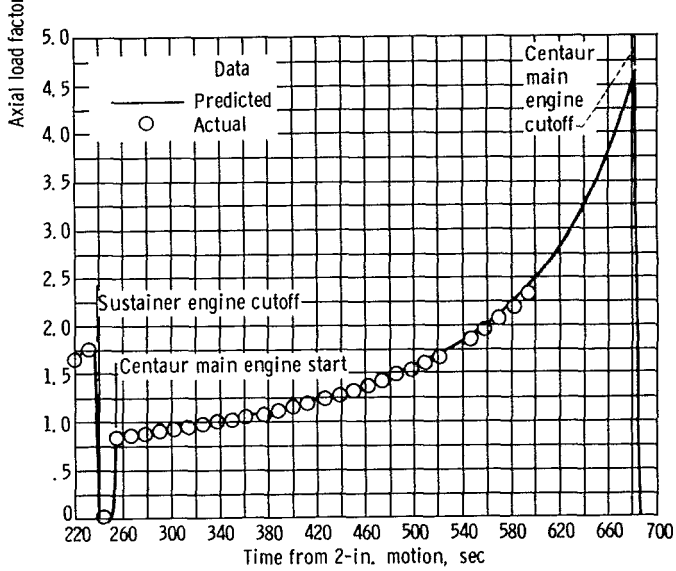

(b) Time, 220 to 700 seconds.

Figure A-7. - Axial load factor as function of time, AC-10.

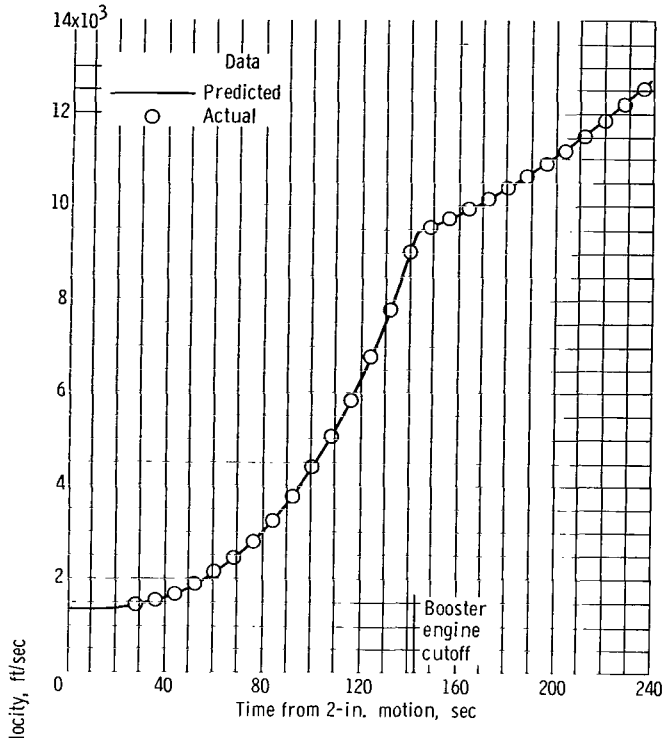

(a) Time, 0 to 240 seconds.

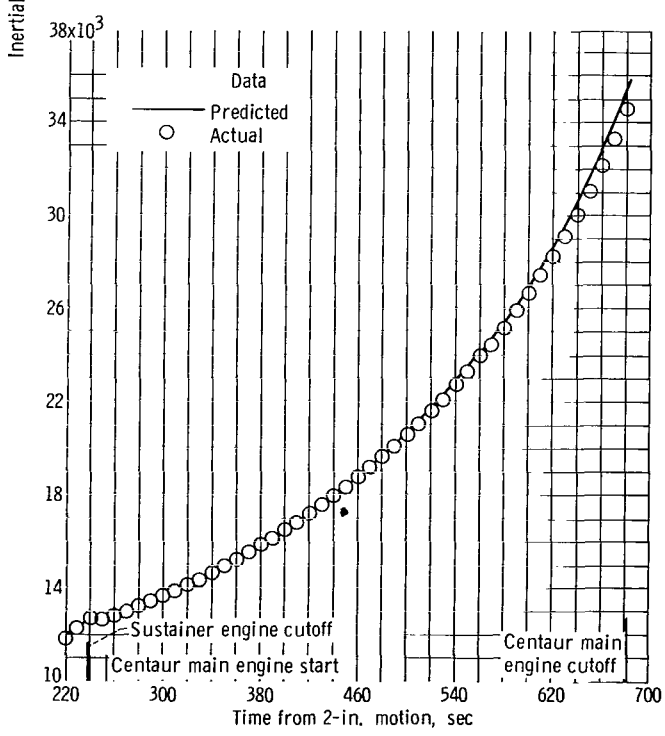

(b) Time, 220 to 700 seconds.

Figure A-8. - Inertial velocity as function of time, AC-10.

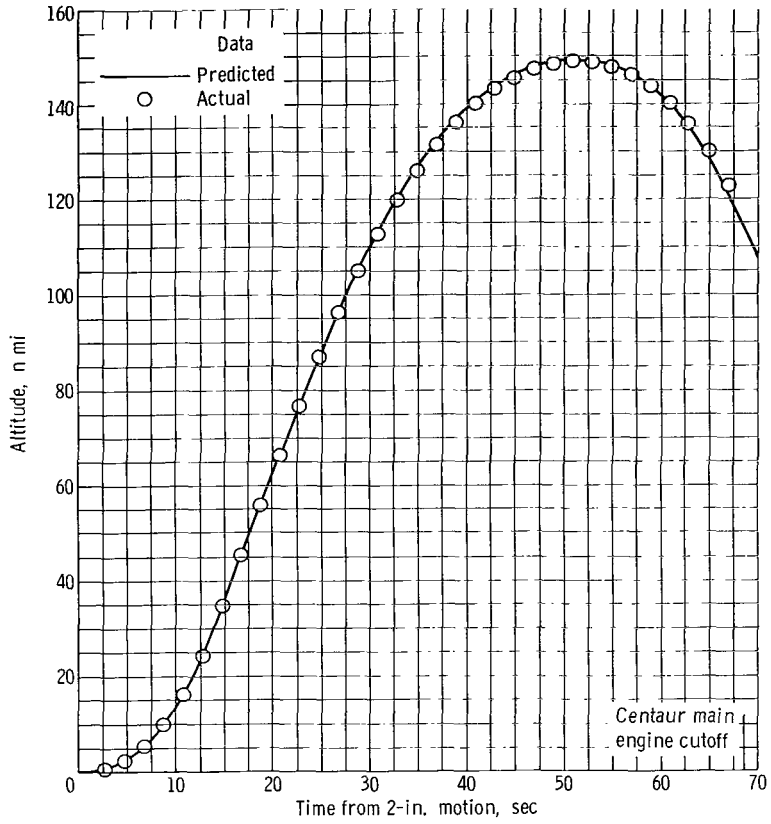

Figure A-9. - Altitude as function of time, AC-10.

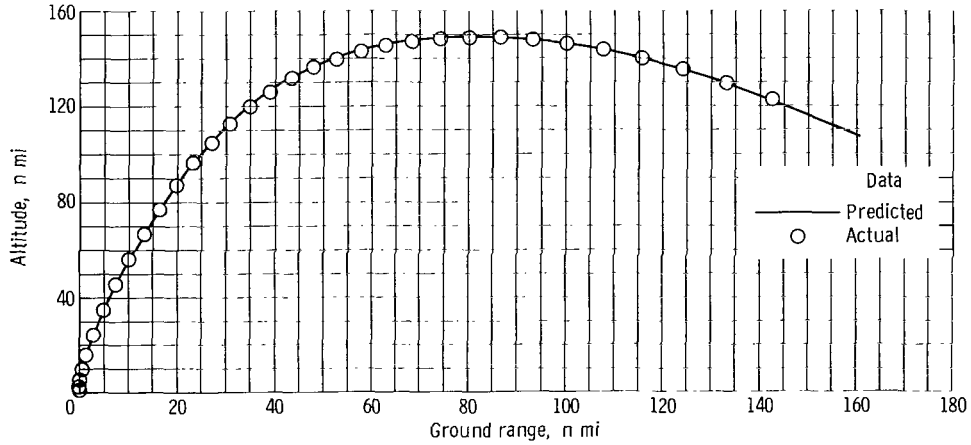

Figure A-10. - Altitude as function of ground range, AC-10.

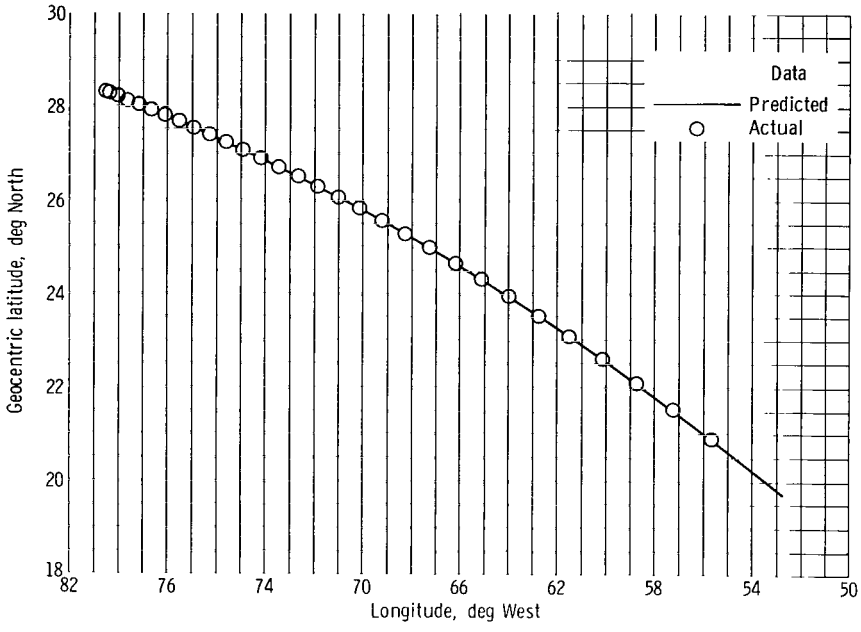

Figure A-11. - Earth trace of vehicle subpoint, latitude as function of longitude, AC-10.

APPENDIX B

CENTAUR ENGINE PERFORMANCE CALCULATIONS

by William A. Groesbeck, Ronald W. Ruedele, and John J. Nieberding

SUMMARY

Calculations of engine specific impulse, engine thrust, and oxidizer to fuel mixture ratio to evaluate engine performance have been made by the Pratt & Whitney characteristic velocity C* iteration and Pratt & Whitney regression methods. In addition, a vehicle specific impulse has been calculated by using data obtained from the guidance system velocity data outputs. The calculated engine specific impulse using the C* method was about 433 to 434 seconds, whereas the vehicle specific impulse was 431.6 seconds. These values are considered to be in good agreement. These methods are discussed in the following section, and a comparison of the engine specific impulse data calculated by two methods (C* and regression) given in table B-I.

METHODS OF CALCULATION

Pratt & Whitney C* Technique

This technique is an iteration process for determining engine performance parameters. Calculated values of hydrogen flow rate along with the measured chamber pressure and engine acceptance test data are used to determine the actual characteristic exit velocity C*, the total propellant weight flow, and finally the specific impulse and engine thrust. The procedure is as follows:

(1) Calculate the hydrogen flow rate by using venturi measurements of pressure and temperature as obtained from telemetry.

(2) Assume a given mixture ratio and calculate the corresponding oxidizer flow rate and total propellant flow rate.

(3) Obtain C* ideal from the performance curve as a function of mixture ratio.

(4) Correct to C* actual by using the characteristic exit velocity efficiency factor obtained from acceptance test results.

(5) Calculate the total propellant flow rate by using C* actual:

TABLE B-I. - CENTAUR MAIN ENGINE PERFORMANCE, AC-10

(a) C-1 engine (serial number 1840)

Time from main engine start, sec	Chamber pressure, psia	Engine thrust, lb		Specific impulse, sec		Oxidizer to fuel mixture ratio	
		Regression[a] equations	C* method	Regression[a] equations	C* method	Regression[a] equations	C* method
10	297.3	14 982	14 994	432.6	433.7	5.053	5.090
50	295.5	14 978	14 901	432.7	433.9	5.046	5.062
90	297.3	14 975	14 997	432.7	433.7	5.037	5.102
100	297.3	14 924	14 974	433.4	434.3	4.935	4.995
150	293.5	14 971	14 889	432.8	434.2	5.030	5.007
200	296.0	14 989	14 937	432.6	433.6	5.060	5.115
250	295.5	14 971	14 896	432.8	434.0	5.022	5.042
300	↓	14 958	14 893	433.0	434.1	4.995	5.024
350		14 940	14 890	433.3	434.2	4.958	5.012
400		14 964	14 891	432.9	434.2	5.007	5.018
435		14 966	14 893	432.8	434.1	5.019	5.025

(b) C-2 engine (serial number 1843)

Time from main engine start, sec	Chamber pressure, psia	Engine thrust, lb		Specific impulse, sec		Oxidizer to fuel mixture ratio	
		Regression[a] equations	C* method	Regression[a] equations	C* method	Regression[a] equations	C* method
10	[b]300.7	15 072	15 347	433.0	434.6	5.129	5.159
50	295.2	15 068	15 057	433.1	435.0	5.120	5.084
90	↓	15 065	15 069	433.1	434.8	5.115	5.124
100		15 022	15 025	433.7	435.5	5.033	4.975
150		15 059	15 059	433.2	435.0	5.102	5.090
200	295.8	15 070	15 109	433.1	434.6	5.116	5.159
250	294.5	15 052	15 025	433.4	434.9	5.080	5.092
300	294.5	15 041	15 028	433.5	434.9	5.059	5.104
350	294.1	15 015	14 986	433.9	435.3	5.004	5.028
400	294.5	15 064	15 029	433.2	434.9	5.098	5.106
435	294.5	15 064	15 015	433.2	435.1	5.106	5.059

(c) Engine acceptance test results

Engine	Chamber pressure, psia	Engine thrust, lb	Specific impulse, sec	Oxidizer to fuel mixture ratio
C-1	296.9	14 994	433	5.05
C-2	294.8	15 051	434	5.07

[a]These values are the acceptance test data adjusted for flight value of pump inlet temperatures and pressure and propellant utilization valve positions

[b]Chamber pressure data questionable at this time. Expected engine performance (for propellant utilization valve at zero); engine thrust, 14 963±263 lb; specific impulse, 434.1±4.3 sec; mixture ratio, 5.014±0.079.

$$\dot{w}_t = \frac{p_o A_* g}{C^*}$$

where $\dot{w}_t$ is the total propellant flow rate in pounds per second, p_o is the measured chamber pressure from telemetry in psi, A_* is the thrust chamber throat area in square inches, g is the gravitational constant, 32. 17 feet per second per second, and C^* is the characteristic exhaust velocity in feet per second.

(6) Determine the mixture ratio by using the calculated total propellant flow rate and measured hydrogen flow rate.

(7) Compare the calculated mixture ratio with that assumed in step (2).

(8) If the two values of mixture ratio do not agree, assume a new value of mixture ratio and repeat the process until agreement is obtained.

(9) When the correct mixture ratio is determined, obtain the ideal specific impulse from the performance curve as functions of actual mixture ratio.

(10) Correct to actual specific impulse by using the specific impulse efficiency factor determined from acceptance test results.

(11) Calculate engine thrust as product of propellant flow rate and specific impulse.

Pratt & Whitney Aircraft Regression Technique

This program determines engine thrust, specific impulse, and propellant mixture ratio from flight values of engine inlet pressures, engine inlet temperatures, and propellant utilization valve angle. The program is strongly dependent on engine ground testing. The method in which ground testing is correlated with the flight is as follows.

A large group of RL10A3-1 engines are ground tested. An average level of engine performance is obtained as a function of engine pump inlet pressures, inlet temperatures, and the propellant utilization valve angle. During any specific engine acceptance test, the differences in performance from this average level are noted.

Flight performance is then determined in two steps: (1) the average engine level of performance is obtained for flight values of engine inlet conditions and propellant utilization valve angle and (2) corrections are made for the difference between the average engine level and the specific engine level as noted during the engine acceptance testing.

Guidance Thrust Velocity Method

The guidance thrust velocity method computes vehicle specific impulse by using guid-

ance computed inertial thrust velocities. Vehicle specific impulse is defined as

$$\left(I_{sp}\right)_v = \frac{|\vec{F}|}{\dot{W}} \tag{B1}$$

where $|\vec{F}|$ is the magnitude of the total Centaur thrust vector and $\dot{W}$ is the time rate of change of instantaneous total Centaur weight.

It should be noted that vehicle specific impulse differs from the engine specific impulse which is defined as

$$\left(I_{sp}\right)_e = \frac{|\vec{F}|}{\dot{w}} \tag{B2}$$

where $\dot{w}$ is the total propellant flow rate through the Centaur main engines. The time rate of change of total Centaur weight in equation (B1) includes weight losses due to hydrogen peroxide used to drive the boost pumps and all other losses in addition to the total propellant flow rate through the main engines. Consequently, the vehicle specific impulse would be less than the engine specific impulse. Vehicle specific impulse is a measure of total vehicle performance, whereas engine specific impulse is an index of engine performance only.

The derivation of vehicle specific impulse is based on the Centaur vehicle vector equation of motion

$$\vec{F} + m\vec{G} - \vec{X} = m\vec{a} \tag{B3}$$

where m is the instantaneous Centaur mass, $\vec{G}$ is the instantaneous Centaur acceleration vector due to gravity, $\vec{X}$ is the instantaneous force vector due to drag or other perturbing forces, and $\vec{a}$ is the instantaneous Centaur total acceleration vector. It was assumed that drag and other perturbing forces are negligible over the time interval of interest, that the time rate of change of total vehicle weight is either constant or at least varies symmetrically about a mean value over this interval, and that only a negligible amount of axial thrust is lost due to engine gimbaling. Based on these assumptions, the equations of motion can be rewritten as

$$\vec{F} = m(\vec{a} - \vec{G})$$

or

$$\frac{\vec{F}}{m} = (\vec{a} - \vec{G}) \tag{B4}$$

The acceleration $\vec{a} - \vec{G}$, designated as the thrust acceleration, is the acceleration imparted to the Centaur by thrust alone. It is obtained as the time rate of change of the inertial thrust velocity which is computed by the Centaur guidance system.

The thrust acceleration is used in a computer program to calculate the vehicle axial load factor, and this load factor is then used to determine the total vehicle specific impulse. Axial load factor, which is defined as the ratio of vehicle thrust minus drag over vehicle weight, is obtained by dividing the magnitude of the thrust acceleration in equation (B4) by g:

$$\frac{|\vec{F}|}{mg} = \frac{|\vec{a} - \vec{G}|}{g} \tag{B5}$$

where g is the gravitational acceleration at the Earth's surface. But

$$\frac{|\vec{F}|}{mg} = \frac{|\vec{F}|}{W} = \alpha \tag{B6}$$

where $W = mg$ is the instantaneous total Centaur weight and α is defined as the axial load factor. If the instantaneous Centaur weight is written as

$$W = W_o - \dot{W}(t - t_o) = W_o - \dot{W}\,\Delta t \tag{B7}$$

where W_o is the total Centaur weight at main engine start, and t_o is the time of main engine start (measured from lift-off), t is the instantaneous time from lift-off, and $\Delta t = t - t_o$, and this substitution is made in equation (B6), the result is

$$\alpha = \frac{|\vec{F}|}{W} = \frac{|\vec{F}|}{W_o - \dot{W}\,\Delta t} \tag{B8}$$

The reciprocal of this equation is

$$\frac{1}{\alpha} = \frac{W_o - \dot{W}\,\Delta t}{|\vec{F}|} = \frac{W_o}{|\vec{F}|} - \frac{\dot{W}\,\Delta t}{|\vec{F}|} \tag{B9}$$

If W and F are constant, a plot of $1/\alpha$ against time is a straight line with a slope equal to $-(\dot{W}/|\vec{F}|)$. Since by definition, the vehicle specific impulse is

$$\left(I_{sp}\right)_v = \frac{|\vec{F}|}{\dot{W}}$$

the slope $-(\dot{W}/|\vec{F}|)$ is the negative reciprocal of the vehicle specific impulse. The computer program therefore determined the specific impulse by

(1) Calculating thrust acceleration based on guidance-computed thrust velocities

(2) Computing axial load factor from equation (B5)

(3) Plotting the reciprocal of axial load factor against time

(4) Curve fitting the reciprocal of axial load factor against time with a straight line using the method of least squares

(5) Taking the negative reciprocal of the line slope to obtain an average value of vehicle specific impulse for the time interval considered

The time interval for calculating the vehicle specific impulse on AC-10 was from T + 370 to T + 595 seconds. During this interval, the propellant utilization valve motion was approximately symmetrical about a mean value; consequently, the mean values of thrust and weight flow could be assumed constant. Calculations were made for 143 data points, and the resultant vehicle specific impulse was 431.6 seconds.

REFERENCES

1. Staff of Lewis Research Center: Postflight Evaluation of Atlas-Centaur AC-6 (Launched August 11, 1965). NASA TM X-1280, 1966.

2. Parks, Robert J.: Surveyor I Mission Report. Part I: Mission Description and Performance. Tech. Rep. No. 32-1023 (NASA CR-77795), Jet Propulsion Lab., California Inst. Tech., Aug. 31, 1966.

3. Latto, William T., Jr.: Experimental Investigation of Spreading Characteristics of Hydrogen Gas Vented from Atlas-Centaur Vehicle at Mach Numbers from 0.9 to 3.5. NASA TM X-1188, 1965.

4. Gerus, Theodore F.; Housely, John A.; and Kusic, George: Atlas-Centaur-Surveyor Longitudinal Dynamics Tests. NASA TM X-1459, 1967.

NASA-Langley, 1968 —— 31 E-3484

"The aeronautical and space activities of the United States shall be conducted so as to contribute . . . to the expansion of human knowledge of phenomena in the atmosphere and space. The Administration shall provide for the widest practicable and appropriate dissemination of information concerning its activities and the results thereof."

—NATIONAL AERONAUTICS AND SPACE ACT OF 1958

NASA SCIENTIFIC AND TECHNICAL PUBLICATIONS

TECHNICAL REPORTS: Scientific and technical information considered important, complete, and a lasting contribution to existing knowledge.

TECHNICAL NOTES: Information less broad in scope but nevertheless of importance as a contribution to existing knowledge.

TECHNICAL MEMORANDUMS: Information receiving limited distribution because of preliminary data, security classification, or other reasons.

CONTRACTOR REPORTS: Scientific and technical information generated under a NASA contract or grant and considered an important contribution to existing knowledge.

TECHNICAL TRANSLATIONS: Information published in a foreign language considered to merit NASA distribution in English.

SPECIAL PUBLICATIONS: Information derived from or of value to NASA activities. Publications include conference proceedings, monographs, data compilations, handbooks, sourcebooks, and special bibliographies.

TECHNOLOGY UTILIZATION PUBLICATIONS: Information on technology used by NASA that may be of particular interest in commercial and other non-aerospace applications. Publications include Tech Briefs, Technology Utilization Reports and Notes, and Technology Surveys.

Details on the availability of these publications may be obtained from:

SCIENTIFIC AND TECHNICAL INFORMATION DIVISION

NATIONAL AERONAUTICS AND SPACE ADMINISTRATION

Washington, D.C. 20546